



**Application of triazolium-based metal complexes for catalytic  
oxidation of octane**

by

Siyabonga Gift Mncube

Dissertation submitted in fulfilment of the requirements for the degree of

Master of Science

in

Chemistry

College of Agriculture, Engineering and Science

University of KwaZulu-Natal

Supervisor: Professor M.D. Bala

2014

# **Application of triazolium-based metal complexes for catalytic oxidation of octane**

by

**Siyabonga Gift Mncube**

Dissertation submitted in fulfilment of the academic requirements for the degree of Master of Science in the  
College of Agriculture, Engineering and Science, University of KwaZulu-Natal,  
Durban, South Africa

As the candidate's supervisor I have approved this dissertation for submission.

Signed \_\_\_\_\_ Name \_\_\_\_\_ Date \_\_\_\_\_

December 2014

## Abstract

A series of related 1,2,3-triazole compounds were synthesised and characterised by spectroscopic methods including NMR, IR, MS and X-ray diffraction. *N*-alkylation of the triazole compounds yielded 1,4-disubstituted triazolium ionic liquids (**3.1-3.6**). The ionic liquids were found to act as “green” solvent systems for the dissolution of an iron-based compound for the catalytic oxidation of n-octane. Recycling and re-usage of the system was found to be reproducible for three cycles and leaching of the catalyst to the product phase was associated with decrease of catalytic activity in subsequent cycles.

Synthesis and characterisation of 1,2,3-triazolium-based nickel carbene complexes (**4.1-4.6**) by modification of reported synthetic methods was described. The molecular structures of three metal complexes (**4.1**, **4.3** and **4.4**) were analysed by single crystal X-ray diffraction and fully discussed. The complexes were then tested for catalytic oxidation of alkanes in the presence of various oxidants under mild reaction conditions. Catalyst (**4.3**) with less bulky substituents on the triazolium ring exhibited the highest catalytic activity (15%) with H<sub>2</sub>O<sub>2</sub> as the most productive oxidant.

The main goals of this study were achieved because the catalyst systems were successfully synthesised, characterised and tested for activity in alkane oxidation. Indeed there was significant activity observed with all prepared catalysts, however from the results obtained, the nickel carbene catalysts in the presence of H<sub>2</sub>O<sub>2</sub> demonstrated the highest efficiency in this work.

## **Dedication**

To my family

## Acknowledgments

I would firstly like to thank my family, especially my parents and siblings for their support throughout this project.

I like to express my sincere gratitude and appreciation to my supervisor, Professor Muhammad D. Bala, for his guidance throughout the difficulties and challenges faced during this study.

I also would like to acknowledge the work by Mr D. Jagjivan for help with recording NMR spectra, Mr S. Zamisa for X-ray crystal structure determination and Mr N. Broomhead for GC analysis.

My extended appreciation goes out to the technical staff at the School of Chemistry: Mr Z. Miya, Mr G. Moodley, Mr R. Somaru and Mrs M. Padayachee.

Special thanks go to my research group colleagues and laboratory mates for their constant support throughout the course of this study.

This study received financial support from the University of KwaZulu-Natal and the DST-NRF Centre of Excellence in Catalysis (c\* change) which is gratefully acknowledged.

## Declarations 1

I, Siyabonga Gift Mncube, hereby certify that this dissertation, titled ‘application of triazolium-based metal complexes for catalytic oxidation of octane’, has been written by me, that it is the record of work carried out by me and has not been submitted in a previous application for a higher degree. This dissertation does not contain other person’s data, pictures, graphs or other information, unless specifically acknowledged as being sourced from other persons. This dissertation does not contain other person’s writing, unless specifically acknowledged as being sourced from other researchers. Where other written sources have been quoted, then:

1. Their words have been re-written but the general information attributed to them has been referenced
2. Where their exact words have been used, then their writing has been placed in italics and inside quotation marks, and referenced.

This dissertation does not contain text, graphics or tables copied and pasted from the Internet, unless specifically acknowledged, and the source being detailed in the dissertation and in the References sections

Signed \_\_\_\_\_ Date \_\_\_\_\_

## Declaration 2

### Scientific Contributions

#### List of planned publications

1. S.G. Mncube and M.D. Bala. Application of triazolium-ionic liquids as “green” solvents for catalytic paraffin oxidations in the presence of  $\text{FeCl}_2$  catalyst and  $\text{H}_2\text{O}_2$ . **2015**. *Manuscript in preparation*.
2. S.G. Mncube and M.D. Bala. Synthesis of 1,2,3-triazolium-based nickel carbene complexes and their application for catalytic oxidation of alkanes. **2015**. *Manuscript in preparation*.

#### Conferences

1. Poster titled “Triazolium-based transition metal carbene complexes and their application as paraffin oxidation catalysts” by S.G. Mncube and M.D. Bala, presented at the CATSA conference 2013, Wild Coast Resort, Eastern Cape, November 2013.
2. Poster titled “Non-precious metal complexes of *N*-heterocyclic carbene ligands applied as paraffin oxidation catalyst” by M.D. Bala and S.G. Mncube, presented at the XXVI International Conference on Organometallic Chemistry (ICOMC 2014), Sapporo, Japan, July 2014.
3. Poster titled “Triazolium-based nickel carbene complexes and their application as paraffin oxidation catalysts” by S.G. Mncube and M.D. Bala, presented at the CATSA conference 2014, St George conference centre, Gauteng, November 2014.

Signed \_\_\_\_\_

Date \_\_\_\_\_

## List of Abbreviations

Å	Angstrom unit, $10^{-10}$ m
A/K	alcohol/ ketone ratio
Cp	cyclopentadiene, cyclopentadienyl
DMF	<i>N,N'</i> -dimethylformamide, Me <sub>2</sub> NCHO
DMSO	dimethyl sulfoxide
DTA	differential thermal analysis
EI-MS	electron impact mass spectrometry
IMes	1,3-dimesitylimidazo-2-ylidene
en	ethane-1,2-diamine
[C <sub><i>n</i></sub> C <sub><i>m</i></sub> mim] <sup>+</sup>	1-alkyl-3-alkylimidazolium cations (where <i>n</i> and <i>m</i> are the lengths of the alkyl chains.)
ES-MS	electrospray mass spectrometry
FT	Fourier Transform
GC-MS	gas chromatography-mass chromatography
Hz	Hertz
HR-MS	high resolution mass spectrometry
<i>J</i>	coupling constant, Hz
M	metal
m/z	mass-to-charge ratio
NHC	<i>N</i> -heterocyclic carbene
OAc	acetate, -O <sub>2</sub> CCH <sub>3</sub>
PPh <sub>3</sub>	triphenylphosphine
Ph	phenyl, -C <sub>6</sub> H <sub>5</sub>
ppm	parts per million
py	pyridine
TGA	thermogravimetric analysis
THF	tetrahydrofuran, C <sub>4</sub> H <sub>8</sub> O
TON	turnover number



## Table of Contents

<b>1</b>	<b>Abstract .....</b>	<b>ii</b>
<b>2</b>	<b>Dedication.....</b>	<b>iii</b>
<b>3</b>	<b>Acknowledgments.....</b>	<b>iv</b>
<b>4</b>	<b>Declarations 1.....</b>	<b>v</b>
<b>5</b>	<b>Declaration 2 .....</b>	<b>vi</b>
<b>6</b>	<b>List of Abbreviations .....</b>	<b>vii</b>
<b>1</b>	<b>Chapter 1 .....</b>	<b>1</b>
	<b>Introduction.....</b>	<b>1</b>
1.1	Paraffins .....	1
1.2	Catalytic oxidation of paraffins.....	2
1.2.1	Chemical catalyst .....	2
1.2.2	Biological catalyst: enzymes.....	6
1.2.3	Biomimetic catalyst .....	6
1.3	Triazole ligands .....	8
1.3.1	Synthesis of 1,4-disubstituted-1,2,3-triazoles.....	10
1.4	NHC ligands.....	12
1.4.1	Synthesis of NHC-metal complexes .....	13
1.5	Ionic liquids.....	15
1.5.1	Application of ionic liquids in oxidations of organic compounds.....	16
1.6	Aims of this dissertation.....	20
1.7	Dissertation outline .....	21
1.8	References .....	22
	<b>Chapter 2 .....</b>	<b>25</b>
	<b>Simple and highly efficient one-pot synthesis of 1,4-disubstituted-1<i>H</i>-1,2,3-triazoles.....</b>	<b>25</b>
2.1	Introduction .....	25
2.2	Results and discussion.....	26
2.2.1	Synthesis of 1,4-disubstituted 1,2,3-triazoles .....	26
2.2.2	IR analysis.....	35

2.2.3	MS analysis .....	36
2.2.4	Single crystal X-ray diffraction studies .....	36
2.3	Summary and conclusion .....	39
2.4	Experimental .....	40
2.4.1	General .....	40
2.4.2	General Procedure.....	40
2.5	Reference list.....	45
<b>3</b>	<b>Chapter 3.....</b>	<b>47</b>
	<b>Synthesis and characterisation of triazolium ionic salts. Application of derived ionic liquids in biphasic catalytic oxidation of octane .....</b>	<b>47</b>
3.1	General introduction.....	47
3.1.1	Ionic liquids in catalysis.....	47
3.2	Results and discussion.....	48
3.2.1	Synthesis of triazolium ionic liquids.....	48
3.2.2	Preparation of the ionic liquid dissolved catalyst .....	49
3.2.3	Syntheses and characterisation of triazolium ionic liquids.....	49
3.3	Catalysis .....	55
3.3.1	Selectivity .....	57
3.3.2	Product extraction and analysis .....	60
3.3.3	Catalyst recycling and reuse .....	61
3.3.4	Testing of systems 3.1-3.6 at the optimum conditions .....	62
3.4	Summary and conclusions.....	63
3.5	Experimental .....	63
3.5.1	Synthesis of ionic salts.....	63
3.5.2	General.....	63
3.5.3	Synthesis of 1,4-triazoles .....	63
3.5.4	Synthesis of 1,2,3-triazolium salts .....	64
3.5.5	Synthesis of ionic liquids .....	65
3.6	Catalytic studies .....	67

3.6.1	Procedure for oxidation of octane to oxygenated products in water .....	67
3.7	Reference list.....	69
<b>4</b>	<b>Chapter 4.....</b>	<b>71</b>
	<b>Synthesis and application of 1,2,3-triazolium-based nickel complexes as catalysts for the oxidation of alkanes.....</b>	<b>71</b>
4.1	General introduction.....	71
4.1.1	Synthesis of triazolium nickel complexes.....	71
4.2	Results and discussion.....	72
4.2.1	Synthesis and characterisation of nickel complexes.....	72
4.3	Catalytic studies .....	78
4.3.1	Oxidation of cyclohexane .....	78
4.3.2	Oxidation of <i>n</i> -octane .....	80
4.3.3	Testing of complexes 4.1-4.6 under the optimised conditions .....	83
4.4	Summary and conclusions.....	86
4.5	Experimental .....	87
4.5.1	General procedure for synthesis of 1,3,4-trisubstituted-1,2,3-triazolium salts .....	87
4.5.2	General procedure for synthesis of [(Cp)Ni(X)(NHC)] complexes. ....	88
4.6	Catalytic studies .....	90
4.7	Reference list.....	92
<b>5</b>	<b>Chapter 5.....</b>	<b>93</b>
<b>6</b>	<b>Conclusions.....</b>	<b>93</b>
	<b>List of compounds synthesised.....</b>	<b>94</b>

## List of Figures

Figure 1.1: The Shilov and Periana systems. ....	5
Figure 1.2: Schematic structure of a chiral manganese(III)-salen complex. <sup>16</sup> .....	7
Figure 1.3: X-ray crystal structure of the Albrecht manganese(III)-salen complex. <sup>16</sup> .....	8
Figure 1.4: General structure of 1,2,3-triazole.....	8
<b>Figure 1.5:</b> Triazole ring mimics the amide bond with potential hydrogen bond capabilities. ....	9
<b>Figure 1.6:</b> Peptidomimetic structures. <sup>18</sup> .....	9
<b>Figure 1.7:</b> Classical NHCs <b>I</b> and <b>II</b> , their mesoionic carbene isomers <b>III–III'</b> , and the first complexes featuring the latter. <sup>39</sup> .....	13
<b>Figure 1.8:</b> General structures of common ionic liquids derived from imidazolium salts. ....	16
Figure 2.1 : 1,4-disubstituted-1,2,3-triazole indicating the ring proton. ....	28
Figure 2.2: <sup>1</sup> H NMR spectrum of <b>2.8</b> in CDCl <sub>3</sub> . ....	30
Figure 2.3 : <sup>1</sup> H NMR spectrum of <b>2.6</b> in CDCl <sub>3</sub> . ....	31
Figure 2.4: <sup>13</sup> C NMR spectrum of <b>2.6</b> in CDCl <sub>3</sub> . ....	32
Figure 2.5 : <sup>1</sup> H NMR spectrum of <b>2.13</b> in CDCl <sub>3</sub> . ....	33
Figure 2.6 : <sup>1</sup> H NMR spectrum of <b>2.10</b> in CDCl <sub>3</sub> . ....	34
Figure 2.7 : Molecular crystal structure of compound <b>2.13</b> ; anisotropic displacement parameters are given at the 50% level.....	37
<b>Figure 2.8 :</b> Structure of <b>2.13</b> showing the key intermolecular atoms engaged in hydrogen bonding. ....	38
Figure 2.9 : A perspective of packing in the crystal structure of compound <b>2.13</b> . ....	39
<b>Figure 3.1 :</b> Structures of azolium salts: <b>i</b> – imidazolium; <b>ii</b> –1,2,3-triazolium. ....	48
<b>Figure 3.2:</b> Crystal structure of compound <b>3.3a</b> ; thermal ellipsoids are drawn at the 50% probability level. ....	51
<b>Figure 4.1 :</b> Triazolium-based nickel complexes prepared in this study.....	72
<b>Figure 4.2 :</b> <sup>1</sup> H NMR spectra of a 1,2,3-triazolium salt (bottom)and the corresponding nickel complex <b>4.6</b> (top).....	73
<b>Figure 4.3 :</b> Molecular structure of <b>4.1</b> . For clarity, all hydrogen atoms have been omitted. Displacement ellipsoids are drawn at the 50% probability. ....	74
<b>Figure 4.4 :</b> Molecular structure of <b>4.3</b> . For clarity, all hydrogen atoms have been omitted. Displacement ellipsoids are drawn at the 50% probability. ....	74
<b>Figure 4.5 :</b> Molecular structure of <b>4.4</b> . For clarity, all hydrogen atoms have been omitted. Displacement ellipsoids are drawn at the 50% probability. ....	75
<b>Figure 4.6 :</b> Thermo gravimetric analysis for <b>4.1</b> .....	77
<b>Figure 4.7 :</b> Effect of temperature in catalytic oxidation of <i>n</i> -octane. ....	80
<b>Figure 4.8 :</b> Effect of time on product distribution. ....	81
<b>Figure 4.9 :</b> Effect of substrate to oxidant ratio.....	82
<b>Figure 4.10 :</b> Effect of catalyst loading. ....	83
<b>Figure 4.11:</b> Total conversion of <i>n</i> -octane at the optimum conditions for catalysts <b>4.1–4.6</b> .....	84
<b>Figure 4.12 :</b> Oxygenated product distribution for catalysts <b>4.1–4.6</b> .....	85
<b>Figure 4.13 :</b> Selectivity and product distribution at C(1) for compounds <b>4.1–4.6</b> . ....	86

## List of Schemes

Scheme 1.1: Oxidation of methane to methanol to methanoic acid.....	1
Scheme 1.2: Fenton (Fe-catalysed) oxidation of alkanes. <sup>5</sup> .....	3
<b>Scheme 1.3:</b> Overall stoichiometries and mechanism proposed by Shilov <i>et al.</i> <sup>7-9</sup> .....	4
Scheme 1.4: Periana's catalyst for oxidation of alkanes: Hg (7) and bipyrimidinePt(II) complex (8).....	5
Scheme 1.5: Enzyme catalysed oxidation of alkanes.....	6
Scheme 1.6: (I) Huisgen's cycloaddition route and (II) its copper (I) catalysed version.....	10
<b>Scheme 1.7:</b> Cu(I)-catalysed one-pot synthesis of 1,4-disubstituted-1,2,3-triazoles. <sup>30</sup> .....	11
Scheme 1.8: Mechanism of 1,3-dipolar reaction catalysed with Cu(I) salt. ....	12
Scheme 1.9: Synthesis of NHC-Metal complex by (a) free carbene generation route and (b) <i>in situ</i> carbene-metal complex route.....	14
Scheme 1.10: Synthesis of $[\text{Ni}(\eta^5\text{-C}_5\text{H}_5)(\text{X})(\text{NHC})]$ .....	14
Scheme 1.11: Example of NHC-ML <sub>n</sub> complex formed via transmetalation technique. <sup>45</sup> .....	15
Scheme 1.12: Illustration of the aqueous-IL biphasic system for benzene hydroxylation to phenol with H <sub>2</sub> O <sub>2</sub> . ....	17
Scheme 1.13: Oxidation of alkanes in ionic liquids in the presence of Re catalyst and H <sub>2</sub> O <sub>2</sub> .....	17
Scheme 1.14: Decomposition of imidazolium salt in a basic environment. ....	18
<b>Scheme 1.15:</b> Synthesis of 1,3,4-trisubstituted 1,2,3-triazolium ionic liquids. ....	19
Scheme 2.1 : Synthesis of 1-benzyl-4-phenyl-H1-1,2,3-triazole (2.1). ....	26
Scheme 2.2 : Diazotisation reaction.....	33
Scheme 2.3 : Synthesis of 2.10. ....	34
<b>Scheme 3.1:</b> Schematic preparation of 1,2,3-triazolium ionic liquids.....	49
<b>Scheme 3.2 :</b> Illustration of inter-ionic interactions in the dissolution of the catalyst in the ionic liquid phase. ....	49
<b>Scheme 3.3:</b> Thermal decomposition of hydrogen peroxide. ....	56
<b>Scheme 4.1 :</b> Synthesis of $[(\eta^5\text{-C}_5\text{H}_5)\text{Ni}(\text{X})(\text{NHC})]$ . ....	71
<b>Scheme 4.2:</b> Possible fragmentation pathways of the generated ions. ....	78

## List of Tables

Table 2.1 : Effect of catalysts and solvents on the formation of triazole 2.1.....	27
Table 2.2: One-pot synthesis of 1,2,3-triazoles from organic halides, NaN <sub>3</sub> , and alkynes.....	28
Table 2.3: IR data obtained for each triazole compound showing significant wave numbers.....	35
Table 2.4: <i>m/z</i> ratios obtained for each triazole .....	36
Table 2.5: Selected bond lengths (Å) and bond angles (°) of 2.13.....	37

# Chapter 1

## Introduction

The aim of this chapter is to give some general introduction on paraffin activation on the basis that they are one of the major constituents of natural gas and petroleum. Also inspired from the activities of natural catalytic enzymes in alkane oxidation, this chapter will review a variety of enzymes that have been used as efficient and selective catalysts for *n*-alkane oxidation reactions under physiological conditions and some critical challenges encountered in biomimetic catalysis and synthesis of complexes. Furthermore, the application of ionic liquids as new and “green” solvents in catalysis will be discussed. Finally the overall aims and objectives of the research described in this dissertation will be outlined.

### 1.1 Paraffins

Paraffins are straight chain chemical compounds that consist only of hydrogen and carbon atoms and are bonded exclusively by single bonds (i.e., they are saturated compounds). They are major constituents of natural gas and petroleum due to the relatively inert nature of the C–H bond. The field of alkane activation still remains a challenge to chemists, biochemists and engineers because it poses a huge challenge, however the field is not only of academic concern but also considerable interest to chemical industries globally.<sup>1</sup> The successful conversion of these compounds into valuable product: alcohols, carboxylic acids and alkenes under controlled catalytic conditions can offer large economic benefits.<sup>1,2</sup> Alkanes derived from natural gas, such as methane, are available in very large quantities at remote locations that is economically challenging to transport. Therefore, conversion of methane into a transportable liquid such as methanol, would improve its economic viability as an energy resource.<sup>2</sup> Currently, alkanes derived from both petroleum and natural gas are converted (Scheme 1.1) to energy, fuel and chemicals at high temperatures and via multiple steps leading to inefficient, environmentally and economically impracticable processes.



**Scheme 1.1:** Oxidation of methane to methanol to methanoic acid.

Light alkanes are mostly found abundant in natural gas which includes methane, ethane, propane etc., with methane being the leading component (80-98%). Exploiting their usage and energy content for heating, transportation and electricity generation is the driving force for continued interest in their exploitation.<sup>3</sup> Employment of natural gas as a fuel and chemical feedstock is known for a few processes. For example, ethane to ethylene by steam cracking, while methane can be used to produce syngas ( $\text{CO} + \text{H}_2$ ) by steam reforming which is used as a starting material for the manufacture of many chemicals including methanol. However, these methods that include steam cracking generally require elevated temperatures and high pressures via multi-step reactions leading to inefficient processes that are environmentally and economically wasteful.<sup>3</sup>

## **1.2 Catalytic oxidation of paraffins**

There are very few operational catalytic processes for the direct conversion of alkanes to value-added products. Considering alkane oxidation, at least two issues need to be addressed: (i) how to selectively activate the C-H bonds using the lowest amount of energy possible and (ii) how to design catalytic systems that will lead to selectively targeted compounds. Many factors affect these reactions, some related to the chemical properties of the feed and products, and others related to the catalyst employed.<sup>2,3</sup>

Metal-mediated C-H bond activation has been studied since the 1970's after a direct interaction of metal centres with C-H bond was confirmed. Due to the need of conversion of these highly accessible hydrocarbons, direct and catalytic transformation of alkanes to higher value chemicals via C-H activation is of considerable interest to chemical industries globally. If catalytic conversion of alkanes into useful products, such as alkenes, alcohols, aldehydes, and carboxylic acids can occur under milder and better controlled catalytic conditions, then this can offer large economic benefits.

### **1.2.1 Chemical catalyst**

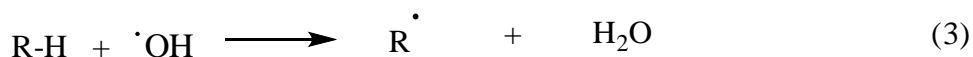
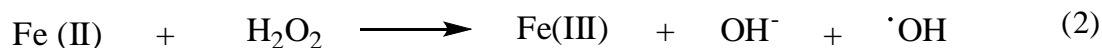
Selective catalytic oxidation of alkanes is an economically attractive process in both the chemical and petroleum industries. However, the well-known chemical catalysts for this process suffer from various disadvantages including difficulty of their recovery, cost, stability at moderate temperatures, and are highly reactive leading to a wide range of side-products.<sup>1,3</sup> Out of the three different broad approaches available for catalysis namely, homogeneous, heterogeneous, and bio-catalysis, the homogeneous soluble metal complexes have been



reported to be the more useful catalysts for CH bond activation. However, a general problem with organometallic complexes is low selectivity from different competing CH bonds in the same molecule as well as low reactivity. Also a major drawback of homogeneous catalysis is the difficulty in separating the relatively expensive catalysts from the reaction mixture at the end of the process.<sup>4</sup> Although in the past decades, there have been intense interests in C-H activation reactions, which are usually part of the catalytic cycle in functionalization of hydrocarbons to more useful products, there are however, very few examples of catalyst systems, that are capable of achieving this process and there are large gaps in our fundamental knowledge in how to design such catalysts.

### 1.2.1.1 Fenton chemistry

Initial success in alkane oxidation *via* transition metal catalysis was achieved as early as 1898 by Fenton<sup>5</sup> who reported the hydroxylation of alkanes catalysed by Fe(II) salts with the oxidant H<sub>2</sub>O<sub>2</sub>. However, the catalyst proved to have very low selectivity for the required alcohol product. Fenton chemistry which was latter known also as Haber-Weiss chemistry<sup>5</sup> was believed to release HO· radicals by Fe-catalysed decomposition of H<sub>2</sub>O<sub>2</sub>, via multiple steps (Scheme 1.2, Eqn. (2)–(4));



**Scheme 1.2:** Fenton (Fe-catalysed) oxidation of alkanes.<sup>5</sup>

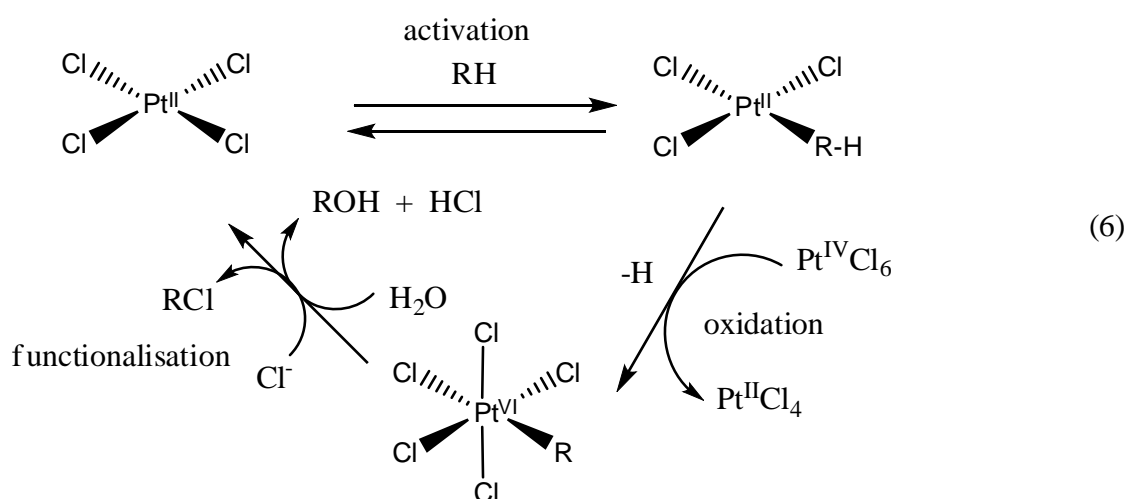
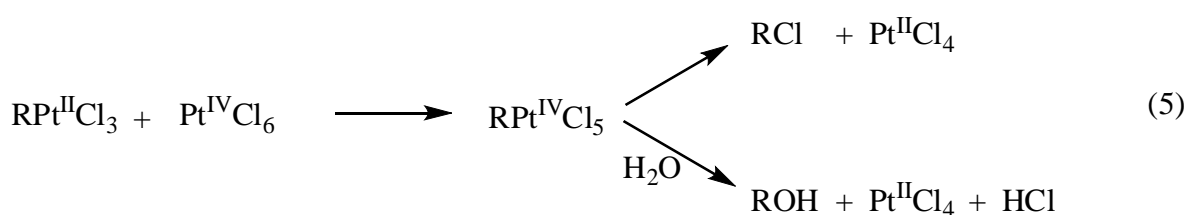
The ROO· radical produced is more reactive than the substrate itself and over-oxidise to give observed products, including ketones and carboxylic acids. However, the selectivity of the target product is then compatible (tert.CH > sec.CH) with radical intermediates, which also further decreases the selectivity.<sup>5, 6</sup>

### 1.2.1.2 Shilov system

The classic Shilov system, discovered in 1969 by Shilov, is perhaps the most important of all alkane oxidation catalysis after “Fenton Chemistry”. Shilov and co-workers<sup>7, 8</sup>, proposed the

pathway involved in the formation of direct metal-carbon bonds, hence the assignment to the organometallic class. The system proved a number of notable features<sup>7</sup>; firstly, the selectivity tend to favour exchange at terminal CH<sub>3</sub> groups rather than the preferential attack at tertiary or benzylic CH bonds, as seen for electrophiles and radicals in “Fenton Chemistry”. This implied a new mechanism (Scheme 1.3) was involved and gave hope for potential practical application, although rates were low. Secondly, multiple exchanges were seen at the earlier stages of the reaction, even for CH<sub>4</sub>.<sup>7-10</sup>

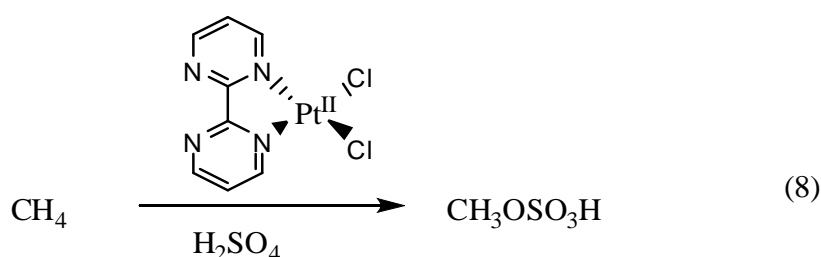
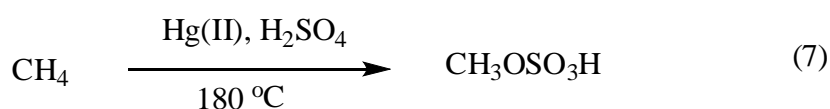
The overall stoichiometries and mechanism proposed by Shilov are as follows:<sup>7-9</sup>



**Scheme 1.3:** Overall stoichiometries and mechanism proposed by Shilov *et al.*<sup>7-9</sup>

The problem with the Shilov system from a practical point of view is that Pt(II) is not an economically viable stoichiometric oxidant which makes it more expensive and it gives large quantities of functionalised product (RX) instead of oxidised alkanes (ROH). Related systems using less expensive alternative stoichiometric oxidants have been revealed. Periana and co-workers<sup>11</sup> first employed mercury (Hg) (as catalyst and then later bipyrimidine complex of Pt(II)); both used sulphuric acid as solvent. The main advantage of their approach was that the

final product  $\text{CH}_3\text{SO}_3\text{H}$ , which was proved to be highly oxidation-resistant as a result of the electron withdrawing character of the sulfonate group. In the mercury case, the reactive ‘soft’  $\text{Hg}(\text{II})$  ion has its highest accessible oxidation state, so it can coexist with oxidants.



**Scheme 1.4:** Periana's catalyst for oxidation of alkanes:  $\text{Hg}$  (7) and bipyrimidine $\text{Pt}(\text{II})$  complex (8).

The limitation in this case is that unlike  $\text{Pt}(\text{II})$ ,  $\text{Hg}(\text{II})$  cannot be readily modified by altering the ligand set in the hope of increasing the rate. Although the Periana system was thought to be remarkably efficient, it was not economically competitive compared with existing heterogeneous industrial processes. The mechanism is similar or very closely related to that of the Shilov system.

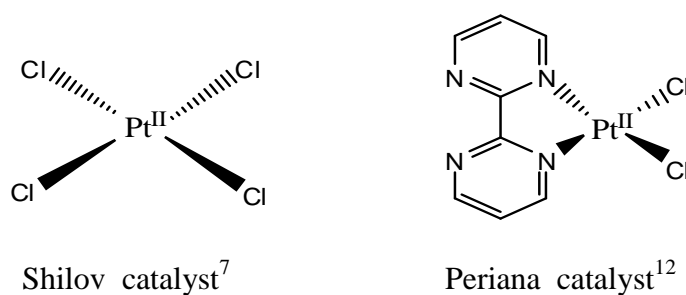
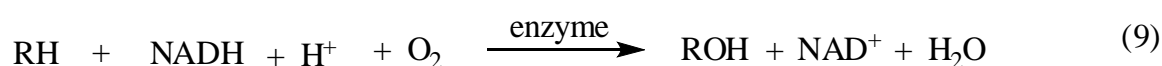


**Figure 1.1:** The Shilov and Periana systems.

### 1.2.2 Biological catalyst: enzymes

A variety of enzymes have been reported as efficient and selective catalysts for *n*-alkane oxidation reactions under physiological conditions.<sup>13</sup> The best examples of selective alkane oxidation to corresponding alcohols are found in nature. There are enzymes that can utilise dioxygen to oxidize saturated hydrocarbons to alcohols at ambient pressures and temperatures. Monooxygenases are among the class of enzymes involved in alkane oxidation found in nature. These enzymes are responsible for catalysing the incorporation of a single atom from molecular oxygen into an organic substrate. Monooxygenases utilise molecular oxygen (O<sub>2</sub>) to oxidize organic substrates by transfer of electrons. The use of molecular oxygen as an oxidant implies that two equivalent (NADH + H<sup>+</sup>) of reducing power must be supplied to the system (see Scheme 1.5). In nature, this reducing power comes from NADH (or NADPH), also commonly known as cofactors in cellular biology.



**Scheme 1.5:** Enzyme catalysed oxidation of alkanes.

Based on eqn. 9, if these biologic catalysts (enzymes) were to be used for alkane activation, then either NADH has to be used in stoichiometric quantities or it must be recycled (regenerated) to retain its reducing power during the catalytic cycle. The stoichiometric requirement for this primary reactant along with the O<sub>2</sub> severely affects the economics of alkane oxidation by this pathway.<sup>2</sup> In practice, these approaches seem to be applicable only to small-scale conversions, and not for large scale bioprocesses for *n*-alkane transformations.

### 1.2.3 Biomimetic catalyst

The idea of biomimetic catalysis refers to the application of synthetic strategy mimics of enzymes with respect to structure and catalytic activity. Recent research on *n*-alkane transformations by biocatalysts has been focused on understanding reaction mechanisms, so as to guide the design of synthetic catalysts mimicking their function, efficiency, and selectivity.<sup>1</sup> Biomimetic catalysis is becoming increasingly admired as enzymes continue to inspire new methods that result in the development of synthetic catalysts. A variety of

enzymes have been used as efficient and selective catalysts for *n*-alkane oxidation reactions under physiological conditions, while the well-known synthetic catalyst systems generally operate under harsh conditions in order to produce conversions and selectivities that satisfy industrial scale applications.<sup>13</sup>

In both biomimetic and enzyme systems that use O<sub>2</sub> as an oxidant along with NADH as reductant, the stoichiometric requirement severely affect the economics of alkane oxidation by these pathways. To avoid the need for an external reductant (NADH) it is necessary to avoid the use of 4-electron oxidants such as O<sub>2</sub> by replacement with 2-electron oxidants such as peroxides. The economic consequences are not so severe in the peroxide case because peroxides, particularly H<sub>2</sub>O<sub>2</sub>, are safe, readily available and cheap reagents. Moreover, using H<sub>2</sub>O<sub>2</sub> as an oxidant means that water is the only by-product which makes it an extremely advantageous source of oxygen.

### 1.2.3.1 Peroxidase models as catalysts for oxidations with hydrogen peroxide

Varieties of metal complexes have been reported to mimic the cytochrome P450 oxidation reactions using hydrogen peroxide as a primary oxidant. Most of the catalysts reported a catalytically active metal centre coordinated to four pyrrole nitrogen and oxygen atoms of heme-ligands and axial supporting ligands.<sup>14</sup> Most of the nitrogen containing ligands such as imidazoles, pyridine and other derivatives have been proven to be beneficial as supporting ligands in metal catalysed oxidations.<sup>15</sup>

One of the most promising heme-model was chiral manganese(III)-salen complex, proposed by Albrecht.<sup>16</sup>

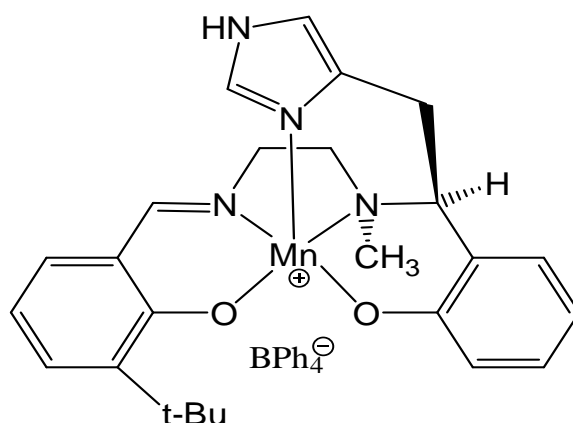


**Figure 1.2:** Schematic structure of a chiral manganese(III)-salen complex.<sup>16</sup>

The structure of the proposed Albrecht catalyst (Figure 1.2) shows an axial-imidazole donor group covalently bonded to a salen type complex. The X-ray crystal structure proved that their ligand design actually afforded the desired pentacoordinated Mn-complexes. The axial coordinated group (imidazole) is expected to bind and activate hydrogen peroxide molecule-just as in heme-peroxidases.<sup>16</sup>

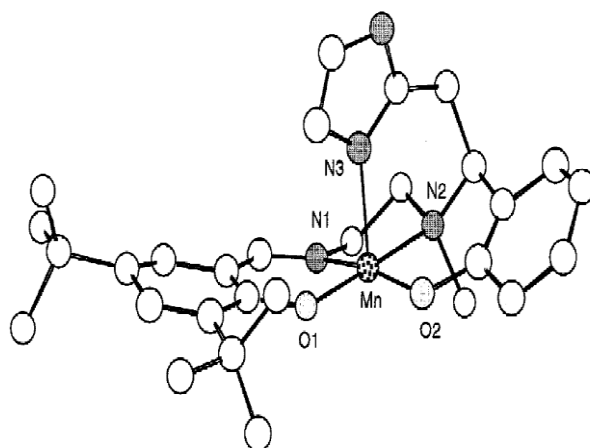


**Figure 1.3:** X-ray crystal structure of the Albrecht manganese(III)-salen complex.<sup>16</sup>

The reported rates are remarkable with  $k_{\text{cat}}$  at  $1.07 \times 10^3 \text{ s}^{-1}$  and  $k_{\text{cat}}/K_{\text{M}}$   $3.4 \times 10^4 \text{ M}^{-1} \text{ s}^{-1}$ , making this complex the most efficient catalase mimic developed to date. However, a mechanism by which the reaction takes place was not demonstrated and has not yet been fully investigated.

### 1.3 Triazole ligands

1,2,3-triazoles belong to a family of five-membered compounds called azoles. They contain two adjacent carbon and three nitrogen atoms (Figure 4). They are very stable compounds compared to other compounds with three adjacent nitrogen atoms.

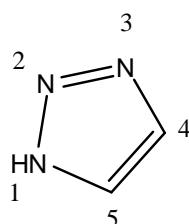


**Figure 1.4:** General structure of 1,2,3-triazole.

Recently, triazoles in general, but more specifically 1,2,3-triazole compounds have received great attention due to their broad application in industrial and medicinal chemistry. Although the structural moiety of triazole compounds does not occur in nature, these compounds have shown some biological activities and numerous examples as anti-HIV and antibiotic agents due to their antimicrobial activity against gram positive bacteria have been demonstrated.<sup>17</sup> It is believed that these compounds structurally mimic some of the amino acids in biological systems. The 1,4-disubstituted-1,2,3-triazoles have attracted increasing attention as mimics of the amide bond moiety of peptides (Figure 1.5). Due to these properties, 1,4-disubstituted-1,2,3-triazole oligomers have been suggested to mimic the structure of  $\beta$ -strands of peptides (Figure 1.6).<sup>18</sup>

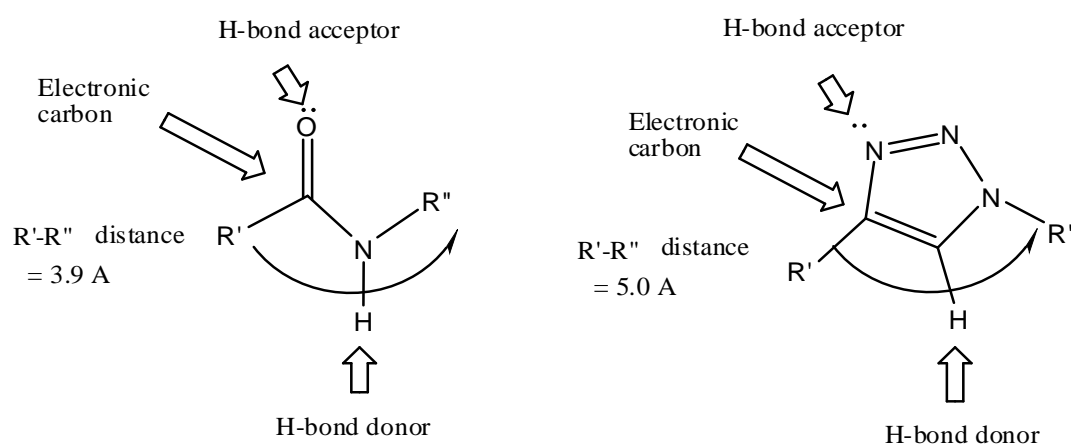


**Figure 1.5:** Triazole ring mimics the amide bond with potential hydrogen bond capabilities.

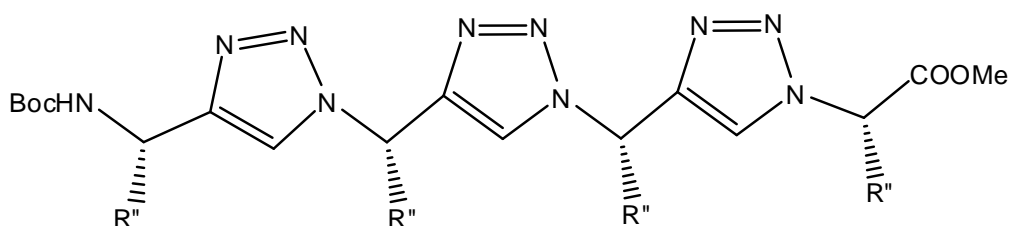


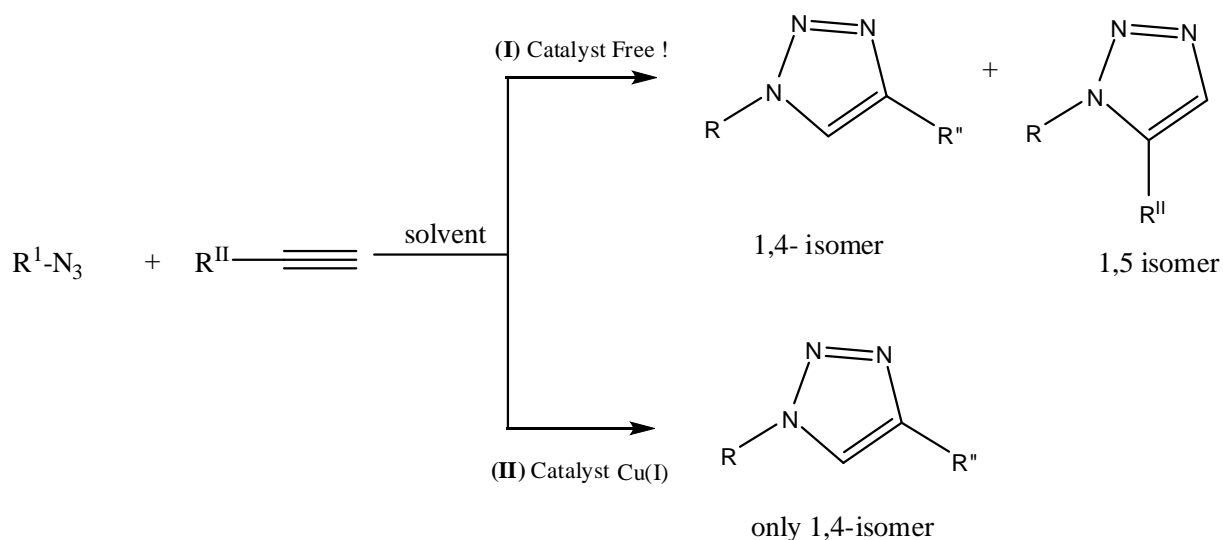
**Figure 1.6:** Peptidomimetic structures.<sup>18</sup>

In chemistry, these compounds have created much attention because they are used as supporting ligands due to the existence of reasonably basic nitrogen atoms in the 1,2,3-triazole rings which act as donor atoms in coordination chemistry.<sup>19</sup>

More recently, Huynh and co-workers<sup>20</sup> and Albrecht and co-workers<sup>21</sup> have shown that 1,2,3-triazolium salts can serve as precursors to *N*-heterocyclic carbenes (NHC) used in the synthesis of metal complexes, thus greatly expanding the family of carbene ligands. The success of 1,2,3-triazolium salts in organometallic chemistry as ancillary ligands has been attributed to four key properties: i) the relatively high covalent contribution to M–NHC bond therefore lessening ligand dissociation; ii) their strong donor ability enabling favourable rates of metal catalysed oxidation addition; iii) the presence of sterically encumbering groups bound to the N-atoms facilitate reductive elimination of the product from the metal and iv) the activity of NHC ligands can be remotely modified by introduction of electronic directing substituents.<sup>22, 23</sup>

### 1.3.1 Synthesis of 1,4-disubstituted-1,2,3-triazoles

Due to increasing number of 1,4-disubstituted-1,2,3-triazole applications, numerous synthetic methods for their preparation have been developed. Among the pioneers is the Huisgen 1,3-dipolar cycloaddition between an alkyne and an azide in the middle of the 20th century.<sup>24, 25</sup> The non-catalysed Huisgen reaction suffers from many draw-backs that include poor regioselectivity and the high temperature and pressure condition required for operation.<sup>24, 26</sup> Following Huisgen, recently Meldal and co-workers have reported that the use of catalytic amounts of copper(I) led to fast, highly efficient and regioselective azide–alkyne cycloaddition at room temperature in an organic medium.<sup>27</sup>

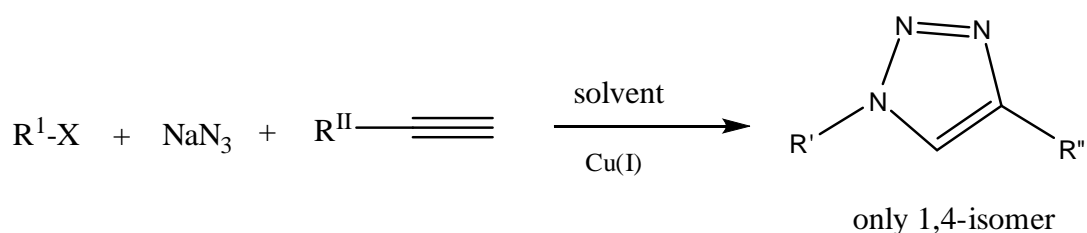


**Scheme 1.6:** (I) Huisgen's cycloaddition route and (II) its copper (I) catalysed version.



Due to numerous advantages of the copper (I) catalysed version over Huisgen's cycloaddition route, copper-catalysed azide-alkyne cycloaddition (CuAAC) has become the reaction-of-choice for the preparation of 1,4-disubstituted-1,2,3-triazole derivatives in many areas of synthetic chemistry. Even though Sharpless and Meldal improved the regioselectivity and reaction conditions, massive research has been focusing on ways to maximise the general efficiency of the process and to look at "greener" alternatives. This has led to the development of the so-called "click" reactions which involves multistep processes within a single pot reaction. This is inspired by the need to avoid the isolation of organic azides which are characterised by highly explosive and toxic nature.<sup>22, 28</sup>

The focus is now on the development of *in situ* generation of organic azides from organic halides and sodium azide in the presence of alkynes in a one-pot synthetic strategy. However, like Huygens's cycloaddition route, this method gave mixtures of regioisomers and very low yields of the target product.<sup>29</sup>

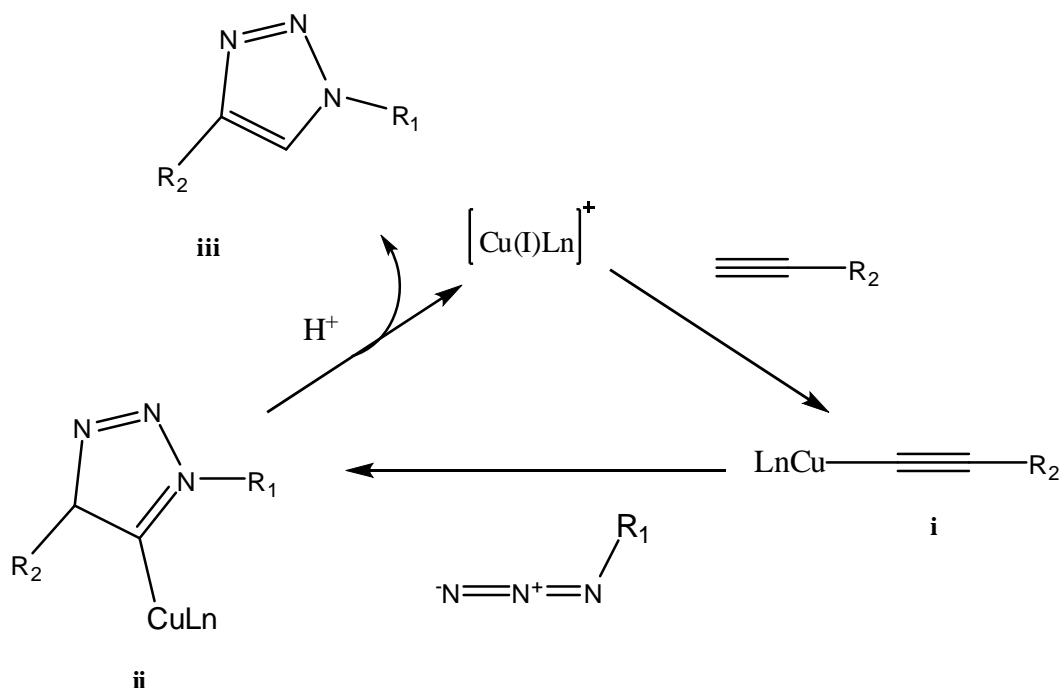


**Scheme 1.7:** Cu(I)-catalysed one-pot synthesis of 1,4-disubstituted-1,2,3-triazoles.<sup>30</sup>

In 2002, Rostovtsev and Fokin showed (Scheme 1.7) a very efficient, fast and regioselective Cu(I)-catalysed one-pot synthesis of 1,4-disubstituted-1,2,3-triazoles from alkyl halides, alkynes and sodium azide. A variety of copper catalysts can be used provided that some species of Cu(I) are generated. The copper catalysts reported include Cu(I) halide salts (CuI, CuBr, and CuCl) with a base to prevent oxidation to Cu(II) or reduction to Cu(0) compounds, or a pre-catalyst in the form of Cu(II) salts usually CuSO<sub>4</sub><sup>22</sup> together with a reducing agent usually sodium ascorbate.<sup>31</sup> One of the great advantages of using CuAAC reaction is that a variety of solvent systems can be used including non-coordinating solvents such as hexane and dichloromethane and even polar ones such as DMF, DMSO and alcohols give good yields. The conditions and variety of solvent systems applicable to CuAAC are listed in the reviews by Meldal and Tornøe.<sup>27, 31</sup>

### 1.3.1.1 CuAAC mechanism

The CuAAC mechanism has been extensively studied by different research groups.<sup>32-34</sup> The general mechanism proposed for this reaction involves formation of the copper(I)-acetylide complex (**i**), which then further reacts with an organic azide and rearrangements result in formation of the product (**III**).<sup>33</sup>



**Scheme 1.8:** Mechanism of 1,3-dipolar reaction catalysed with Cu(I) salt.

## 1.4 NHC ligands

The 1,2,3-triazol-5-ylidenes (**III**, Figure 1.7) carbene belong to a family of ligands referred to as N-Heterocyclic carbenes (NHCs). These ligands have become very predominant in organometallic chemistry due to their efficiency in improving the catalyst activity.<sup>35</sup> Their superiority over classic  $2e^-$  ligands such as amines, ethers, phosphines and Schiff base ligands is due to the formation of a stable covalent metal-ligand bond ( $M-C_{\text{carbene}}$ ) and their strong  $\sigma$ -donor ability.<sup>36, 37</sup> Herrmann, *et al.*<sup>38</sup> reported one of the NHC-metal complexes that are relevant to catalysis today. In the family of NHC ligands, the imidazolin-2-ylidene based metal complexes (**A**, **B**, **C**, Figure 1.7) have been widely studied and reported.

The main focus of this dissertation lies on the synthesis and use of nickel complexes of N-heterocyclic carbenes in catalytic oxidation of alkanes.

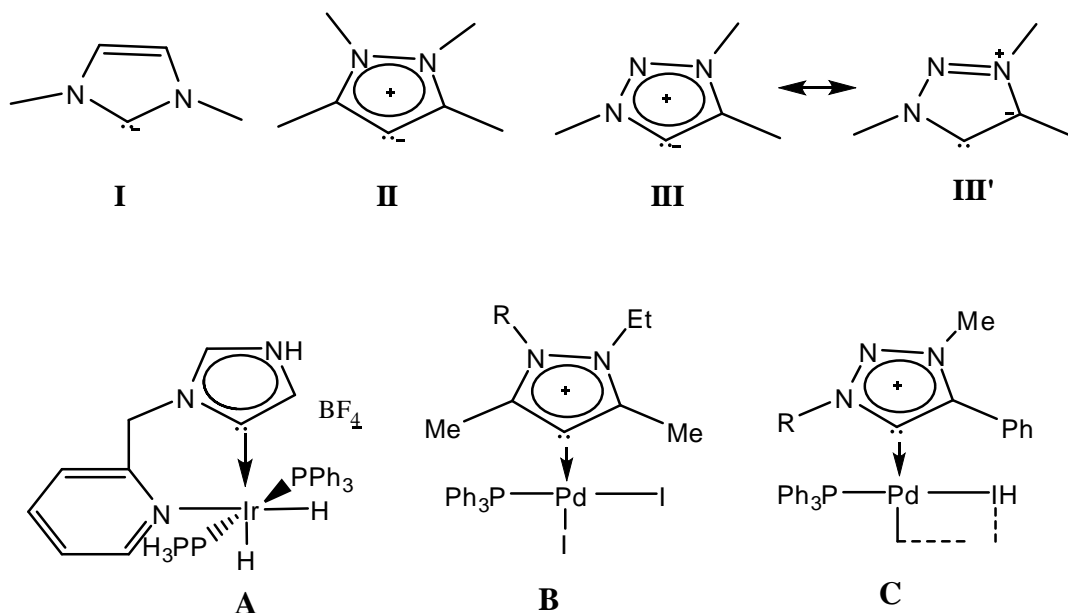


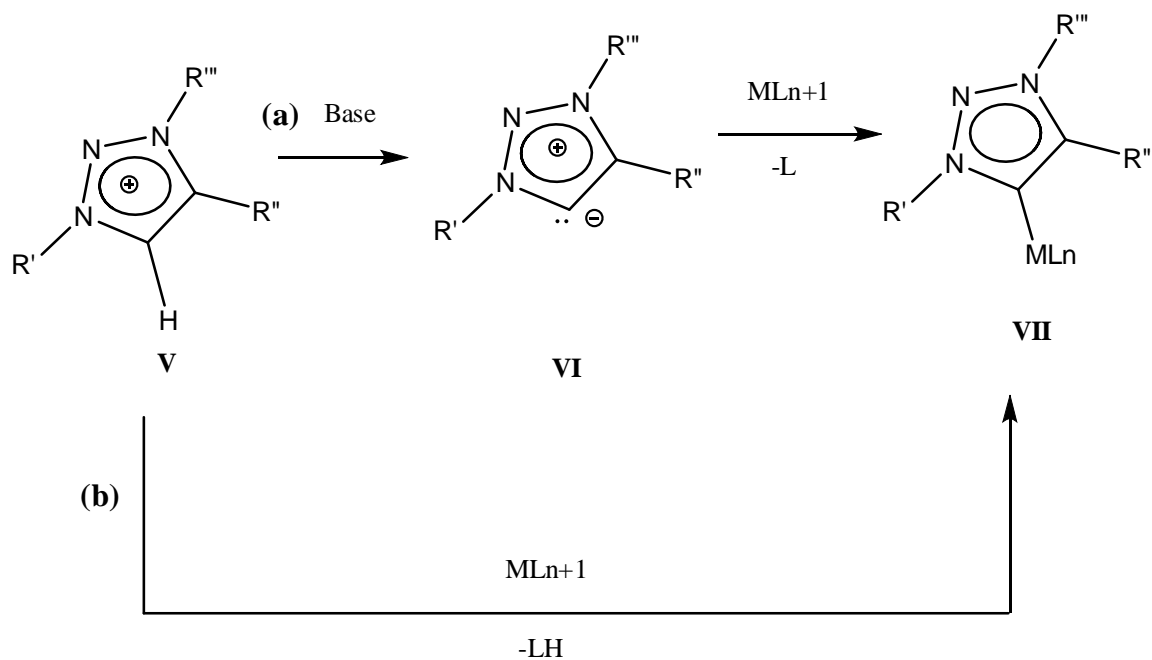
**Figure 1.7:** Classical NHCs **I** and **II**, their mesoionic carbene isomers **III–III'**, and the first complexes featuring the latter.<sup>39</sup>

#### 1.4.1 Synthesis of NHC-metal complexes

Due to the growing number of application of metal-NHC complexes, a variety of methods have been reported for their synthesis. However the most widely used synthetic methods are based on three pathways;

##### I. Synthesis of free carbene

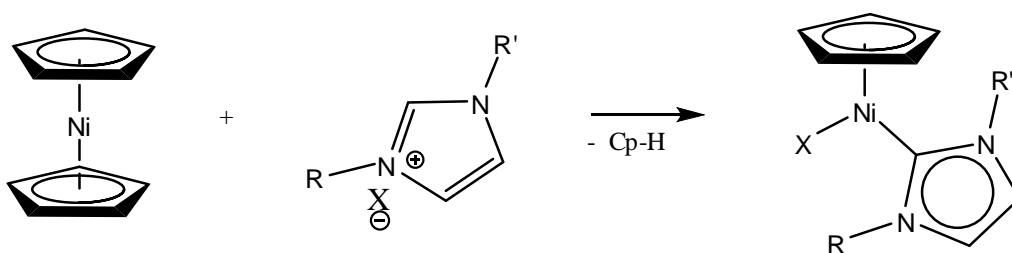
The common route for synthesis of NHC-metal complexes, is the generation of free carbene (**VI**, Scheme 10), obtained by deprotonation of the corresponding azolium salts with a strong base ((**a**), Scheme 1.9) in suitable solvent under inert conditions. The free carbene obtained can then be reacted with metal precursor to obtain the corresponding metal-NHC complex (**VII**, Scheme 1.9).<sup>38</sup> However due to some difficulties (which includes decomposition) of isolated free carbene, an alternative methods have been generated which involves *in situ* (**b**, Scheme 1.9) generation of free carbene, by reacting azolium salts with a basic ligand of a suitable metal precursor generating the carbene followed by binding of the metal to the free carbene *in situ* forming the NHC-metal complex.



**Scheme 1.9:** Synthesis of NHC-Metal complex by (a) free carbene generation route and (b) *in situ* carbene-metal complex route.

Abernethy and co-workers<sup>40</sup> first reported the *in situ* synthesis of diamagnetic complex  $[\text{Ni}(\eta^5\text{-C}_5\text{H}_5)(\text{Cl})(\text{IMes})]$  by reaction of nickelocene with 1,3-dimesitylimidazolium chloride in refluxing THF in high yield. Following this, a number of NHC complexes  $[\text{Ni}(\eta^5\text{-C}_5\text{H}_4\text{R})(\text{X})(\text{NHC})]$  (R = H or alkyl; X = Cl, Br, or I) have been reported in similar fashion.<sup>41-</sup>

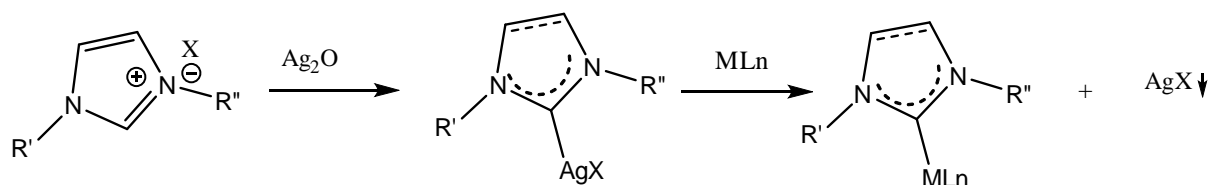
43



**Scheme 1.10:** Synthesis of  $[\text{Ni}(\eta^5\text{-C}_5\text{H}_5)(\text{X})(\text{NHC})]$

## II. Transmetalation

Alternatively, another recently widely used route is transmetalation, which involves the transfer of ligands from one metal to another. During this process the metal-carbon bond is activated, leading to the formation of new metal-carbon bonds. After the first report of NHC-silver complex by Arduengo and co-workers.<sup>44</sup>, first silver carbene transfer using imidazolium salt and Ag<sub>2</sub>O was reported by Wang and Lin.<sup>45</sup> These applications have received much attention due to different advantages which includes avoiding harsh experimental conditions and works efficiently. Due to this NHC-metal complexes of Au<sup>46,47</sup>, Cu<sup>48</sup>, Ni<sup>49</sup>, Pd<sup>50</sup>, Pt<sup>51,52</sup> and Ru<sup>53</sup> have been prepared using this method.



**Scheme 1.11:** Example of NHC-ML<sub>n</sub> complex formed via transmetalation technique.<sup>45</sup>

### 1.5 Ionic liquids

By general definition, ionic liquids (ILs) are organic salts mainly composed of organic cations and inorganic anions, which are liquid below 100 °C and exhibit in most cases relatively low viscosities.<sup>54</sup> These compounds have many applications, which include use as solvents in organic synthesis, as electrical conducting fluids, in commercial pharmaceutical industry, in electrode-electrolyte interfaces for ultra-high vacuum systems, in heat transfer and storage media for solar thermal energy systems, etc.

The main advantages of ionic liquids over ordinary volatile organic solvents include:

- ✓ non-flammability, which make them safer to use as solvents,
- ✓ very low vapour pressures, allows for high temperature reactions without the requirement of a pressure vessel to contain the vapours,
- ✓ they can be recycled, which makes them potential green solvents,
- ✓ highly thermally stable, large working temperature range (-40 to +200 °C),

- ✓ additionally, they can be easily used in biphasic separations due to their immiscibility with a range of solvents.

They are referred to as “green solvents” mainly due to the fact that they are non-volatile used at normal conditions and they can be recycled after the reaction by simple extraction with organic solvents or by distillation of product.<sup>55, 56</sup> Due to these properties, ionic liquids have opened a wide field for investigations. The imidazolium salts (Figure 1.8) have been extensively studied as ionic liquids and a number of them are now commercially available.<sup>57,</sup>

58

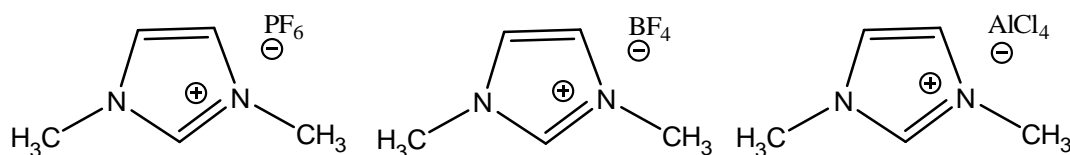
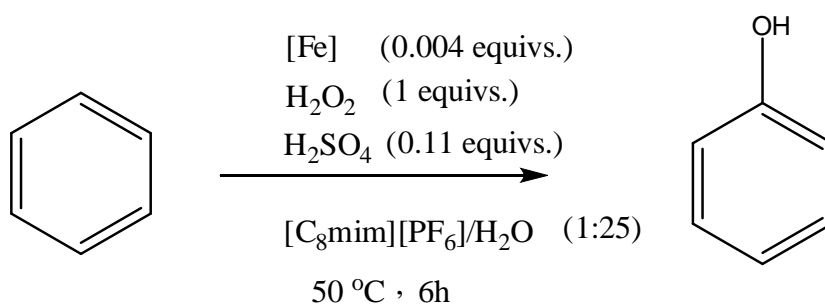


**Figure 1.8:** General structures of common ionic liquids derived from imidazolium salts.

### 1.5.1 Application of ionic liquids in oxidations of organic compounds

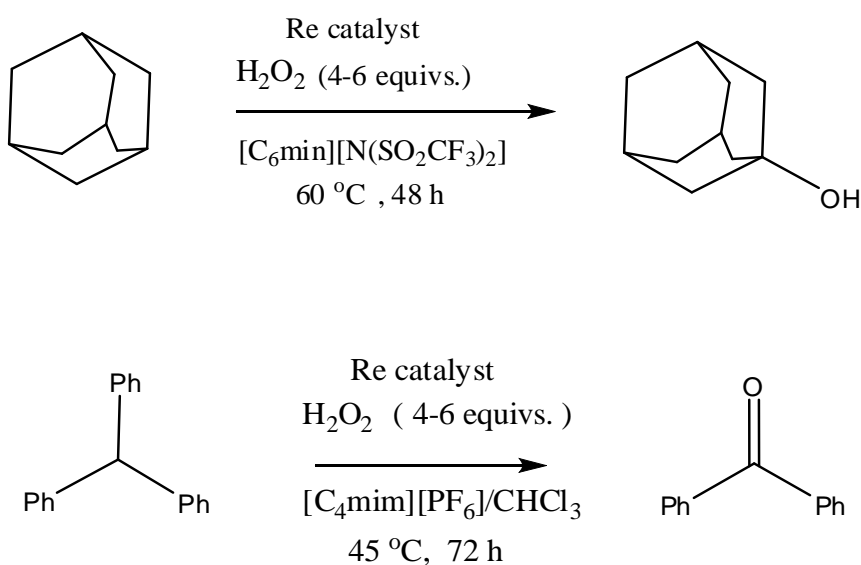
Ionic liquids have gained much attention in the last decades due to large the number of their applications. Growing interest has led to increased number of publications describing their applications.<sup>59-63</sup> The applications of ILs in homogeneous catalysis is more than just as alternative “green” solvents, but also as enhancers of catalytic performance and aids for catalyst separation and recycling.<sup>64</sup> The application of ILs in oxidation reactions has also been reported, mainly by the adaptation of traditional organic solvents. For example, Peng and co-workers<sup>65</sup> have reported the selective aqueous-IL biphasic hydroxylation of benzene to phenol with H<sub>2</sub>O<sub>2</sub> and metal dodecanesulfonate salts of Co(II), Fe(II), Fe(III), Cu(II) and Ni(II) in aqueous-[C<sub>n</sub>mim][X](n=4,8,10; X=PF<sub>6</sub>, BF<sub>4</sub>).



**Scheme 1.12:** Illustration of the aqueous-IL biphasic system for benzene hydroxylation to phenol with  $\text{H}_2\text{O}_2$ .

In Peng's aqueous-IL biphasic system, both the catalyst and benzene were dissolved in the IL, whereas,  $\text{H}_2\text{O}_2$  was mainly dissolved in the aqueous phase (Scheme 1.12). The produced phenol was contained in the aqueous phase helping to minimise its contact with the catalyst and over-oxidation to the acid. Following that, Xiao-ke, *et al.*<sup>66</sup> has also reported the application of triethylammonium acetate ( $[\text{Et}_3\text{NH}][\text{CH}_3\text{COO}]$ ) as a medium for the hydroxylation of benzene to phenol where benzene was both the substrate and the solvent for the product. The system protected the phenol from contact with the catalyst and oxidant which reduced its over-oxidation.

The Re-catalysed selective oxidation of the tertiary C-H bond of *cis*-1,2-dimethylcyclohexane and adamantane with  $\text{H}_2\text{O}_2$  in biphasic solvents  $\text{CHCl}_3/[\text{C}_4\text{mim}][\text{PF}_6]$  and  $\text{CHCl}_3/[\text{C}_6\text{mim}][\text{N}(\text{SO}_2\text{CF}_3)_2]$  and the oxidation of triphenylmethane with  $\text{H}_2\text{O}_2$  in  $\text{CHCl}_3/[\text{C}_4\text{mim}][\text{PF}_6]$  to afford benzophenone were reported by Bianchini, *et al.*<sup>67</sup> (Scheme 1.13)

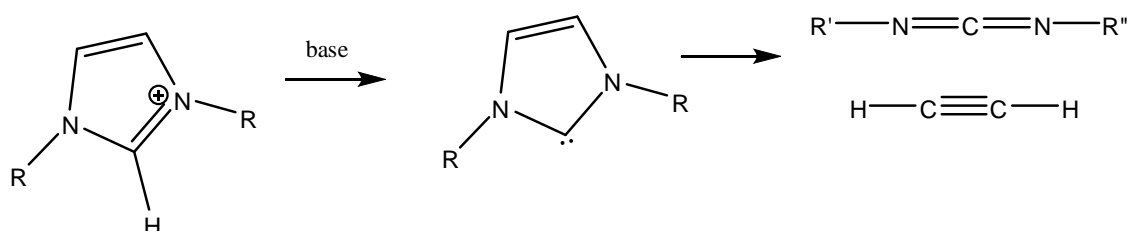


**Scheme 1.13:** Oxidation of alkanes in ionic liquids in the presence of Re catalyst and  $\text{H}_2\text{O}_2$ .

According to Bianchini, heterogeneous analogues of the Re catalyst resulted in lower conversions and selectivity compared to the IL dissolved catalysts. The application of methylrhenium trioxide (MTO) as a catalyst for the epoxidation of alkenes has gained some attention.<sup>61</sup> However, poor solubility of H<sub>2</sub>O<sub>2</sub> in organic solvents has led to low yields and selectivity. The application of ILs as solvents, have however resulted in excellent yields and selectivity of epoxides. In addition, the products can be easily extracted and the catalyst recycled.<sup>60</sup>

### 1.5.1.1 Application of triazoles as ionic liquids

Imidazolium-based salts present the most prominent subclass of *N*-heterocyclic cations; however the limitation of using imidazolium salts is their decomposition under strongly basic conditions due to deprotonation of the C-2 proton leading to formation of free carbenes which are not stable under normal conditions. Although, the two *N*-atoms around the free carbene (C-2 carbon) of the imidazolium ion help in its stabilisation, it is still highly susceptible to decomposition under a basic environment due to increased acidity of the C-H bond (Scheme 1.14).



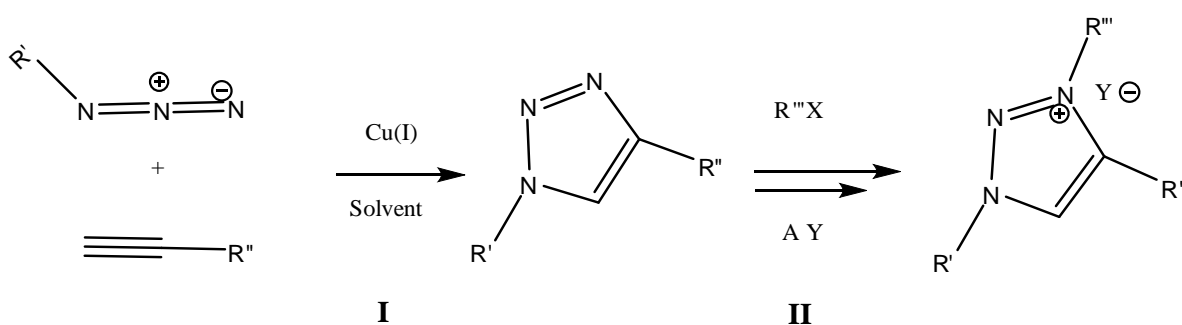
**Scheme 1.14:** Decomposition of imidazolium salt in a basic environment.

Acidity of the C-H bond of 1,2,3-triazolium salts is much lower than that of corresponding imidazolium counterparts hence more stable with many advantages as solvents.<sup>68</sup> 1,2,3-triazolium salts were neglected as potential ionic liquids until recently, even though reports on them have appeared as early as 1887.<sup>69</sup>



### 1.5.1.2 Synthesis of 1,2,3-triazolium ionic liquids

The synthesis of 1,2,3-triazolium salts consists of two major steps (Scheme 1.15): building the 1,2,3-triazole ring system (I) and its *N*-alkylation (II).<sup>68</sup>



**Scheme 1.15:** Synthesis of 1,3,4-trisubstituted 1,2,3-triazolium ionic liquids.

The anion-exchange may be conducted via a Lewis acid-base reaction or via anion metathesis.<sup>54</sup> From the literature, when 1,4-disubstituted-1,2,3-triazoles are alkylated by soft substituting reagents such as alkyl-, benzyl- and allyl-halides, sulphates or sulphonates, only 1,3,4-trisubstituted-1,2,3-triazolium salt products were obtained in high regioselectivity i.e. the 1,4,5-trisubstituted isomer was not formed.<sup>70</sup> According to Yacob and Liebscher<sup>68</sup>, the *N*-substitution reactions are done in excess quantities of the reagents which also serve as solvents. After the reaction, excess reagents are removed by simple evaporation under reduced pressure. Facile anion exchange with another counter-anion via salt metathesis may be performed to impart desired properties such as miscibility with required media.

### 1.5.1.3 Properties of 1,3,4-trisubstituted-1,2,3-triazolium ionic liquids

Chemically, 1,2,3-triazolium salts are relatively stable, however, their thermal stability depends on the type of counter-ions, e.g. with iodide and TfO<sup>-</sup> as counter-ions, the salts decompose above 100 °C, while bulky anions such hexafluorophosphate and tetrafluoroborate are known to be stable even at much higher temperatures.<sup>71</sup> Reported literature data shows that thermal stability also depends on the substituents on the triazolium ring (R', R'' and R''', Scheme 1.15).

## 1.6 Aims of this dissertation

The field of alkane activation still remains a challenge to chemists, biochemist and engineers because of the relatively inert nature of the C-H bonds. Successful conversion of these compounds into valuable products such as alcohols, carboxylic acids and alkenes under mild and controlled catalytic conditions can offer large economic benefits. A variety of enzymes have been used as efficient and selective catalysts for *n*-alkane oxidation reactions under physiological conditions. However, these approaches seem to be applicable only to small scale applications, and not for large scale transformations. Hence, inspired from metal based enzymes such as the monooxygenases which are highly active catalysts for many transformations at physiological temperatures and pressures, one of the aims of this work is to mimic the biologically active catalysts with respect to structure and catalytic activity by employing Fe, Co and Ni metal centres with triazolylidene ligands for paraffin activation in the presence of H<sub>2</sub>O<sub>2</sub> as the oxidant.

Well established synthetic catalyst systems for paraffin activation generally operate under harsh conditions in order to produce conversions and selectivity that are satisfactory to industrial scale applications. The crucial challenges and key lingering questions still pertinent to biomimetic oxidation catalysis are: (i) how to develop a truly biomimetic catalyst, (ii) gain thorough understanding of the mechanism of operation of the developed catalyst and (iii) develop a set of mild conditions that allow the catalyst to perform at its optimum operational efficiency which should be as close to that of the natural oxygenases it is attempting to mimic as possible.

In this work, we have applied the [2+3] cycloaddition of acetylene with azides (“click” chemistry) as a versatile and flexible method for the synthesis of several 1,4-disubstituted-1,2,3-triazole compounds. This reaction has recently received considerable attention due to its regiospecificity, quantitative yields and the capacity to tolerate a wide variety of functional groups. The prepared 1,4-disubstituted-1,2,3-triazoles are then *N*-alkylated using reported methods to afford 1,3,4-trisubstituted-1,2,3-triazolium salts. Finally, the synthesised salts are then complexed to biologically active metal centres and used as catalysts for *n*-alkane activation. Some salts are also converted into ionic liquids (ILs) by anionic metathesis and used as ‘green solvents’ in a biphasic IL/water solvent system for octane activation with H<sub>2</sub>O<sub>2</sub> in the presence of iron chloride as the catalyst.

By introducing different substituents at positions 1, 3 and 4 of the triazole ring it is envisaged to remotely alter the electronic character of the metal centre or alternatively the *N*-substituents would allow the topography around the metal to alter, to ensure the required steric bulk for reductive elimination of products in a catalytic cycle.

## **1.7 Dissertation outline**

In the second chapter, the synthesis and characterisation of 1,4-disubstituted-1,2,3-triazole ligands is reported. Chapter 3 describes the synthesis, characterisation and application of 1,3,4-trisubstituted-1,2,3-triazolium salts as ionic liquids for octane activation in the presence of FeCl<sub>2</sub> as catalyst. Chapter 4 deals with the synthesis, characterisation and catalytic activity of metal complexes of ligands derived from the triazolium salts. In the final chapter, concluding remarks are presented.

## 1.8 References

1. A. Sivaramakrishna, P. Suman, E. V. Goud, S. Janardan, C. Sravani, C. S. Yadav and H. S. Clayton, *Res. Rev. Mat. Sci. Chem.*, 2012, **1**, 75–103.
2. R. H. Crabtree, *J. Chem. Soc., Dalton Trans.*, 2001, 2437–2450.
3. J. Z. M. Sun, Piotr Putaj, Valerie Caps, Frédéric Lefebvre, J. Pelletier, and J.M. Basset, *Chem. Rev.*, 2014, **114**, 981–1019.
4. C. Jia, T. Kitamura and Y. Fujiwara, *Acc. Chem. Res.*, 2001, **34**, 633–639.
5. F. Haber and H. Weiss, *Proc. R. Soc.*, 1934, **147**, 332–351.
6. W. G. Barb, J. H. Baxendale, P. George and K. R. Hargrave, *Trans. Faraday Soc.*, 1951, **47**, 591–616.
7. A. E. Shilov and G. B. Shul'pin, *Chem. Rev.*, 1997, **97**, 2879–2932.
8. A. E. Shilov, *Riedel, Dordrecht*, 1984, pp. 245–249.
9. N. F. Gol'dshleger, V. V. Eskova, A. E. Shilov and A. A. Shteinman, *Russ. J. Phys. Chem.*, 1972, **46**, 785–789.
10. A. E. Shilov and A. A. Shteinman, *Kinet. Katal.*, 1973, **14**, 117–120.
11. R. A. Periana, D. J. Taube, E. R. Evitt, D. G. Loffler, P. R. Wentreck, G. Voss and T. Masuda, *Science*, 1993, **259**, 340–345.
12. R. A. Periana, D. J. Taube, S. Gamble, H. Taube, T. Satoh and H. Fujii, *Science*, 1998, **280**, 560–565.
13. D. A. Kopp and S. J. Lippard, *Curr. Opin. Chem. Biol.*, 2002, **38**, 568–576.
14. B. Meunier, ed. B. Meunier, Imperial College Press, London 2000, vol. 171, pp. 91–169.
15. P. Battioni, J. P. Renaud, J. F. Bartoli, M. Reina-Artiles, M. Fort and D. Mansuy, *J. Am. Chem. Soc.*, 1988, **110**, 8462–8470.
16. M. Albrecht, P. Mathew, *J. Mol. Catal. A-Chem.*, 1997, **117**, 339–346.
17. P. Li and L. Wang, *Lett. Org. Chem.*, 2007, **4**, 23–26.
18. D. Margetic, D. N. Butler and R. N. Warrener, *Aust. J. Chem.*, 2000, **12**, 959–963.
19. H. Struthers, T. L. Mindt and R. Schibli, *Dalton Trans.*, 2010, **39**, 675–696.
20. Y. Han, H. V. Huynh and G. K. Tan, *Organometallics*, 2007, **26**, 6581–6585.
21. P. Mathew, A. Neels and M. Albrecht, *J Am Chem Soc.*, 2008, **130**, 13534–13535.
22. V. V. Rostovtsev, L. G. Green, V. V. Fokin and K. B. Sharpless *Angew. Chem. Int. Ed.*, 2002, **41**, 2596–2599.
23. W. A. Herman, *Angew. Chem. Int. Ed.*, 2002, **41**, 1290–1309.
24. R. Huisgen in *1,3-Dipolar Cycloaddition Chemistry* (Ed.: A. Padwa), Wiley, New York, 1984, pp. 1–176.
25. R. Huisgen, *Angew. Chem*, 1963, **2**, 633–645.
26. R. Huisgen, *Angew. Chem*, 1963, **2**, 565–598.
27. C. W. Tornøe, C. Christensen and M. Meldal, *J. Org. Chem.*, 2002, **67**, 3057–3064.
28. S. Bräse, C. Gil, K. Knepper and V. Zimmermann, *Angew Chem. Int. Ed.*, 2005, **44**, 5188–5240.
29. A. V. Maksikova, E. S. Serebryakova, L. G. Tikhonova and L. I. Vereshagin, *Chem. Heterocycl. Comp.*, 1980, **16**, 1284–1285.
30. V. V. Rostovtsev, L. G. Green, V. V. Fokin and K. B. Sharpless, *Angew. Chem.* 2002, **114**, 2708–2711.
31. L. Liang and D. Astruc, *Coord. Chem. Rev.*, 2011, **255**, 2933–2945.
32. V. O. Rodionov, V. I. Presolski, D. D. Diaz, V. V. Fokin and M. G. Finn, *J. Am. Chem. Soc.*, 2007, **129**, 12705–12712.
33. J. E. Hein and V. V. Fokin, *Chem. Soc. Rev.*, 2010, **39**, 1302–1315.

34. V. O. Rodionov, V. V. Fokin, M. G. Finn and *Angew. Chem., Int. Ed.*, 2005, **44** 2210–2215.
35. E. A. B. Kantchev, C. J. O. O'Brien and M. G. Organ, *Angew. Chem., Int. Ed.*, 2007, **46**, 2768–2813.
36. S. N. Sluijter and C. J. Elsevier, *Organometallics*, 2014, **33**, 6389–6397.
37. M. Paulson, N. Antonia and A. Martin, *J. Am. Chem. Soc.*, 2008, **41**, 13534–13535.
38. W. A. Herrmann, O. Runte and G. R. J. Artus, *J. Organomet. Chem.*, 1996, **2**, 1627–1636.
39. G. Guisado-Barrios, J. Bouffard, B. Donnadiou and G. Bertrand, *Angew. Chem. Int. Ed.*, 2010 **28**, 4759–4762.
40. C. D. Abernethy, A. H. Cowley and R. A. Jones, *J. Organomet. Chem.*, 2000, **596**, 3–5.
41. W. Buchowicz, A. Koziół, L. B. Jerzykiewicz, T. Lis, S. Pasynkiewicz, A. Pecherzewska and A. Pietrzykowski, *J. Mol. Catal. A: Chem.*, 2006, **257**, 118–123.
42. V. Ritleng, C. Barth, E. Brenner, S. Milosevic and M. J. Chetcuti, *Org. Lett.*, 2008, **27**, 4223–4228.
43. R. A. Kelly, N. M. Scott, S. Díez-González, E. D. Stevens and S. P. Nolan, *Org. Lett.*, 2005, **24**, 3442–3447.
44. A. J. Arduengo, H. V. R. Dias, J. C. Calabrese and F. Davidson, *Organometallics*, 1993, **12**, 3405–3409.
45. H. M. J. Wang and I. J. B. Lin, *Organometallics*, 1998, **17**, 972–975.
46. S. K. Schneider, W. A. Herrmann and E. Z. Herdtweck, *Anorg. Allg. Chem.*, 2003, **629**, 2363–2368.
47. V. J. Catalano, M. A. Malwitz and A. O. Etogo, *Inorg. Chem.*, 2004, **43**, 5714–5718.
48. C. Y. Legault, C. Kendall and A. B. Charette, *Chem. Commun.*, 2005 3826–3830.
49. X. Wang, S. Liu and G. X. Jin, *Organometallics* 2004, **23**, 6002–6004.
50. C. K. Lee, J. C. C. Chen, K. M. Lee, C. W. Liu and I. J. B. Lin, *Chem. Mater.*, 1999, **11**, 1237–1240.
51. M. Poyatos, A. Maise-Francois, S. Bellemin-Laponnaz and L. H. Gade, *Organometallics* 2006, **25**, 2634–2638.
52. E. M. Prokopchuk and R. J. Puddephatt, *Organometallics*, 2003, **22**, 563–568.
53. G. Xu and S. R. Gilbertson, *Org. Lett.*, 2005, **7**, 4605–4609.
54. P. Wasserscheid and W. Keim, *Angew. Chem. Int. Ed.*, 2000, **39**, 3772–3789.
55. E. A. Turner, C. C. Pye and R. D. Singer, *J. Phys. Chem. A.*, 2003, **107**, 2277–2288.
56. R. S. Varma and V. V. Namboodiri, *Chem. Commun.*, 2001, 643–644.
57. H. Zhao, J. E. Holladay, H. Brown and Z. C. Zhang, *Science* 2007, **316**, 1597–1601.
58. C. Jork, M. Seiler, Y. A. Beste and W. Arlt, *J. Chem. Eng. Data*, 2004, **49**, 852–858.
59. J. S. Wilkes, *J. Mol. Catal. A: Chem.*, 2004, **214**, 11–17.
60. T. W. Welton, *Chem. Rev.*, 1999, **99**, 2071–2083.
61. T. Welton, *Coord. Chem. Rev.*, 2004, **248**, 2459–2477.
62. J. Dupont, C. S. Consorti, J. Spencer and J. Braz, *Chem. Soc. Rev.*, 2000, **11**, 337–344.
63. P. Wasserscheid and W. Keim, *Angew. Chem. Int. Ed.*, 2000, **39**, 3772–3789.
64. J. Muzart, *Adv. Synth. Catal.*, 2006, **348**, 275–295.
65. J. Peng, F. Shi, Y. Gu and Y. Deng, *Green Chem.*, 2003, **5**, 224–226.
66. H. Xiao-ke, Z. Liang-fang, G. Bin, L. Qiu-yuan, L. Gui-ying and H. Chang-wei, *Chem. Res. Chin. Univ.* 2011, **27**, 503–507.
67. G. Bianchini, M. Crucianelli, F. d. Angelis, V. Neri and R. Saladino, *Tetrahedron Lett.*, 2005, **46**, 2427–2432.
68. Z. Yacob and J. Liebscher, in *Ionic Liquids as Advantageous Solvents for Preparation of Nanostructures*, ed. S. T. Handy, 2011 pp. 3–22.

69. T. Zincke and A. T. Lawson, *J. Org. Chem.*, 1995, **20**, 1167–1176.
70. R. Gompper, *Chem. Angew Chem. Int. Ed.*, 1987, **90**, 374–382.
71. Y. Jeong and J. S. Ryu, *J. Org. Chem.*, 2010, **75**, 4183–4191.

## Chapter 2

### Simple and highly efficient one-pot synthesis of 1,4-disubstituted-1*H*-1,2,3-triazoles

#### 2.1 Introduction

This chapter reports on the synthesis of 1,4-disubstituted-1,2,3-triazole derivatives via the utilisation of a “click” chemistry approach. This involved the use of a commercially available and inexpensive catalyst - copper(I) bromide (CuBr) for the cycloaddition of terminal alkynes to alkyl- or benzyl-halides promoted by sodium azide in DMF/H<sub>2</sub>O (4:1) at room temperature. It was achieved via an efficient, safe and green one-pot synthesis strategy with all the prepared compounds fully characterised by spectroscopic and analytical techniques.

In fact, any variety of copper catalysts can be used provided that some species of Cu(I) is generated. The copper catalysts that have been tested include Cu(I) halides ( CuI, CuBr, and CuCl) with a base to prevent generation of Cu(II) or Cu(0) compounds, or a pre-catalyst that may be a Cu(II) salt (usually CuSO<sub>4</sub>) together with a reducing agent (usually sodium ascorbate).<sup>5-7</sup> Numerous solvent systems have been reported to be very active for the “click” reaction, which include polar solvents such as DMSO, DMF, acetone and MeCN and less polar or non-coordinating solvents like toluene, chloroform and dichloromethane. A biphasic media involving mixtures of aqueous and organic solvents have been reported.<sup>7, 8</sup>

One-pot synthesis/reaction has been found to be an efficient and “greener” method since it cuts down unnecessary steps, which include isolation, handling and chromatography, hence better yields and atom efficiency. Even though some organic azides are safe at room temperature, those of low molecular weight can be unstable and difficult to handle. The *in situ* generation of organic azides followed by addition of alkynes in a “one-pot CuAAC”, helps reduce the amount of time consuming and waste generation steps and also aids in preventing difficulties associated with the generation and handling of explosive azides.<sup>9, 10</sup>

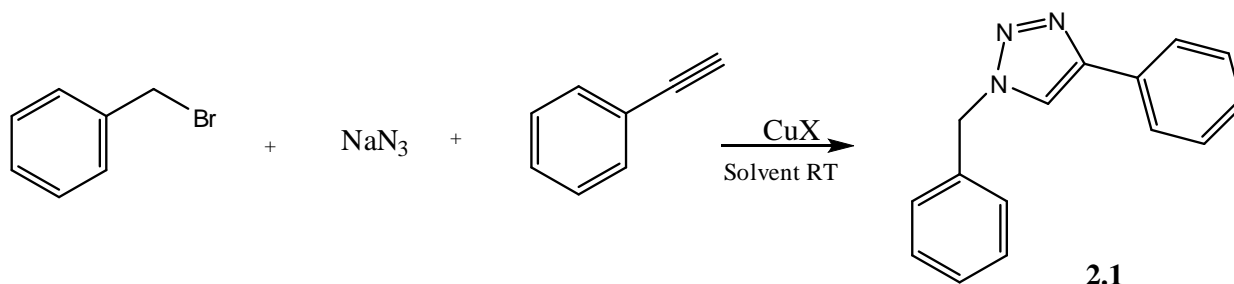
## 2.2 Results and discussion

One of the main aims of this project is to design a suitable method utilising green chemistry conditions for the synthesis of a variety of 1,4-disubstituted-1,2,3-triazoles to be used as ligands for the synthesis of transition metal complexes for the catalytic activation of alkanes. In planning the method, the main guidelines are: i) use cheap, available chemicals, ii) that are less toxic and easier to handle than current ones, iii) avoid unnecessary steps (maximise atom economy) wherever possible.

To achieve the above aims, the study focused on using a one-pot synthetic strategy for the preparation of the triazole compounds straight from alkyl halides, sodium azide and terminal alkynes. The system is efficient and “greener” since it cuts down several unnecessary steps, which include isolation, handling and chromatography.

### 2.2.1 Synthesis of 1,4-disubstituted 1,2,3-triazoles

Basic parameters for realising the cycloaddition reaction at optimum conditions were first tested with the result presented in Table 2.1. These include testing a variety of Cu salts (CuSO<sub>4</sub>, CuBr, CuI and CuCl) as catalysts with benzyl bromide, sodium azide and phenylacetylene as substrates. The reaction was conducted in DMSO at room temperature to afford 1-benzyl-4-phenyl-1H-1,2,3-triazole (**2.1**, Scheme 2.1). TLC and <sup>1</sup>H-NMR analysis confirmed the formation of only one compound and the <sup>1</sup>H- and <sup>13</sup>C-NMR spectra were comparable with those published by Huisgen <sup>12</sup>



**Scheme 2.1** : Synthesis of 1-benzyl-4-phenyl-1H-1,2,3-triazole (**2.1**).



**Table 2.1** : Effect of catalysts and solvents on the formation of triazole **2.1**.

Entry	Catalyst	Solvent	Yield (%)
1	CuBr (20%)	DMSO	67
2	CuI (20%)	DMSO	34
3	CuCl (20%)	DMSO	52
4	CuBr (10%)	DMSO	69
5	CuBr (5%)	DMSO	89
6	CuSO <sub>4</sub> .6 H <sub>2</sub> O	DMSO	72
7	CuBr (5%)	DMF	73
8	CuBr (5%)	DMF/H <sub>2</sub> O (1:1)	82
9	CuBr (5%)	DMF/H <sub>2</sub> O (4:1)	94
10	CuBr (5%)	DMSO/ H <sub>2</sub> O (4:1)	87
11	CuBr (5%)	MeOH	57
12	CuBr (5%)	H <sub>2</sub> O	42
13	CuBr (5%)	THF	25
12	CuBr (5%)	CH <sub>2</sub> Cl <sub>2</sub>	25

→ Reaction conditions: benzyl bromide (0.2 mmol), NaN<sub>3</sub> (1 equiv.), phenylacetylene (1 equiv.) and sodium ascorbate as reducing agent. All reactions were carried at room temperature for 24 h.

It is clear after the initial tests that CuBr is the best catalyst for this study as it resulted in the highest isolated yield of 94% when a 4:1 mixture of DMF/H<sub>2</sub>O was used as the solvent (entry 9).

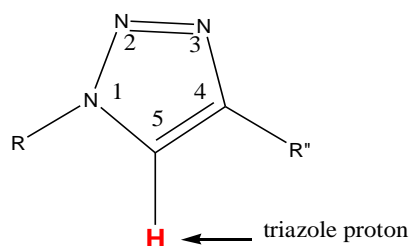
Because organic azides are used as precursors for the preparation of many essential compounds, methodologies for their synthesis have been extensively studied. But, it is also well known that some organic azides are unstable and difficult to handle, therefore the *in situ* method which involve the reaction of alkyl (aryl) halides, sodium azide and alkynes in a one-pot process for the synthesis of triazoles is the preferred routine.

Further synthesis of all the 1,4-disubstituted-1,2,3-triazoles was performed *in situ* under the following conditions as a standard:

- CuBr (5%) as catalyst,
- Sodium ascorbate as reducing agent,
- DMF/H<sub>2</sub>O (4:1) as medium,
- At room temperature, open to the atmosphere.

Good to excellent yields were obtained from a variety of organic halides, sodium azide and terminal alkynes (Table 2.2).

The synthesised triazoles were grouped on the basis of the substituent groups ( $-R$ ,  $-R''$ ) on the 1,4-positions of the ring (Figure 2.1). The substituent groups range from straight chain alkyl groups to bulkier benzyl and phenyl groups. In all cases, the products were isolated by simple extraction with  $\text{CH}_2\text{Cl}_2$  or by recrystallisation from water with isolated yields that are comparable to reported literature values for known compounds such as **2.1**.<sup>9</sup>

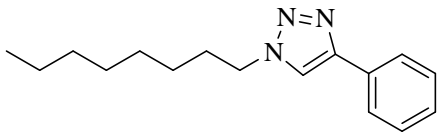
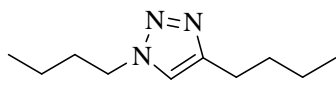
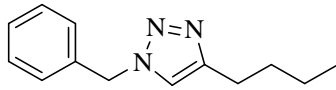
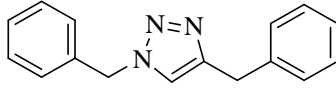
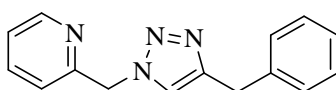
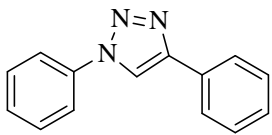
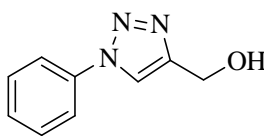
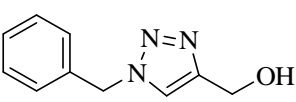
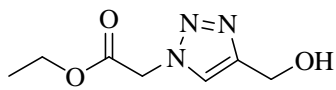
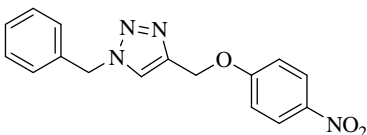


**Figure 2.1** : 1,4-disubstituted-1,2,3-triazole indicating the ring proton.

With reference to published data, all the compounds are easily identified by the triazole ring proton (Figure 2.1) resonating downfield as a singlet around 7.5-8.5 ppm (Table 2.2).<sup>18</sup>The NMR data of representative compounds are presented and further discussed below.

**Table 2.2:** One-pot synthesis of 1,2,3-triazoles from organic halides,  $\text{NaN}_3$ , and alkynes.

Compound	Triazole	Triaz.-H*	m.p.	Yield
2.1		7.69	129-131°C	92
2.2		7.81	-	89
2.3		7.51	46-48 <sup>13, 14</sup>	90
2.4		7.75	72-74 <sup>14</sup>	92

2.5		7.76	67-71	86
2.6		7.08	-	84
2.7		8.33	105-107	88
2.8		7.91	102-105	93
2.9		7.77	60-63	89
2.10		8.19	183-185 <sup>15-17</sup>	94
2.11		8.44	114-116	78
2.12		7.49	77-79	82
2.13		7.95	94-96	89
2.14		7.59	-	76

\* Triaz-H = Triazole proton

Fig. 2.2 presents the  $^1\text{H-NMR}$  spectrum of **2.1** where it is observed that the  $-\text{CH}_2-$  from benzyl bromide shifted downfield from 4.4 ppm in the starting material to 5.5 ppm in the product **2.1**, appearing as a singlet. The aromatic region integrated to the 10 protons expected for the proposed structure. The  $^1\text{H-NMR}$  spectrum shows that no residual starting material was present. The proton chemical shifts were further compared with literature spectral data and found to be in agreement.<sup>9, 10, 18, 19</sup>

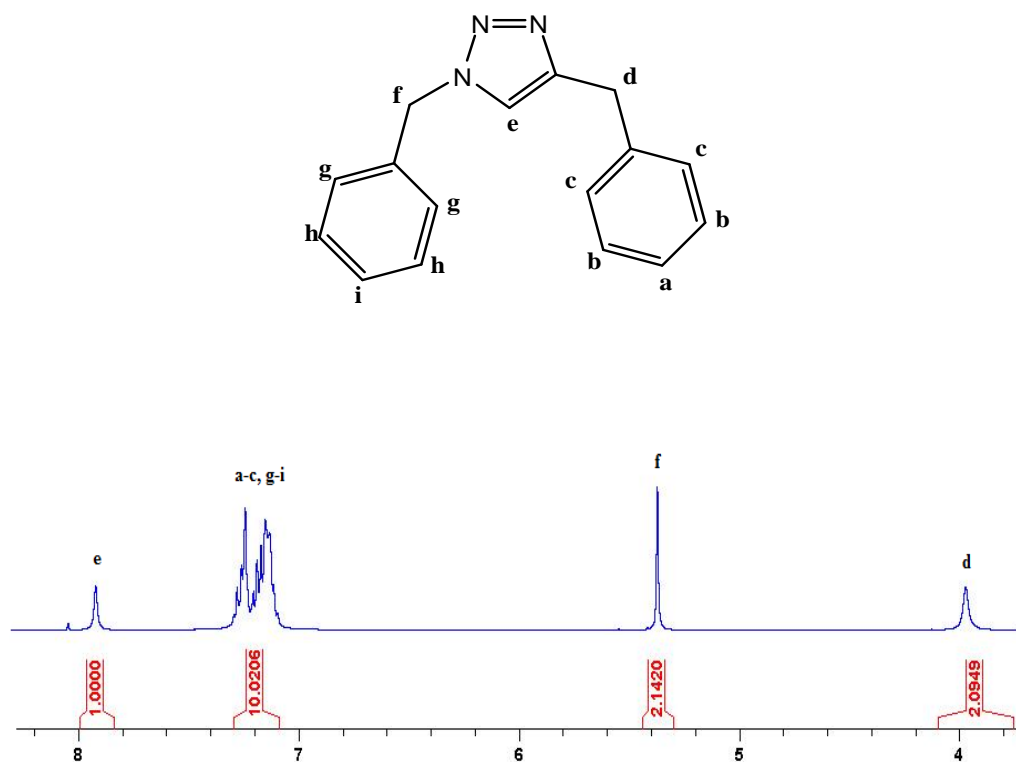


**Figure 2.2:**  $^1\text{H-NMR}$  spectrum of **2.8** in  $\text{CDCl}_3$ .

Product identification based on  $^{13}\text{C-NMR}$  chemical shifts focused on a comparison of the benzyl  $-\text{CH}_2-$  carbon of the product triazole and the reactant benzyl bromide, which resonates around 33 ppm in benzyl bromide was observed to shift downfield to 54 ppm in the triazole. The rest of the  $^{13}\text{C-NMR}$  chemical shifts were comparable to literature data.<sup>2, 9, 10, 18-21</sup>

Figs. 2.3 and 2.4 present the NMR data of an alkyl chain bearing compound **2.6** with the characteristic alkyl chain protons observed upfield around  $\delta = 1-3$  ppm in the  $^1\text{H-NMR}$  spectrum. The triazole ring proton (e, Fig. 2.3) appeared further downfield at  $\sim 7$  ppm

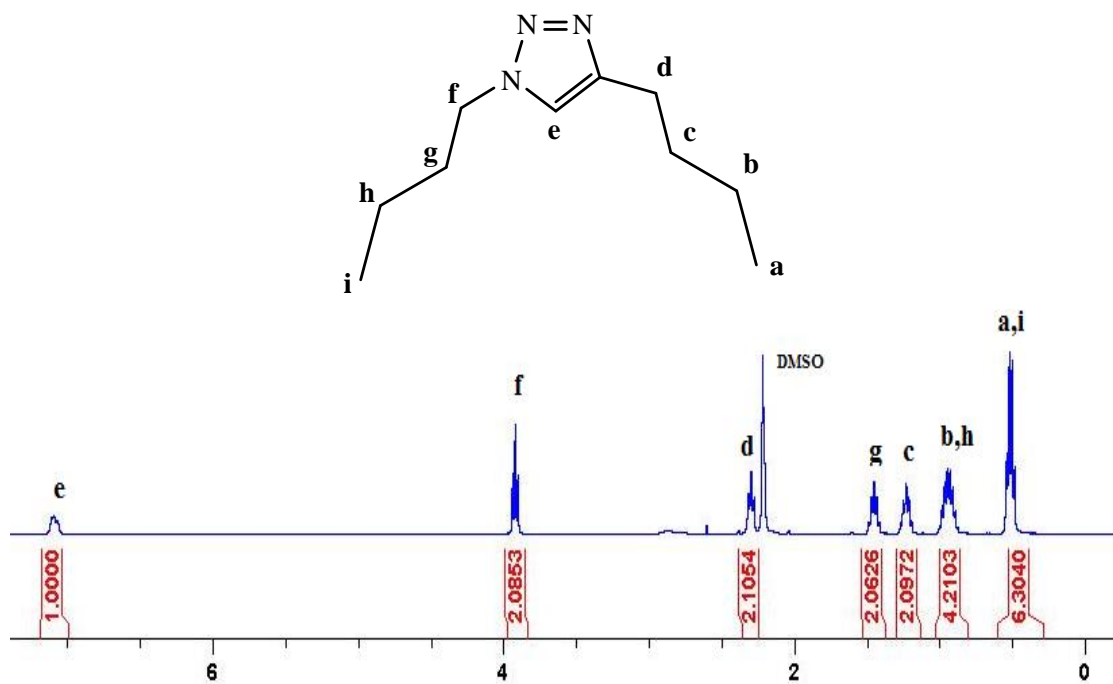


**Figure 2.3 :** <sup>1</sup>H NMR spectrum of **2.6** in CDCl<sub>3</sub>.

Based on <sup>13</sup>C-NMR data, the peak around 147 ppm (**f**, Fig. 2.4) confirmed the formation of the 1,4-disubstituted-1,2,3-triazole. The carbon peaks assignable to CH<sub>3</sub>- and -CH<sub>2</sub>- in the proposed structure shifted upfield as compared to the reactant.

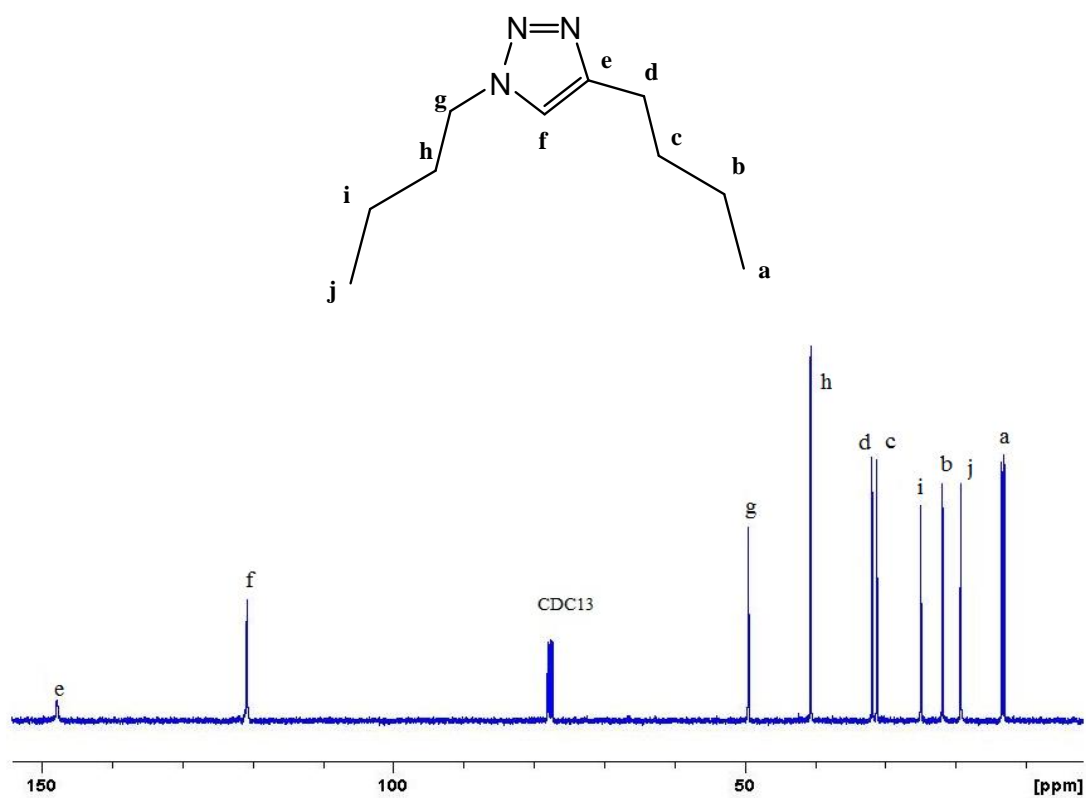


**Figure 2.4:**  $^{13}\text{C}$  NMR spectrum of **2.6** in  $\text{CDCl}_3$ .

The reaction of  $\alpha$ -halo esters with one equivalent of sodium azide in organic solvents has been reported for the synthesis of organic azides to occur within short reaction times.<sup>13</sup> A two-step one-pot synthesis that involve the reaction of ethyl bromoacetate with one equivalent of sodium azide in DMF for two hours followed by the addition of terminal alkyne in the presence of  $\text{CuBr}$  and sodium ascorbate was conducted, with the result that the triazole (**2.13**) was obtained regioselectively in very good yield and purity.

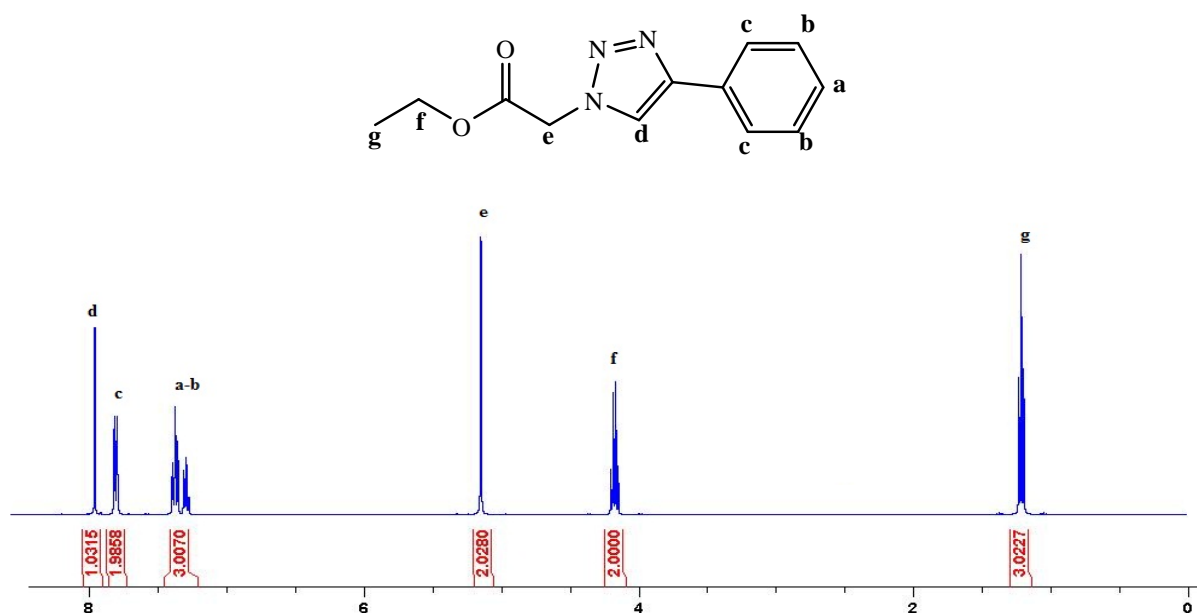
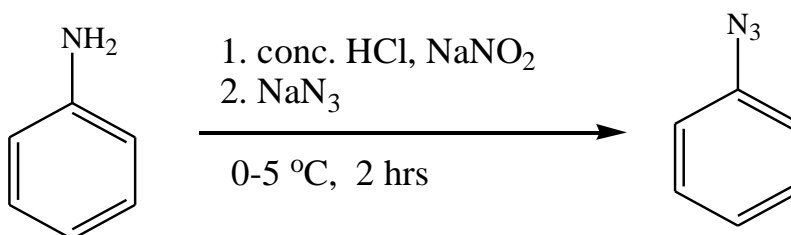


**Figure 2.5 :**  $^1\text{H}$  NMR spectrum of **2.13** in  $\text{CDCl}_3$ .

It was noted that when an aryl halide was used as the phenyl source, no reaction was observed. This was due to the fact that halides are weak deactivators which make the intermediate cations formed via  $\text{S}_{\text{N}}1$  reaction less stable compared to benzyl halides which typically react very readily with sodium azide via  $\text{S}_{\text{N}}2$  pathways. Alternative substrates were explored to replace the unreactive organic halides. It was observed that anilines can be used as sources of the phenyl group for the synthesis of aromatic azides (Scheme 2.2).<sup>2, 20, 22</sup>

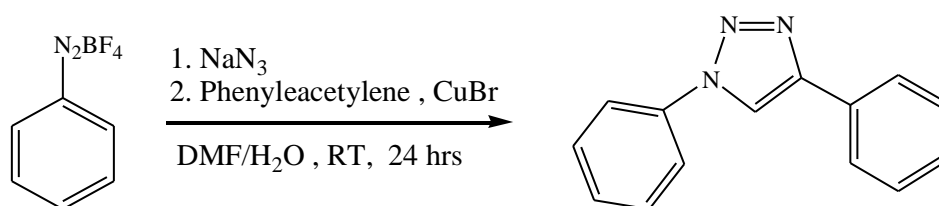


**Scheme 2.2 :** Diazotisation reaction.

However, anilines are not suitable for one-pot synthesis of triazoles due to the acidic medium required for the diazotisation reaction (Scheme 2.2). Therefore preparation of triazoles using anilines required more steps which include isolation and chromatography of heat sensitive, toxic and potentially explosive azides.<sup>23</sup>

Fletcher *and co-workers* reported that commercially available diazonium salts are potential replacements for anilines for the one-pot synthesis of aryl azides using sodium azide.<sup>23</sup>

Therefore, benzenediazonium tetrafluoroborate was used as a precursor for the two-step one-pot synthesis of 1,4-disubstituted-1,2,3-triazoles using the same conditions used for the alkyl halides. The process involved the reaction of sodium azide with a diazonium salt in DMF with vigorous stirring. The evolution of a brown gas was observed and then alkyne, CuBr and sodium ascorbate were added and stirred overnight. Upon reaction workup, the crude product was obtained and purified by chromatography to obtain high yield (94 %) of a yellow powder (Scheme 2.3).



**Scheme 2.3** : Synthesis of **2.10**.

The melting point and NMR data of the powder agreed with literature values.<sup>20</sup> With  $^1\text{H}$ -NMR, the aromatic region for the product integrated to account for 10 protons as expected for the proposed triazole structure. The triazole proton (**d**, Figure 2.6) was observed as a singlet at a considerably downfield position (8.2 ppm) as expected.

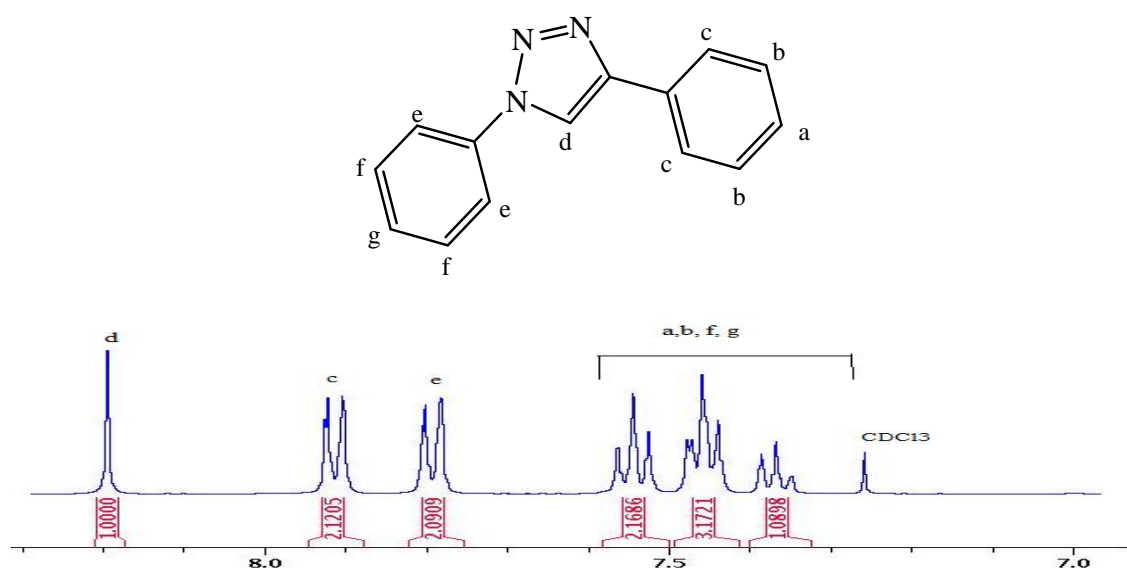


**Figure 2.6** :  $^1\text{H}$  NMR spectrum of **2.10** in  $\text{CDCl}_3$ .



## 2.2.2 IR analysis

Infrared (IR) spectroscopy was used to investigate functional group vibrational modes of the synthesised products. The main frequencies for each triazole are presented in Table 2.3 along with the designated functional group to which the signals belong. Characteristic bands that correspond to 1,2,3-triazole compounds were observed for the triazole ring C–C stretch (in-ring) around  $1600\text{ cm}^{-1}$ , the sharp bands in the range  $1350\text{--}1500\text{ cm}^{-1}$  were assigned to the stretching vibrations of the triazole ring due to the presence of  $\text{--HC=N--}$  group.<sup>24</sup>

The appearance of a medium intensity band in the range  $1470\text{--}1450\text{ cm}^{-1}$  was assigned to the C–H bend of alkyl chains and methylene groups, while C–H rocking was observed typically in the  $750\text{--}720\text{ cm}^{-1}$  region.<sup>25</sup> A strong intensity, broad O–H stretch around  $3500\text{--}3200\text{ cm}^{-1}$  was observed for the O–H containing compounds **2.11** and **2.12**, while a sharp intense C=O stretch was observed for **2.13**. All the IR spectra for the triazole compounds are presented in Appendix A2.

**Table 2.3:** IR data obtained for each triazole compound showing significant wave numbers

Compound	Triazole (ring)	C–H (aromatic)	C–H (alkyl)	C–C (aromatic)	C–H bend (alkyl)
<b>2.1</b>	1605	3135	2966, 2914, 2856	1589, 1572	1451
<b>2.2</b>	1608	3122	2987, 2940, 2871	1589, 1573	1483
<b>2.3</b>	1608	3119	2955, 2934, 2821	1565, 1521	1464
<b>2.4</b>	1609	3120	2928, 2917, 2923	1590, 1571	1463
<b>2.5</b>	1607	3113	2948, 2919, 2856	1589, 1572	1462
<b>2.6</b>	1604	3121	2987, 2940, 2871	-	1481
<b>2.7</b>	1608	3114	2959, 2957, 2823	1556, 1521	1448
<b>2.8</b>	1609	3120	2928, 2917, 2923	1590, 1571	1463

<b>2.9</b>	1601	3113	-	1540,1500	-
<b>2.10</b>	1600	3122	-	1597	-
<b>2.11</b>	1607	3138	2936, 2917	1552, 1496	1457
<b>2.12</b>	1607	3138	2924	1496, 1454	1454
<b>2.13</b>	1602	3134	2993, 2970, 2948	1487, 1466	1441
<b>2.14</b>	1604	3137	2987, 2974, 2961	1478, 1462	1456

### 2.2.3 MS analysis

Table 2.4 presents the found  $m/z$  ratios of the synthesised triazole ligands which were comparable with calculated values represented in parentheses. Only new compounds were analysed by HRMS.

**Table 2.4:**  $m/z$  ratios obtained for each triazole

<b>Ligand</b>	<b><math>m/z</math> [M+H]<sup>+</sup> (Calculated)</b>
<b>2.2</b>	187.1 (190.0)
<b>2.4</b>	229.1 (229.08)
<b>2.6</b>	181.31 (181.61)
<b>2.8</b>	250.13 (249.13)

### 2.2.4 Single crystal X-ray diffraction studies

A single crystal of **2.13** suitable for X-ray diffraction studies was grown by slow diffusion of diethyl ether into a dichloromethane solution at ambient temperature. Selected bond lengths and bond angles are presented in Table 2.5.

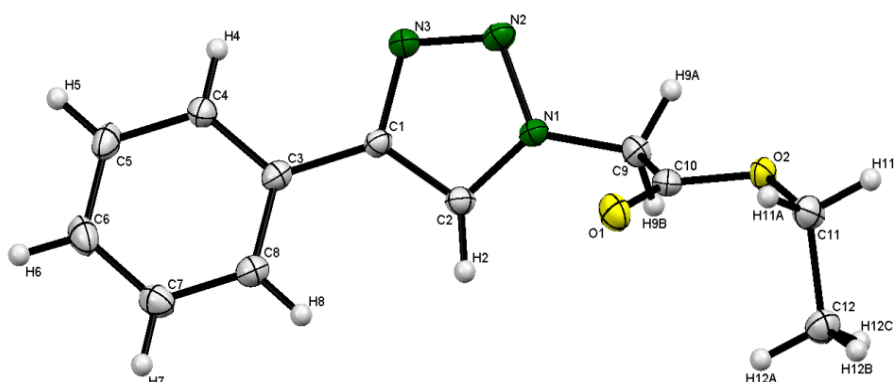


**Figure 2.7** : Molecular crystal structure of compound **2.13**; anisotropic displacement parameters are given at the 50% level.

**Table 2.5:** Selected bond lengths (Å) and bond angles (°) of **2.13**

N1 – N2	1.355(5)	C10 – O1	1.204(5)	N2 – N3 – C1	108.7(3)
N2 – N3	1.317(6)	C10 – O2	1.340(5)	N3 – C1 – C2	108.7(3)
N1 – C2	1.354(5)	N3 – C1	1.366(4)	C9 – C10 – O2	108.5(3)
C1– N3	1.366(4)	N1– C2– C1	104.7(3)		
C1– C2	1.370(6)	N1– N2– N3	107.3(3)		
C2 – H2	0.930(4)				

The ORTEP diagram of a molecule of ethyl-2-(4-phenyl-1H-1,2,3-triazol-1-yl)acetate (**2.13**) is shown in Figure 2.7. The compound crystallises in the triclinic crystal system with P-1 space group symmetry. Bond distances (Table 2.5) between N(1)-N(2) = 1.355(5), N(2)-N(3) = 1.317(6) and C(1)-C(2) = 1.370(6) Å are in the range for partial double bonds, as these bond lengths are shorter than C-N single bond length (1.470 Å), but longer than the C-N double bond length (1.265 Å), supporting delocalisation of electron density within the triazole ring.<sup>26-29</sup>

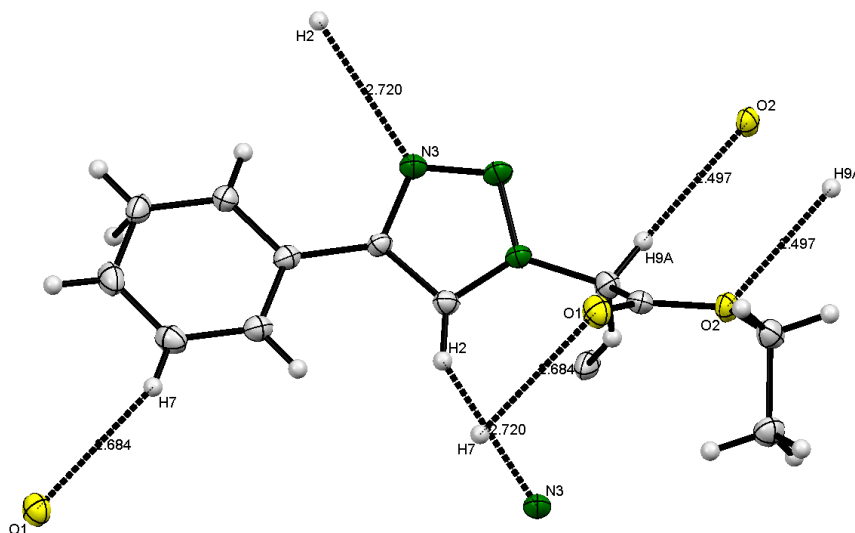


**Figure 2.8** : Structure of **2.13** showing the key intermolecular atoms engaged in hydrogen bonding.

Many structures have been reported to be strengthened by hydrogen bonding along the chain of repeating units. Packing in the crystal of **2.13** (Figs. 2.8 and 2.9) shows the formation of parallel layers with multiple hydrogen bonding sites that help in stabilising the linear form of the compound. A strong hydrogen bond between the triazole proton H(2) and the triazole nitrogen N(2) was observed (C-H(2)⋯N(2) distance of 2.720 Å). Both oxygen atoms (O(1) and O(2)) are involved in hydrogen bonding with neighbouring protons from the phenyl ring and the alkyl chain. The carbonyl oxygen O(1) is involved in hydrogen bonding with phenyl ring hydrogen (C-H(7)⋯O(1) distance of 2.684 Å), while O(2) is involved in hydrogen bonding with acidic proton H(9A) adjacent to the carbonyl group (C-H(9A)⋯O(2) distance of 2.497 Å).

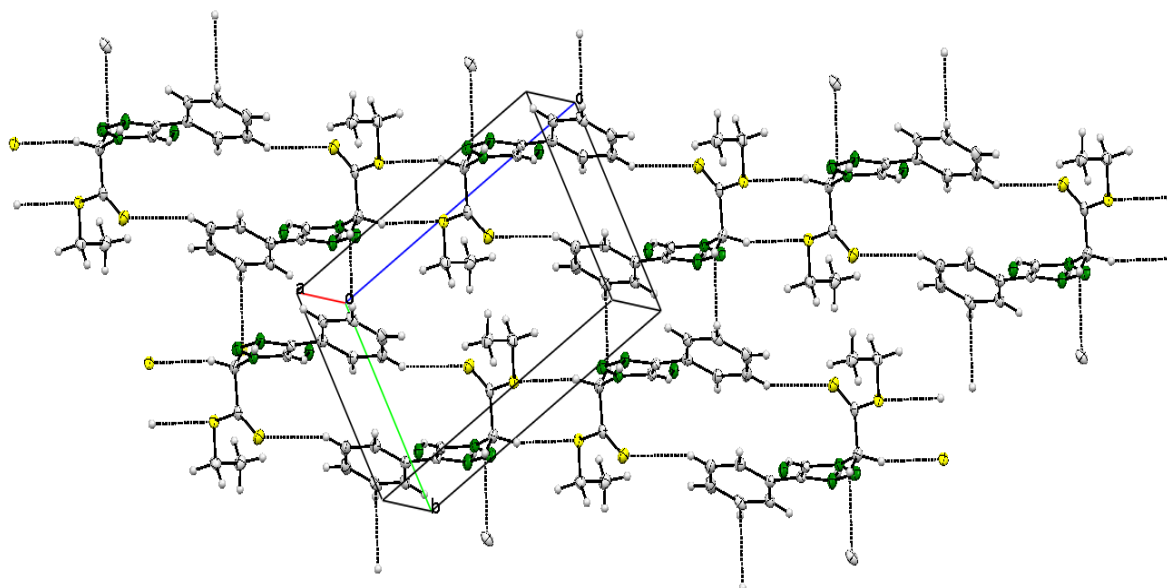


**Figure 2.9** : A perspective of packing in the crystal structure of compound **2.13**.

### 2.3 Summary and conclusion

Due to increasing number of applications for triazoles, numerous synthetic methods for their preparation have been developed with over 1000 research articles published. In this study, a two-step-one-pot synthetic method which involves *in situ* formation of organic azides followed by copper-catalysed Huisgen 1,3-dipolar cycloaddition to form corresponding 1,2,3-triazoles was used. Different copper salts were tested as catalysts with CuBr showing the highest catalytic activity. The biphasic (DMF/H<sub>2</sub>O) system with CuBr as catalyst returned the highest yield. The method used did not only give high yields but also avoided well documented difficulties of isolating potentially explosive organic azides.

## 2.4 Experimental

### 2.4.1 General

Unless stated otherwise, all reagents and solvents were purchased from commercial suppliers and were used without further purification. Glassware were oven dried at 110 °C. All NMR experiments were done using a 400 MHz Bruker ultrashield spectrometer and samples were dissolved in deuterated solvents. The solvents used in column chromatography were obtained from commercial suppliers and used without distillation. Infrared spectra (FTIR) were recorded on a Perkin Elmer FT-IR 1600 spectrophotometer.

### 2.4.2 General Procedure

In a 100 ml round bottom flask containing a stirrer bar was charged with the organic halide (1 equiv.) and sodium azide (1 equiv.) in DMF (20 ml). The mixture was heated and stirred at 80 °C for 4 h. The reaction was monitored by TLC for disappearance of alkyl halide. When the reaction was complete, the solution was cooled to room temperature and CuBr (5% equiv.), sodium ascorbate (0.1 equiv.) and terminal alkyne (1.0 equiv.) in 5 ml water were added and stirred at room temperature for 24 hr. The suspension was then partitioned between aqueous NH<sub>4</sub>OH/EDTA (100 ml) and CH<sub>2</sub>Cl<sub>2</sub> (100 ml) from which the organic layer separated. The organic phase was washed with H<sub>2</sub>O (100 ml) and brine (100 ml) then dried over MgSO<sub>4</sub> and the solvent was removed under reduced pressure to give high yields (76-94%) product. The same procedure was used to prepare all the 1,4-disubstituted-1,2,3-triazoles in good yields from several organic halides, sodium azide and terminal alkynes.

**1-Benzyl-4-phenyl-1*H*-1,2,3-triazole**<sup>9,17,30</sup> (**2.1**). The starting materials used were benzyl bromide (4.681 g, 28.2 mmol), sodium azide (1.840 g, 1 equiv.) and phenylacetylene (0.890 g, 8.6 mmol, 1.1 equiv.) off-white powder product. (6.351 g, 96%); mp: 129-131 °C; <sup>1</sup>H NMR (CDCl<sub>3</sub> 400 MHz): δ 7.77 (d, 2H, Ar), 7.69 (s, 1H, triazole C=CH), 7.39-7.26 (m, 8H, Ar), 5.532 (s, 2H, Ar-CH<sub>2</sub>); <sup>13</sup>C NMR (CDCl<sub>3</sub> 400 MHz): δ 126.5, 148.1, 134.7, 130.5, 129.1, 128.7, 128.1, 125.6, 119.6, 54.1. IR v<sub>max</sub> (cm<sup>-1</sup>): 3143 (s), 2977 (m), 2096 (s), 1665 (s), 1607 (m), 1468 (s), 1450 (s), 1362 (s), 1223 (s), 767 (m), 727 (s), 694 (m), 480 (s).

**1-Propyl-4-(phenyl)-1H-1,2,3-triazole (2.2).** The starting materials used were 1-bromopropane (3.101 g, 25.1 mmol), sodium azide (1.625 g, 1 equiv.) and phenylacetylene (2.552 g, 1equiv). Brown oily product (4.012 g , 86%);  $^1\text{H}$  NMR ( $\text{CDCl}_3$  400 MHz ):  $\delta$  7.83 (t, 2H, Ar), 7.81 (s, 1H, triazole C=CH), 7.47 (t, 2H, Ar), 7.38 ( t, 1H, Ar ), 4.27 (m, 2H,  $\text{CH}_2$ ), 1.90-1.88 (m, 2H,  $\text{CH}_2$ ) , 0.91 (m, 3H,  $\text{CH}_3$ );  $^{13}\text{C}$  NMR ( $\text{CDCl}_3$  400 MHz):  $\delta$  147.4, 132.0, 130.6, 125.6, 122.0, 119.8, 51.8, 36.3, 31.2, 23.6, 10.9; IR  $\nu_{\text{max}}$  ( $\text{cm}^{-1}$ ): 3122 (s), 2987 (m), 2940 (m), 1608 (m), 1483(s), 1433 (s), 819 (m), 765 (m), 691 (m), 508 (m). HRMS (ESI)  $m/z$  for  $\text{C}_{11}\text{H}_{13}\text{N}_3[\text{M}+\text{H}]$ : calculated 187.1, found : 190.1.

**1-Butyl-4-phenyl-1H-1,2,3-triazole<sup>13</sup> (2.3).** The starting materials used were 1-bromobutane (5.08 g, 37.1 mmol), sodium azide (2.411 g, 1 equiv.) and phenylacetylene (3.781 g, 1.0 equiv.). off-white crystalline product (6.262 g , 84%); mp: 46-48 °C;  $^1\text{H}$  NMR ( $\text{CDCl}_3$  400 MHz):  $\delta$  7.79 (s, 1H, triazole C=CH), 7.44-7.26 (m, 5H, Ar), 4.28 (t, 2H,  $\text{CH}_2$ ), 1.82-1.76 ( t, 2H,  $\text{CH}_2$ ), 1.30-1.27 (m, 2H,  $\text{CH}_2$ ), 0.89 (t, 3H,  $\text{CH}_3$ );  $^{13}\text{C}$  NMR ( $\text{CDCl}_3$  400 MHz):  $\delta$  147.4, 132.0, 130.8, 128.7, 125.6, 49.9, 32.1, 19.6, 13.3. IR  $\nu_{\text{max}}$  ( $\text{cm}^{-1}$ ): 3119 (s) 3064 (m), 2955 (m), 2934 (m), 1674 (m), 1608 (s), 1464 (s), 1078 (s), 839 (s), 761 (m) ,693 (m).

**1-Hexyl-4-(phenyl)-1H-1,2,3-triazole (2.4).** The starting materials used were 1-bromohexane (4.681 g, 28.2 mmol), sodium azide (1.842 g, 1 equiv.) and phenylacetylene (2.890 g, 1.0 equiv.). Off-white crystalline product (5.601 g , 87%); mp: 72-74 °C;  $^1\text{H}$  NMR ( $\text{CDCl}_3$  400 MHz ):  $\delta$  7.82 (m, 2H, Ar), 7.75 (s, 1H, triazole C=CH), 7.41-7.39 (m, 2H, Ar), 7.34-7.27( t, 1H, Ar), 4.38 (t, 2H,  $\text{CH}_2$ ), 1.95-1.91(m, 2H,  $\text{CH}_2$ ), 1.32-1.32 (m, 6H,  $\text{CH}_2$ ), 0.88 (t, 3H, $\text{CH}_3$ );  $^{13}\text{C}$  NMR ( $\text{CDCl}_3$  400 MHz):  $\delta$  147.7, 130.7, 128.8, 128.0, 125.6, 119.4, 50.4, 36.4, 31.1, 30.2, 26.1, 22.4, 13.9; IR  $\nu_{\text{max}}$  ( $\text{cm}^{-1}$ ): 3120 (s) 3095 (m), 2928 (m), 2917 (m), 1609 (s), 1463 (s), 1078 (s), 839 (s), 761 (m), 693 (m). HRMS (ESI)  $m/z$  for  $\text{C}_{14}\text{H}_{19}\text{N}_3[\text{M}+\text{H}]$ : calculated 229.13 , found 229.02.

**1-Octyl-4-phenyl-1H-1,2,3-triazole<sup>31</sup> (2.5).** The starting materials used were 1-bromooctane (4.416 g, 23.3 mmol), sodium azide (1.491 g, 1.0 equiv.) and phenylacetylene (2.403 g, 1.0 equiv.). Off-white crystalline product (5.313 g, 87%); mp: 67-71 °C;  $^1\text{H}$ -NMR ( $\text{CDCl}_3$  400 MHz ):  $\delta$  7.83 (m, 2H, Ar), 7.74 (s, 1H, triazole C=CH), 7.38-7.42 (m, 2H, Ar), 7.33-7.29( t, 1H, Ar), 4.38 (t, 2H,  $\text{CH}_2$ ), 1.90-1.94 (m, 2H,  $\text{CH}_2$ ), 1.25-1.32(m, 10H,  $\text{CH}_2$ ), 0.88 (t, 3H, $\text{CH}_3$ );  $^{13}\text{C}$  NMR ( $\text{CDCl}_3$  400 MHz):  $\delta$  147.7, 130.7, 128.8, 128.0, 125.6, 119.4, 50.4,

31.7, 31.1, 30.3, 28.9, 26.5, 22.6, 22.4, 14.0; IR  $\nu_{\max}$  (cm<sup>-1</sup>): 3113 (m), 2948 (m), 2919 (m), 1607 (s), 1462 (s), 1088 (s), 839 (s), 761 (m), 693 (m).

**1,4-Dibutyl-1H-1,2,3-triazole (2.6).** The starting materials used were 1-bromobutane (5.501 g, 40 mmol), sodium azide (2.610 g, 1 equiv.) and 1-hexyne (3.300 g, 1 equiv.). Yellow oily-liquid (6.213 g, 85%); <sup>1</sup>H-NMR (CD<sub>3</sub>OD 400 MHz):  $\delta$  7.089 (s, 1H, triazole C=CH), 3.914 (t, 2H, CH<sub>2</sub>), 2.309 (m, 2H, CH<sub>2</sub>), 1.255 (m, 2H, CH<sub>2</sub>), 0.959 (m, 4H, CH<sub>2</sub>), 0.514 (m, 6H, CH<sub>3</sub>); <sup>13</sup>C NMR (CD<sub>3</sub>OD, 400 MHz):  $\delta$  147.8, 120.7, 49.5, 40.6, 31.9, 31.2, 24.2, 21.8, 19.2, 13.4. IR  $\nu_{\max}$  (cm<sup>-1</sup>): 3121 (s), 3098 (m), 3059 (s), 1654 (m), 1604(m), 1513(s), 1481 (s), 1078 (s), 836(s), 764 (m), 693 (m). HRMS (ESI) m/z for C<sub>10</sub>H<sub>19</sub>N<sub>3</sub>[M+H]: calculated 181.13, found 181.63.

**1-Benzyl-4-butyl-1H-1,2,3-triazole<sup>32</sup> (2.7).** The starting materials used were benzyl bromide (3.212 g, 18.7 mmol), sodium azide (1.221 g, 1 equiv.) and 1-hexyne (1.451 g, 1 equiv.). Pale green solid (3.421 g, 85%); mp 105-107 °C; <sup>1</sup>H-NMR (CD<sub>3</sub>OD 400 MHz):  $\delta$  8.33 (s, 1H, triazole C=CH), 7.84 (d, 2H, Ar), 7.60-7.40 (m, 3H, Ar), 2.78 (t, 2H, CH<sub>2</sub>), 1.79 (t, 2H, CH<sub>2</sub>), 1.43 (m, 2H, CH<sub>2</sub>), 0.97 (t, 3H, CH<sub>3</sub>); <sup>13</sup>C-NMR (CD<sub>3</sub>OD 400 MHz):  $\delta$  138.6, 131.0, 129.9, 121.4, 116.4, 40.7, 32.6, 26.1, 23.3, 14.4. IR  $\nu_{\max}$  (cm<sup>-1</sup>): 3114 (s), 3063 (m), 2959 (s), 2923 (m), 2857 (m), 1556 (s), 1495 (s), 1448 (s), 1051 (s), 747 (m), 703 (s), 673 (m), 469 (s).

**1,4-Dibenzyl-1H-1,2,3-triazole (2.8).** The starting materials used benzyl bromide (6 g, 35.1 mmol), sodium azide (2.280 g, 1 equiv.) and prop-2-ynylbenzene (4.069 g, 1 equiv.). Brown solid (7.124 g, 91%); mp 102-105 °C; <sup>1</sup>H NMR (CD<sub>3</sub>OD 400 MHz):  $\delta$  7.91 (s, 1H, triazole C=CH), 7.13-7.25 (m, 10H, Ar), 5.36 (s, 2H, Ar-CH<sub>2</sub>), 3.96 (s, 2H, Ar-CH<sub>2</sub>); <sup>13</sup>C NMR (CD<sub>3</sub>OD 400 MHz):  $\delta$  161.5, 159.7, 137.8, 134.3, 133.7, 127.9, 127.6, 127.5, 127.5, 126.9. IR  $\nu_{\max}$  (cm<sup>-1</sup>): 3113 (s), 3058 (m), 3059 (s), 1601 (m), 1540(m), 1494(s), 1457 (s), 726 (s), 693 (m). HRMS (ESI) m/z for C<sub>16</sub>H<sub>15</sub>N<sub>3</sub>[M+H]: calculated 249.13, found 250.13.

**2-((4-Phenyl-1H-1,2,3-triazol-1-yl)methyl)pyridine<sup>33</sup> (2.9).** The starting materials used were 2-(bromomethyl) pyridine (4.186 g, 24.6 mmol), sodium azide (1.601g, 1 equiv.) and phenylacetylene (2.403 g, 1.0 equiv.). Yield (4.982 g, 86%). Off white solid; mp 60-63 °C; <sup>1</sup>H-NMR (CDCl<sub>3</sub> 400 MHz):  $\delta$  8.59 (s, 1H, N=CH, Ar), 7.83 (s, 1H, triazole, C=CH), 7.71-7.52 (m, 3H, Ar), 7.33-7.12 (m, 3H, Ar), 6.712 (d, 2H, Ar), 5.621 (s, 2H, Ar-CH<sub>2</sub>); <sup>13</sup>C-NMR (CDCl<sub>3</sub> 400 MHz):  $\delta$  154.5, 149.7, 137.3, 130.5, 128.1, 123.4,



122.4, 120.2, 55.72. IR  $\nu_{\max}$  ( $\text{cm}^{-1}$ ): 3465 (s), 3334 (b), 3214 (s), 1627 (m), 1614 (m), 1500 (s), 1435 (s), 805 (s), 758 (s), 724 (m), 523 (m), 484 (m).

**1,4-Diphenyl-1H-1,2,3-triazole**<sup>15, 16, 34</sup> (2.10). The starting materials used benzenediazonium tetrafluoroborate (4.013 g, 20.9 mmol), sodium azide (1.495 g, 1 equiv.) and phenylacetylene (2.392 g, 1.1 equiv.). Yellow powder (4.325 g, 85%); mp 184-186 °C ; <sup>1</sup>H NMR ( $\text{CD}_3\text{OD}$  400 MHz ):  $\delta$  8.192 (s, 1H, triazole C=CH), 7.923 (d, 2H, Ar), 7.920 (d, 2H, Ar ), 7.803 (t, 2H, Ar), 7.470 (t, 3H, Ar ), 7.366 (t, 1H, Ar); <sup>13</sup>C NMR ( $\text{CD}_3\text{OD}$  400 MHz):  $\delta$  147.4, 137.0, 130.2, 129.7, 128.9, 128.7, 128.4, 125.8, 117.6. IR  $\nu_{\max}$  ( $\text{cm}^{-1}$ ): 3122 (s), 3098 (m), 3054 (m), 1657 (m), 1597 (s), 1451 (s), 1078 (s), 826 (s), 754 (m), 687 (m).

**(1-Phenyl-1H-1,2,3-triazol-4-yl)methanol** (2.11). The starting materials used benzenediazonium tetrafluoroborate (4.013 g, 20.9 mmol.), sodium azide (1.495 g, 1 equiv.) and prop-2-yn-1-ol (1.194 g, 1 equiv.). Pale-yellow powder ( 2.875 g, 79%); mp 113-115 °C; <sup>1</sup>H-NMR ( $\text{CDCl}_3$  400 MHz ):  $\delta$  7.49 (s, 1H, triazole C=CH), 7.43-7.23 (m, 5H, Ar), 5.47 (s, 2H, Ar-CH<sub>2</sub>), 4.00 (s ,2H, CH<sub>2</sub>); <sup>13</sup>C-NMR ( $\text{CDCl}_3$  400 MHz):  $\delta$  134.4, 129.0, 128.7, 128.1, 54.2, 40.7. IR  $\nu_{\max}$  ( $\text{cm}^{-1}$ ): 3444 (b), 3138 (m), 3088 (m), 2936 (m), 1662 (m), 1607 (s), 1552 (s), 1496 (s), 1457 (m), 717 (m), 690 (m).

**(1-Benzyl-1H-1,2,3-triazol-4-yl)methanol**<sup>6</sup> (2.12). The starting materials used benzyl bromide (6.012 g, 35.1 mmol) sodium azide (3.001 g, 1.1 equiv.) and prop-2-yn-1-ol (2.580 g, 1.1 equiv.). Pale yellow powder (4.621 g, 70%); mp 76-77 °C; <sup>1</sup>H-NMR ( $\text{CDCl}_3$  400 MHz):  $\delta$  7.49 (s, 1H, triazole C=CH), 7.43-7.23 (m, 5H, Ar), 5.47 (s, 2H, Ar-CH<sub>2</sub>), 4.72 (s, 1H, OH), 4.00 (s, 2H, Ar-CH<sub>2</sub>); <sup>13</sup>C-NMR ( $\text{CDCl}_3$  400 MHz):  $\delta$  134.4, 129.0, 128.7, 128.1, 54.2, 40.7. IR  $\nu_{\max}$  ( $\text{cm}^{-1}$ ): 3444 (b), 3138 (m), 3088 (m), 2936 (m), 1662 (m), 1607 (s), 1552 (s), 1496 (s), 1457 (m) ,717 (m), 690 (m).

**Ethyl-2-(4-phenyl-1H-1,2,3-triazol-1-yl)acetate**<sup>35-37</sup> (2.13). The starting materials used ethyl bromoacetate (4.013 g, 17.3 mmol), sodium azide (1.126 g, 1 equiv.) and phenylacetylene (1.766 g, 1 equiv.). Pale-green powder (3.473 g, 87%); mp 94-95 °C ; <sup>1</sup>H NMR ( $\text{CDCl}_3$  400 MHz ):  $\delta$  7.95 (s, 1H, triazole C=CH), 7.38 (t , 2H, Ar), 7.28-7.37 (m , 3H, Ar), 5.14 (s, 2H, N-CH<sub>2</sub>), 4.18-4.16 (m, 2H, O-CH<sub>2</sub>), 1.21 (t , 3H, CH<sub>3</sub>); <sup>13</sup>C NMR ( $\text{CDCl}_3$  400 MHz):  $\delta$  166.4, 147.9, 130.4, 128.8, 128.1, 125.7, 121.1, 62.2, 50.8, 1.397. IR  $\nu_{\max}$  ( $\text{cm}^{-1}$ ): 3134 (s) 2993 (m), 2948 (m), 1752 (m), 1466 (m), 1441 (s), 1197 (m), 1014 (s), 763 (m), 692 (m).

**1-Benzyl-4-((4-nitrophenoxy)methyl)-1H-1,2,3-triazole<sup>37</sup> (2.14).** The starting materials used benzyl bromide (6.115 g, 35.08 mmol), sodium azide (1.126 g, 1 equiv.) and 1-nitro-4-(prop-2-ynyloxy)benzene (6.195 g, 1 equiv.). White powder (3.473 g, 87%); mp 98-100 °C ; <sup>1</sup>H NMR (CDCl<sub>3</sub> 400 MHz): δ 8.181 (s, 2H, Ar), 7.593 (s, 1H, triazole C=CH), 7.275-7.385 (m, 5H, Ar), 7.038-7.061 (m, 2H, Ar), 5.547 (s, 2H, Ar-CH<sub>2</sub>) 5.267 (s, 2H, Ar-CH<sub>2</sub>); <sup>13</sup>C NMR (CDCl<sub>3</sub> 400 MHz): δ 163.1, 141.8, 134.2, 129.2, 128.1, 125.8, 123.0, 114.8, 62.4, 54.3. IR ν<sub>max</sub> (cm<sup>-1</sup>): 3131 (s) 2977 (m), 2951 (m), 1716 (m), 1543 (m), 1538 (s), 1010 (s), 768 (m), 596 (m).

## 2.5 Reference list

1. R. Huisgen, G. Szeimies and L. Moebius, *Chem. Ber.*, 1965, **98**, 4014–4021.
2. R. Huisgen in *1,3-Dipolar Cycloaddition Chemistry* (Ed.: A. Padwa), Wiley, New York, 1984, pp. 1–176.
3. R. Huisgen, *Pure Appl. Chem.*, 1989, **61**, 613–628.
4. V. V. Rostovtsev, L. G. Green, V. V. Fokin and K. B. Sharpless, *Angew. Chem. Int. Ed.*, 2002, **41**, 2596-2599.
5. F. Himo, T. Lovell, R. Hilgraf, V. V. Rostovtsev, L. Noodleman, K. B. Sharpless and V. V. Fokin, *J. Am. Chem. Soc.*, 2005, **127**, 210-216.
6. R. A. Periana, D. J. Taube, E. R. Evitt, D. G. Loffler, P. R. Wentrcek, G. Voss and T. Masuda, *Science*, 1993, **259**, 340-345.
7. R. A. Periana, D. J. Taube, S. Gamble, H. Taube, T. Satoh and H. Fujii, *Science*, 1998, **280** 560-565.
8. D. A. Kopp and S. J. Lippard, *Curr. Opin. Chem. Biol.*, 2002, **38**, 568-576.
9. P. Li and L. Wang, *Lett. Org. Chem.*, 2007, **4**, 23-26.
10. J. D. Lipscomb, *Annu. Rev. Microbiol.*, 1994, **48**, 371-376.
11. D. M. Nguyen and D. H. Miles, *Int. J. Rap. Commun. Synth. Org. Chem.*, 2011, **41**, 1759-1771.
12. R. Huisgen, *Angew. Chem*, 1963, **2**, 565-569.
13. L. Pinhua and L. Wang, *Lett. Org. Chem.*, 2007, **4**, 23-26.
14. L. H. Lu, J. H. Wu and C. H. Yang, *J. Chin. Chem. Soc.*, 2008, **55**, 414-417.
15. J. Z. Miao Sun , P. Putaj, V. Caps, F. Lefebvre, J. Pelletier and J.-M. Basset, *Chem. Rev.*, 2014, **114**, 981–1019.
16. C. Jia, T. Kitamura and Y. Fujiwara, *Acc. Chem. Res.*, 2001, **34**, 633-639.
17. F. Wang, H. Fu, Y. Jianga and Y. Zhao, *Green Chem.*, 2008, **10**, 452–456.
18. L. Zhang, X. Chen, P. Xue, H. H. Sun, I. D. Williams, K. B. Sharpless, V. V. Fokin and G. J. Jia, *J. Am. Chem. Soc.*, 2005, **127**, 15998-15999.
19. L. D. Pachón, J. H. Maarseveen and G. Rothenberg, *Adv. Synth. Catal.*, 2005, **347**, 811-814.
20. C. W. Tornøe, C. Christensen and M. Meldal, *J. Org. Chem.* , 2002, **67**, 3057–3064.
21. L. Liang and D. Astruc, *Coord. Chem. Rev.*, 2011, **255**, 2933-2945.
22. F. Alonso, Y. Moglie, G. Radivoy and M. Yusa, **50**, 2358-2362.
23. J. T. Fletcher and J. E. Reillya, *Tetrahedron Lett.* , 2011, **52(42)**, 5512–5515.
24. M. A. Iqbal, R. A. Haque, M. B. K. Ahamed, M. A. M. Abdul and S. Al-Rawi, *Med. Chem. Res.* 2013, **22**, 2455-2466.
25. R. A. Haque and M. A. Iqbal, *Asian J. Chem.*, 2013, **25**, 3049-3054.
26. A. Bondi, *J. Phys. Chem.* , 1964, **68**, 441-445.
27. G. A. Adamson and C. W. Rees, *J.C.S. Perkin I*, 1996, 1535.
28. A. L. Rheingold, L. M. Liable-Sands and S. Trofimenko, *Angew. Chem., Int. Ed. Engl.*, 2000, **39**, 3321-3326.
29. A. R. Katritzky, J. Cobo-Domingo, B. Yang and P. G. Steel, *J. Chem. Res.* , 1999, **162**, 452-456.
30. J. C. Sheehan, *J. Am. Chem. Soc.*, 1951, **73**, 1207-1210.
31. S. Lal and S. Díez-González, *J. Org. Chem.*, 2011, **76**, 2367-2373.
32. N. Candelon, D. Lastécouères, A. K. Diallo, J. R. Aranzaes, D. Astruc and J. M. Vincent, *Chem. Commun.*, 2008, **6**, 741-747.
33. J. D. Crowley, P. H. Bandeen and L. R. Hanton, *Polyhedron*, 2010, **29**, 70-83.

34. A. Sivaramakrishna , P. Suman, E. V. Goud, S. Janardan, C. Sravani, C. S. Yadav and H. S. Clayton, *Res. Rev. Mat. Sci. Chem.*, 2012, **1**, 75-103.
35. C. W. Tornøe, C. Christensen and M. Meldal, *J. Pept. Sci.* 2000, **6**, 594-602.
36. K. Odlo, E. A. Høydahl and T. V. Hansen, *Tetrahedron Lett.* 2007, **48** 2097–2099.
37. K. Barral, *Org. Lett.*, 2007, **9**, 1809-1811.

## Chapter 3

### Synthesis and characterisation of triazolium ionic salts. Application of derived ionic liquids in biphasic catalytic oxidation of octane

#### 2.6 General introduction

This chapter reports on the chemistry of 1,3,4-trisubstituted-1,2,3-triazolium salt derivatives synthesised via the highly efficient “click” chemistry approach followed by *N*-alkylation and anion exchange by salt metathesis reaction to yield a series of ionic liquids (ILs). The ILs were then used as “green” solvents in a modified Fenton-type catalytic biphasic oxidation of octane in the presence of H<sub>2</sub>O<sub>2</sub> and FeCl<sub>2</sub>.

##### 2.6.1 Ionic liquids in catalysis

The applications of room temperature<sup>1</sup> ILs in chemistry<sup>2</sup>, biology<sup>3, 4</sup> and industry<sup>5-7</sup> have received great attention due to their uniqueness that include high ionic conductivity, non-flammability, non-volatility, high thermal stability, wide temperature range for the liquid phase (40 to 200 °C) and their highly solvating and non-coordinating properties. The high interest of their utilisation in catalysis is due to the possibility of catalyst/solvent recycling and the fact that they have an acceleration effect on some catalytic chemical reactions. Their recycling ability varies depending on the stability of the IL and catalyst used with several reported recyclable applications in the literature.<sup>3, 8-10</sup> Recycling is basically possible due to the non-volatile nature of ILs and the solubility of some organic compounds in water. Hence, the product may be easily separated by simple distillation or through extraction with non-polar solvents.

Oxidation is one of the most important topics in organic C-H activation due to the abundant nature of alkanes. Successful conversion of alkanes into valuable products such as alcohols, carboxylic acids and alkenes under controlled catalytic conditions can offer large economic benefits.<sup>9, 11, 12</sup>

The well-known chemical catalytic methods for this process suffer from various disadvantages including difficulty of catalyst recovery, comparatively expensive, decomposition at moderate temperatures, and uncontrolled reactivity leading to a wide range of side-products.<sup>11</sup>

The application of ILs in oxidation reactions has also recently drawn considerable attention due to the easy catalyst recycle and product recovery, which also makes them economically viable and environmentally friendly. Until now, most of the research in this field has mainly focused on alkyimidazoles (**i**, Figure 3.1) as source of ILs and their applications which have been extensively reported on.<sup>13-17</sup> But there are growing stability concerns about the decomposition of the imidazolium based ILs via bond cleavage at position C-2 under basic conditions leading to formation of side products. The two *N*-atoms around C-2 make it more acidic, thus accessible to basic environment for deprotonation, while 1,2,3-triazolium salts (**ii**, Figure 3.1) lack a carbon atom flanked by two *N*-atoms.<sup>18</sup> When compared structurally, the C-2 atom in imidazolium salts has been replaced by *N*-atom in triazolium salts resulting in more stability to decomposition under basic reaction conditions. This is a distinct advantage utilised in this study.

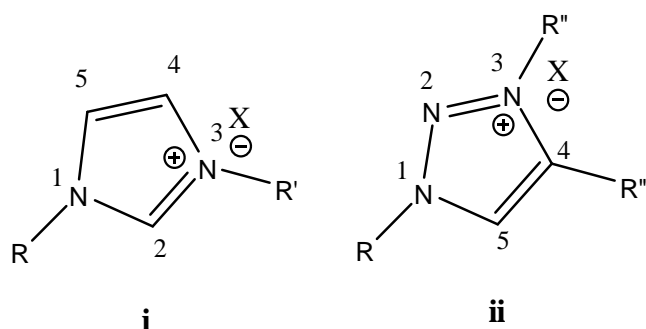
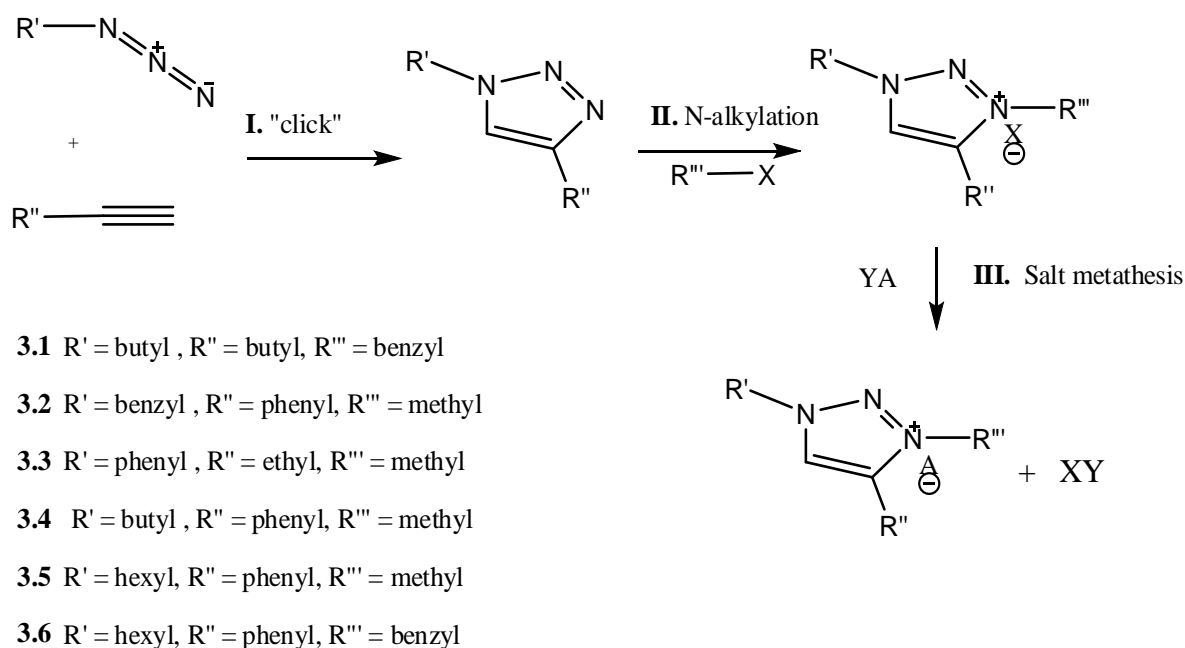


**Figure 3.1** : Structures of azolium salts: **i**– imidazolium; **ii**–1,2,3-triazolium.

## 2.7 Results and discussion

### 2.7.1 Synthesis of triazolium ionic liquids

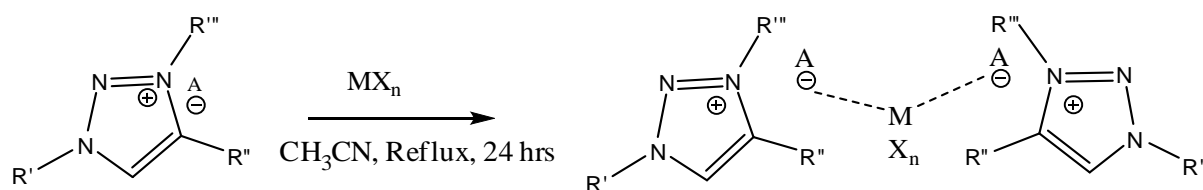
1,2,3-triazolium-based salts (**3.1-3.7**) were synthesised in a three-step procedure consisting of Cu-catalysed cycloaddition reaction of azides with alkynes (**I**, Scheme 3.1), *N*-alkylation of the resulting 1,2,3-triazoles (**II**, Scheme 3.1) followed by salt metathesis (**III**, Scheme 3.1).



**Scheme 3.1:** Schematic preparation of 1,2,3-triazolium ionic liquids.

### 2.7.2 Preparation of the ionic liquid dissolved catalyst

The catalyst composite was achieved by mixing appropriate amounts of the required triazolium ionic salt with the metal salt [M] in acetonitrile under nitrogen and refluxing at 80 °C for 24 hours (Scheme 3.2).



**Scheme 3.2 :** Illustration of inter-ionic interactions in the dissolution of the catalyst in the ionic liquid phase.

### 2.7.3 Syntheses and characterisation of triazolium ionic liquids

One of the key objectives of this project was the design of cheap, non-toxic, efficient and easy to handle system that can be used for the catalytic oxidation of octane. The first target was the preparation of a series of related halide-free triazolium salts which were later used as ILs for

biphasic metal catalysed oxidation catalysis. A general route to the preparation of the ionic salts is presented in Scheme 3.1. The triazole compounds (**I**) were synthesised by the adaptation of previously reported methods based on “click” chemistry.<sup>19-23</sup> The triazolium nitrate-based ionic salts (**II**) were synthesised by *N*-alkylation of the 1,4-disubstituted triazole compounds, followed by (**III**) salt metathesis between the triazolium halide salts and silver nitrate to give desired triazolium nitrate ILs. To purify the salts, the residue was re-dissolved in dichloromethane and washed with excess water to remove impurities. All the synthesised ILs were isolated as oily liquids at room temperature after workup.

### 2.7.3.1 NMR analysis

NMR studies showed significant chemical shifts in the salts when compared to the starting neutral triazoles. The formation of formal (+1) charge on the nitrogen of the triazolium ring resulted in decrease of electron density in the ring which was indicated by a downfield shift of the triazolium proton (*C-H*) resonance peak. The chemical shifts for the aryl and alkyl groups bonded to the triazole ring were also noted to shift downfield when compared to neutral triazole.

The study of anion exchange was further performed using nitrogen-15 isotope (<sup>15</sup>N-) NMR. Electronic and structural changes due to bonded groups around the nitrogen containing ILs are usually reflected on the NMR chemical shift of the nitrogen nucleus.<sup>24</sup> <sup>15</sup>N-NMR spectra of compounds (**3.1-3.6**) are presented in Appendix A3. All the ILs showed expected characteristic nitrogen peaks which corresponded to the nitrogen atoms from the triazolium ring and from the anion (nitrate) present in the compounds.

### 2.7.3.2 Single crystal XRD studies

Due to increasing interest in the applications of substituted 1,2,3-triazolium salts in various fields,<sup>25-28</sup> they have been studied extensively by a variety of techniques including full structural studies by single crystal X ray diffraction. Single crystals of **3.3a** and **3.6a** suitable for X-ray diffraction studies were grown by slow diffusion of diethyl ether into a dichloromethane solution of the salts at ambient temperatures. Selected bond lengths and angles for **3.3a** and **3.6a** are presented in Tables 3.1 and 3.2 respectively.

Figure 3.2 presents an ORTEP diagram of 4-ethyl-3-methyl-1-phenyl-1H-1.2.3-triazol-3-ium iodide (**3.3a**) which crystallised in the monoclinic crystal system with P21/c space group symmetry.



Bond distances (Table 3.1) between N(1)-N(2) = 1.333(6) Å and N(2)-N(3) = 1.295(8) Å are in the range for partial double bonds, supporting delocalization of electron density in the triazole ring.<sup>29-31</sup> However, the increase of N(1)-N(2) = 1.324(2) Å compared to that of a cyclic amino group was due to strong hydrogen bond with C(9) (Figure 3.3 ).

**Table 3.1:** Selected bond lengths (Å) and angles (°) for **3.3a**.

N1 – N2	1.333(6)	N3 – C3	1.460(9)	N2 – N3 – C1	114.3(5)
N2 – N3	1.295(8)	C1 – C4	1.471(8)	N3 – C1 – C2	103.7(5)
N1 – C2	1.336(7)	N1 – C6	1.433(6)		
N3 – C1	1.349(8)	N1 – C2 – C1	107.0(5)		
C1 – C2	1.353(8)	N1 – N2 – N3	103.4(5)		
C2 – H2	0.949(7)	N2 – C1 – C4	130.6(6)		

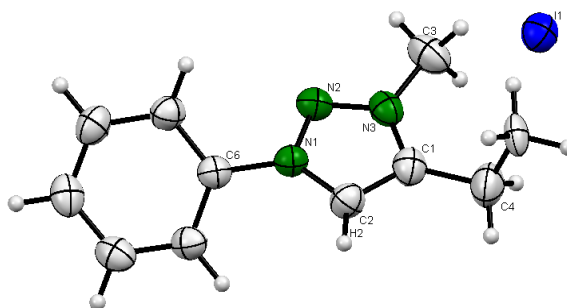


**Figure 3.2:** Crystal structure of compound **3.3a**; thermal ellipsoids are drawn at the 50% probability level.

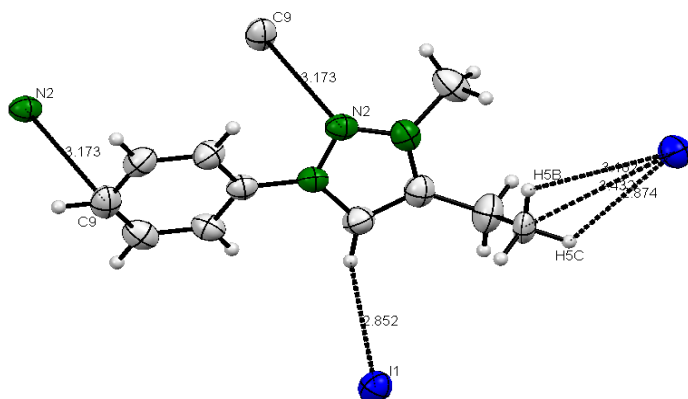


**Figure 0.3:** Structure of **3.3a** showing the key atoms engaged in hydrogen bonding.

The strong hydrogen bond between the acidic hydrogen H(2) and counter anion iodide I(1), C(2)-H(2)...I(1) = 0.852 Å resulted in a slight increase in the bond distance C(4)-H(4) = 0.949(7) Å. N(2) is involved in close contacts with the substituent phenyl group carbon (C(9)···N(2) = 3.173 Å).

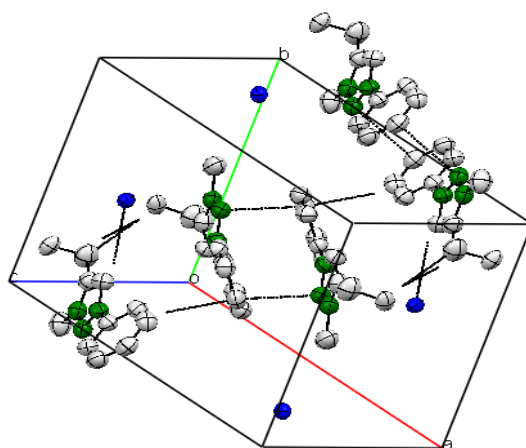


**Figure 0.4** : Close contacts in the crystal structure of compound **3.3a**.

The crystal packing shows a network of intermolecular hydrogen bonding and  $\pi\cdots\pi$  interactions between the centres of gravity of the phenyl rings (C6-C11) which stabilise the triazolium structure in parallel layers of interacting species (Figure 3.4).

It is interesting to note that both edge-to-face (Figure 3.5a, also known as T-shaped or edge-on) and parallel displaced (Figure 3.5b, also referred to as parallel off-centered)  $\pi$  stacking was observed for the crystal packing in **3.3a**.

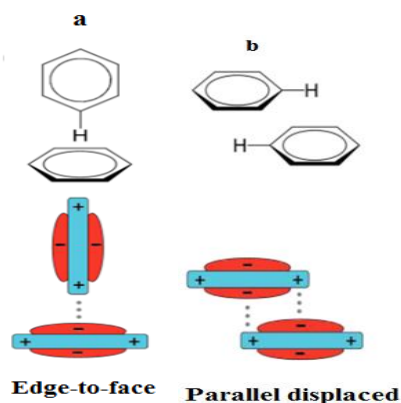


**Figure 0.5** : Schematic representation of interaction geometries of a benzene ring.<sup>32, 33</sup>

**Table 3.2:** Selected bond lengths (Å) and angles (°) for **3.6a**.

N1 – N2	1.318(2)	C1 – C2	1.375(3)	N2 – N3 – C1	112.6(2)
N2 – N3	1.324(2)	C1 – N3	1.373(3)	N3 – C1 – C2	103.8(2)
N3 – C9	1.474(3)	N1 – C2	1.347(3)		
C1- N3	1.373(3)	N2 – N1 – C2	112.3(2)		
C1– C3	1.472(3)	N1 – C2 – C1	106.7(2)		
C2 – H2	0.930(2)	N1 – N2 – N3	104.6(2)		

Figure 3.6 presents an ORTEP diagram of 3-benzyl-1-hexyl-4-phenyl-1H-1,2,3-triazol-3-ium bromide (**3.6a**) which crystallised in the monoclinic crystal system with P-1 space group symmetry. When compared to **3.3a** similar structural patterns were observed for the crystal structure of **3.6a** especially in terms of bond angles and distances with no major differences that warrant further discussion. Similar trend explained in **3.3a** for the role of hydrogen bonding is also evident in **3.6a**.

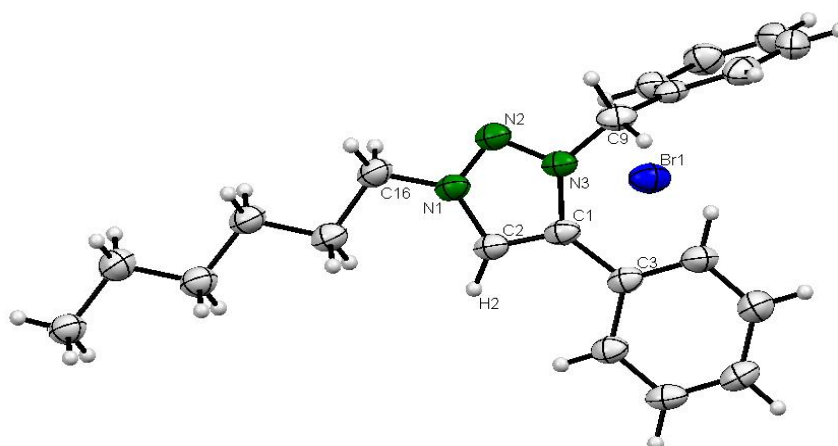


**Figure 0.6 :** Crystal structure of compound **3.6a**; thermal ellipsoids are drawn at the 50% probability level.

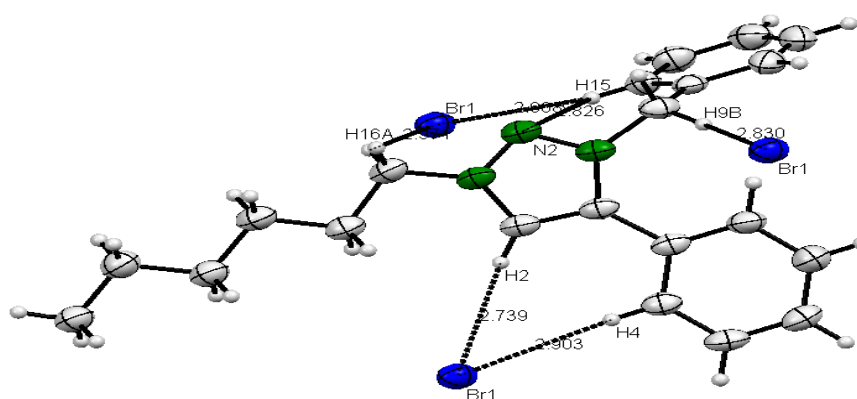


**Figure 0.7 :** Structure of **3.6a** showing the key atoms engaged in hydrogen bonding.

Likewise, the triazole ring acidic proton H(2) was involved in hydrogen bonding (Figure 3.7) with the bromide anion ( $\text{Br}(1)\text{c}\dots\text{H}(2)\text{-C}(2) = 2.739 \text{ \AA}$ ). The neighbouring protons from the phenyl ring and the alkyl chain were also involved in hydrogen bonding with the bromide anion ( $\text{Br}(1)\dots\text{H}(15)\text{-C}(15) = 2.739 \text{ \AA}$ ,  $\text{Br}(1)\dots\text{C}(16\text{A})\text{-H}(16\text{A}) = 2.908 \text{ \AA}$ ). The crystal packing of **3.6a** shows the intermolecular hydrogen bonds and  $\pi\dots\pi$  interactions between the centres of gravity of the phenyl rings which are involved in stabilising the triazolium “dimer” orientation, thus forming a cage-like arrangement with anions in the opposite sides of the cage (Figure 3.8). Similar phenomenon has been reported in biological systems where the interactions between aromatic rings are largely involved in protein–ligand complexation<sup>33, 34</sup> and stabilisation of the double helical structure of DNA<sup>35</sup>.

The packing of **3.6a** may help explain the interaction between the transition metal salt and ionic salts (liquids) in the formation of the  $\text{FeCl}_2/\text{IL}$  catalyst composite. Compound **3.6a** packs in a cage-like form with a central void the volume of which is the right size to fit the metal ion.

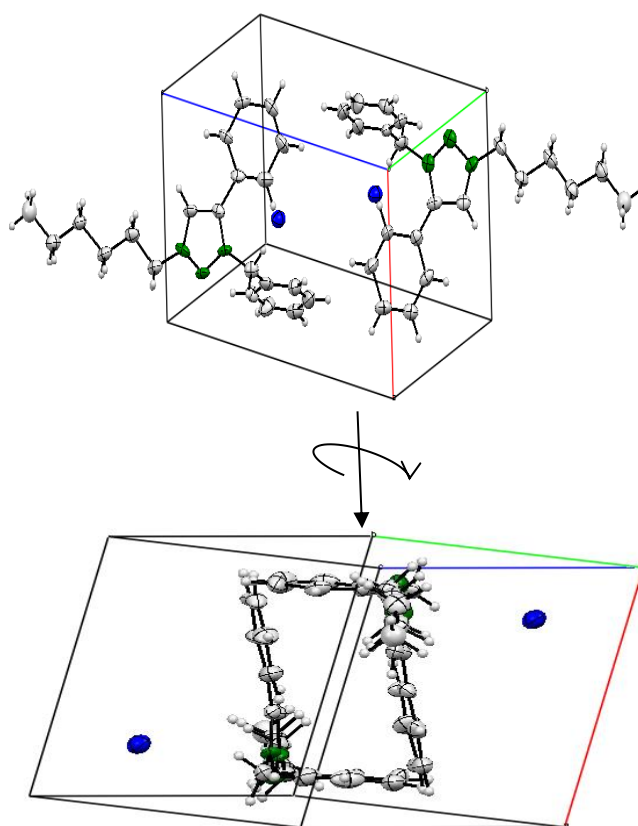


**Figure 0.8** : Crystal structure packing of **3.6a**

It is interesting to note that the use of coordinating ILs as recyclable solvents has led to a variety of applications in catalysis in which they are believed to form IL-metal composites.<sup>38, 39</sup> The orientation of the species in the crystal structure of **3.6a** (Figure 3.8) gives a picture of how they will be involved in the formation of a cage-like structure that stabilises metal ions inside the cage. A similar phenomenon has been noted and reported by Hu *et al.*<sup>40</sup>

### 2.7.3.3 MS analysis

Table 3.3 presents data of the  $m/z$  compounds **3.1a-3.6a**. The parent molecular ions were not detected, however, the fragmented ions  $(M-X)^+$  ( $X = I, Br$ ) were observed and the observed results were comparable with the expected calculated data. A similar fragmentation pattern was observed for both ILs and their precursor salts. Note that only the new compounds were analysed using HRMS.

**Table 3.3:**  $m/z$  ratios obtained for each triazolium salt.

Triazolium salts	$m/z$ (M-X) <sup>+</sup> (Calculated)
<b>3.3a</b>	190.0 (189.0)
<b>3.4a</b>	250.1 (250.1)
<b>3.5a</b>	237.2 (236.1)
<b>3.6a</b>	320.2 (320.2)

## 2.8 Catalysis

The catalytic study was initiated by running a series of preliminary studies to determine the optimum reaction conditions. To optimise the system, the influence of temperature was first investigated, as it has

been established that alkane oxidation reactions are enhanced by elevated temperatures. The performance of the system was investigated at temperatures in the range 40-100 °C using FeCl<sub>2</sub> dissolved in IL **3.5** as the model catalyst system. As expected, the results show a direct correlation between conversion of octane and increase in temperature from 40 to 80 °C (Figure 3.9). Beyond 80 °C, conversion began to drop due to the decomposition of H<sub>2</sub>O<sub>2</sub> at higher temperatures (Scheme 3.3).



**Scheme3.3:** Thermal decomposition of hydrogen peroxide.

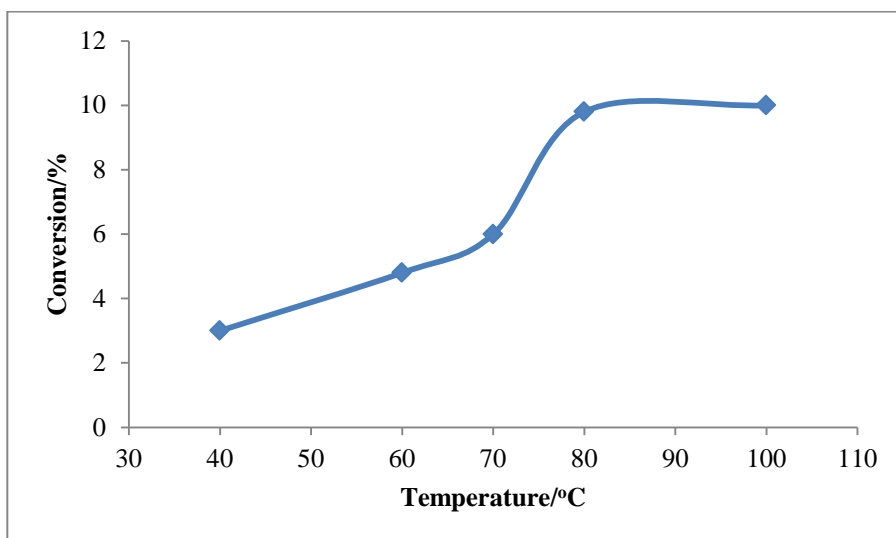


**Figure 0.9:** Effect of temperature on conversion of octane to oxygenated products.

Control reactions (without octane) were performed to compare the rate of thermal decomposition of  $\text{H}_2\text{O}_2$  in pure water with dissolved  $\text{FeCl}_2$  salt (system **A**, Figure 3.10) versus the  $\text{FeCl}_2$ -composite aqueous-IL system (system **B**, Figure 3.10) developed for this study.

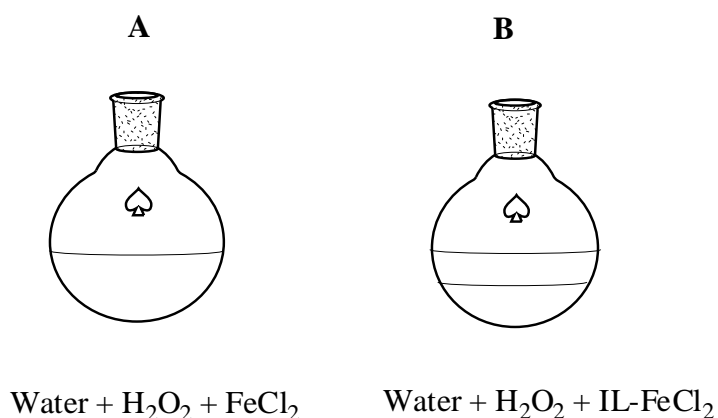


**Figure 3.10 :** System **A** (with only water as solvent) and system **B** (with water and IL as solvents).

It was observed that in both systems the  $\text{H}_2\text{O}_2$  decomposition rate increased with temperature increases. However, after 20 min at 60 °C only traces of  $\text{H}_2\text{O}_2$  were detected in **A**, while in **B** about 40 % remained. Since the decomposition of the oxidant  $\text{H}_2\text{O}_2$  is much faster in system **A** with soluble  $\text{FeCl}_2$ , it shows that dissolution of the  $\text{FeCl}_2$  to the IL phase enhances the

availability of useful oxidant even at higher temperatures which may lead to better productivity of system **B** for the oxidation of substrates. Hence, when both systems (**A** and **B**) were tested for the catalytic activation of octane at 80 °C (Fig. 3.11), system **A** was active for the first 12 h, which tends to level off with time. System **B** showed increased conversion of octane with time up to 50 h after which the system also levelled off. A blank reaction (system **C**) was also performed with a metal-free system based on the same reaction conditions as systems **A** and **B**. No conversion of octane was observed indicating that the metal salt was necessary for any catalytic activation of the substrate.

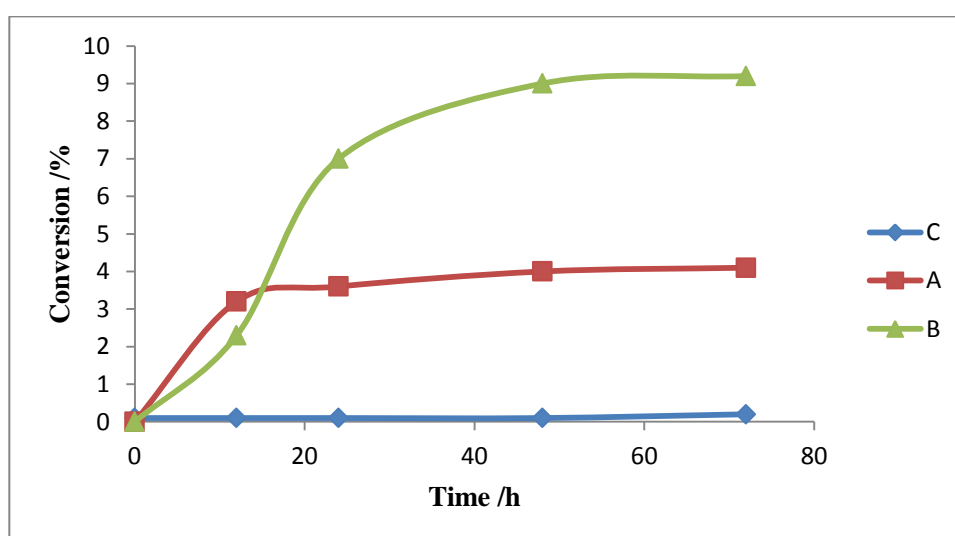


**Figure 0.11:** Effect of time on conversion of octane with systems **A**, **B** and **C** at 80 °C.

A variety of transition metal complexes have been reported to be active as catalysts for alkane activation. Recently, most research has been focused on understanding and mimicking biological enzymes through the use of biologically compatible metals that include Fe, Co and Ni.<sup>41</sup> Hence, in this study, various metal salts ( $\text{FeCl}_3$ ,  $\text{FeCl}_2$ ,  $\text{NiCl}_2$  and  $\text{CoCl}_2$ ) were tested as IL-composite catalysts based on salt **3.5** as the model IL. The result is summarised in Table 2 (Appendix 3), indicating that conversion of octane was highest with  $\text{FeCl}_2$  as the catalyst.

### 2.8.1 Selectivity

The selective oxidation of straight chain hydrocarbons to desired terminal products (alcohols, aldehydes and carboxylic acids) under normal experimental conditions is very difficult to

achieve. This has been associated with order of reactivity which decreases as follows:  $3^\circ\text{CH} > 2^\circ\text{CH} > 1^\circ\text{CH} > \text{CH}_4$ , which then favours the formation of internal oxygenated product with the terminal C-H bond being the least reactive.

When system **B** was employed for the catalytic oxidation of octane, a number of oxygenated products were observed depending on the temperature used. From the GC analysis, the alcohols and ketones were the dominant products at low temperature (40 °C). However, increase in the temperature provided a major increase in substrate conversion but decreased selectivity by greatly increasing the product range (ketones, aldehydes and carboxylic acids). The increased variety of products at higher temperatures was associated with over-oxidation of alcohols to the corresponding ketones, aldehydes and eventually carboxylic acids.



The application of an aqueous–IL biphasic system by Peng *et al.*<sup>42</sup> in the oxidation of benzene resulted in alcohols been extracted into the aqueous phase while the catalyst remained dissolved in the IL phase which dramatically increased the selectivity by reducing the contact between the catalyst and the alcohol. At very high temperatures however, the system formed a homogenised-phase which then increased the contact between the alcohol and the catalyst resulting in a preferential oxidation of the more reactive initial product (alcohol). The same phenomenon was observed when the hybrid **3.5**/FeCl<sub>2</sub> catalyst system was tested.

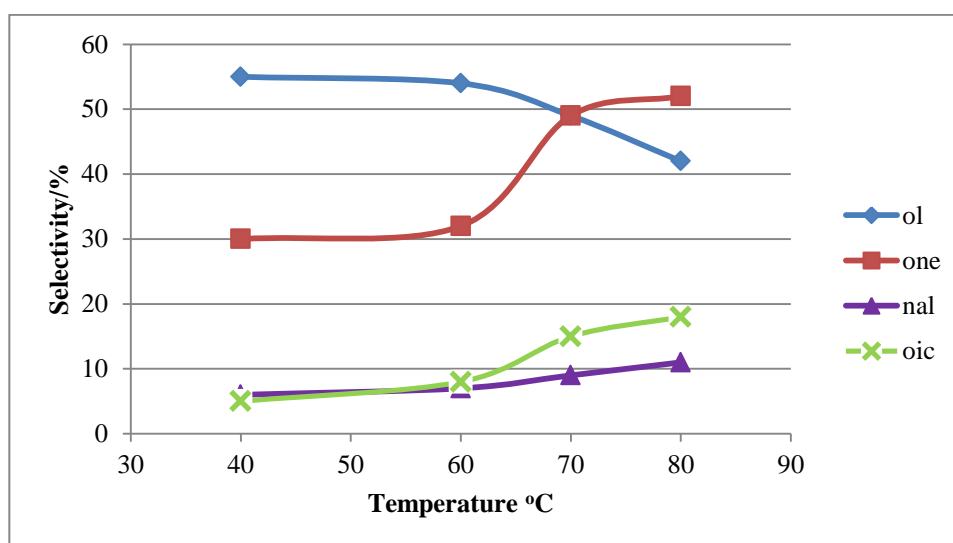


**Figure 3.12:** Effect of temperature on selectivity of oxygenated product using system **B**.



After analysis of product distribution among the carbon atoms on the octane chain C(1)-C(4), it was observed that the C(2) position was the most productive at all temperatures.

For example, at 60 and 80°C (Figures 3.13 and 3.14 respectively) carbon C(2) yielded the highest total regioselectivity to alcohol and ketone products. It is obvious that more alcohol products formed at the lower temperature (Fig. 3.13) which over-oxidised in favour of ketones (Fig. 3.14) at the higher temperature.

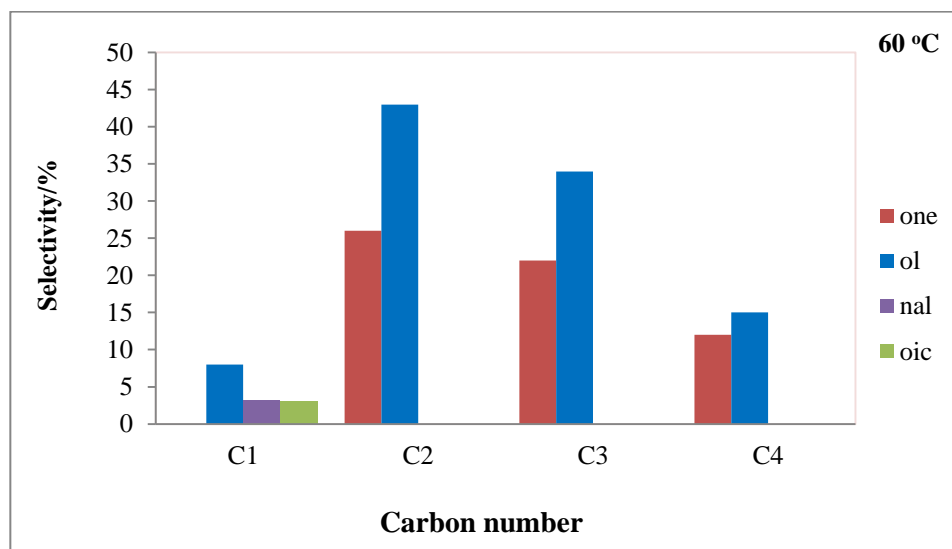


**Figure 3.13:** Regioselectivity (C1-C4) and product distribution at 60 °C.

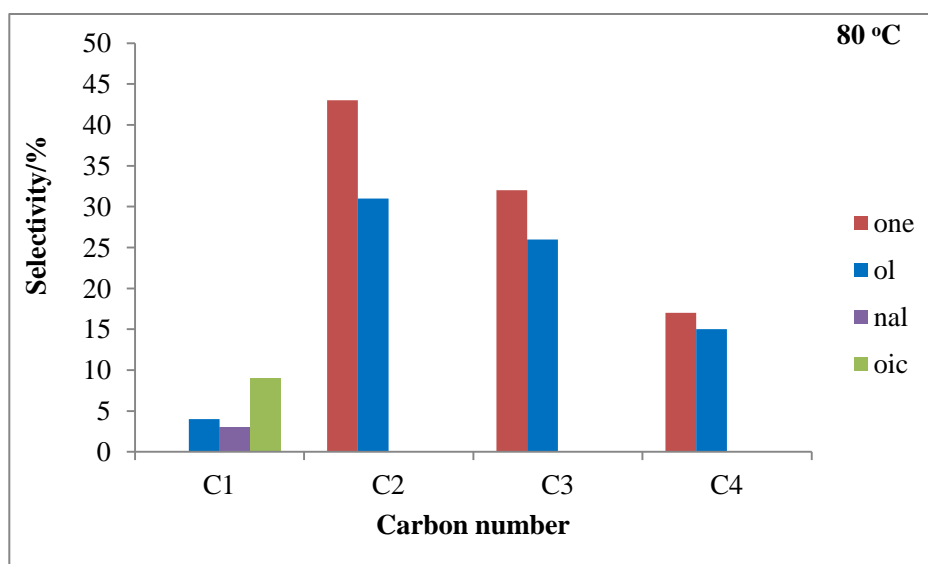


**Figure 3.14:** Effect of temperature on regioselectivity (C1-C4) at 80 °C.

To demonstrate that higher oxidation products (ketones, acids) were produced from the oxidation of alcohols, especially at higher temperatures, a control reaction was performed using 2-octanol as the substrate under similar reaction conditions. The oxidation of 2-octanol to 2-octanone was observed to increase with increase in temperature from 40 to 80 °C (Figure 3.15). Selectivity for 2-octanone was high at elevated temperature (80 °C) compared to a low temperature (40 °C) under the same conditions monitored for 12 hours .

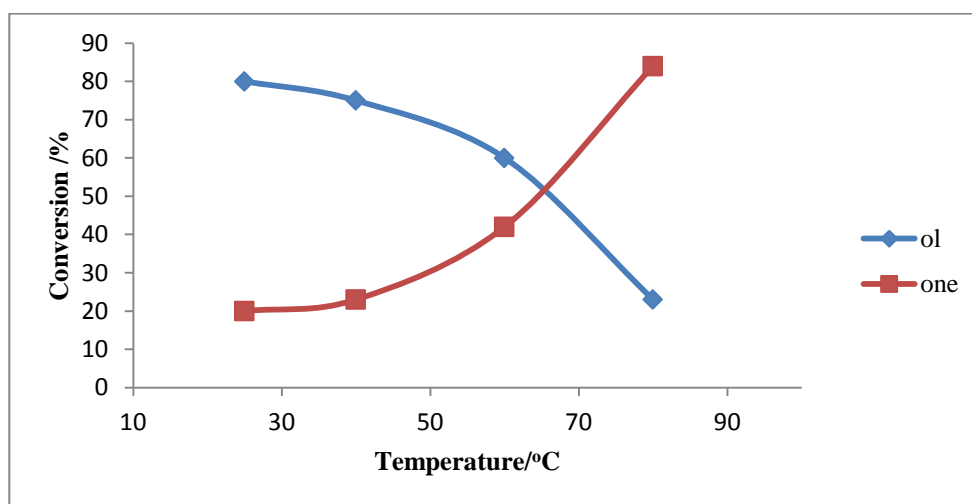


**Figure 3.15:** Effect of temperature on % conversion of 2-octanol to 2-octanone.

## 2.8.2 Product extraction and analysis

After the oxidation reaction, the mixture of crude oxidation products was extracted out of the aqueous-IL biphasic medium using ether. After evaporation of the ether under reduced pressure, the product was analysed using NMR, FTIR and GC-MS. The NMR analysis, confirmed the mix product stream observed by GC. From the  $^1\text{H}$  NMR, a broad proton peak around ~5 ppm was assigned to the hydroxyl proton (O-H), thus indicating the presence of alcohol products (1-octanol, 2-octanol etc.). Far downfield peak (~9 ppm) was assigned to aldehydes ( $-\text{CO}-\text{H}$ ) proton which was formed from the over-oxidation of terminal alcohols. However, no peaks assignable to carboxylic acid was observed, further indicating the limited reactivity of the terminal C(1) carbon.

Interesting FT-IR features confirming successful formation of oxygenated products were observed. The presence of a strong broad band around  $3500\text{--}3200\text{ cm}^{-1}$  indicated the presence of hydroxyl alcohol products. A strong sharp band in the range  $1760\text{--}1665\text{ cm}^{-1}$  was assigned to the stretching  $\text{C}=\text{O}$  vibrations of ketones. The NMR and IR spectra are presented in Appendix 3.

### 2.8.3 Catalyst recycling and reuse

The main reason for interest in application of ILs in catalysis is due to the possibility for preferential dissolution of the catalyst in the IL phase which allows for its recycling.<sup>15, 42</sup> Hence, an attempt to recycle the catalytic system (Trz-FeCl<sub>2</sub>) was explored. Upon the completion of the first reaction cycle, the products were extracted with ether and the system was further washed with more ether and dried under vacuum. The cycle was repeated over six cycles. The results of the catalyst recycling studies are presented in Figure 3.16. The system was found to be recyclable up to the third cycle without significant loss of activity, however, after the third run; a noticeable drop in catalytic conversion was recorded.

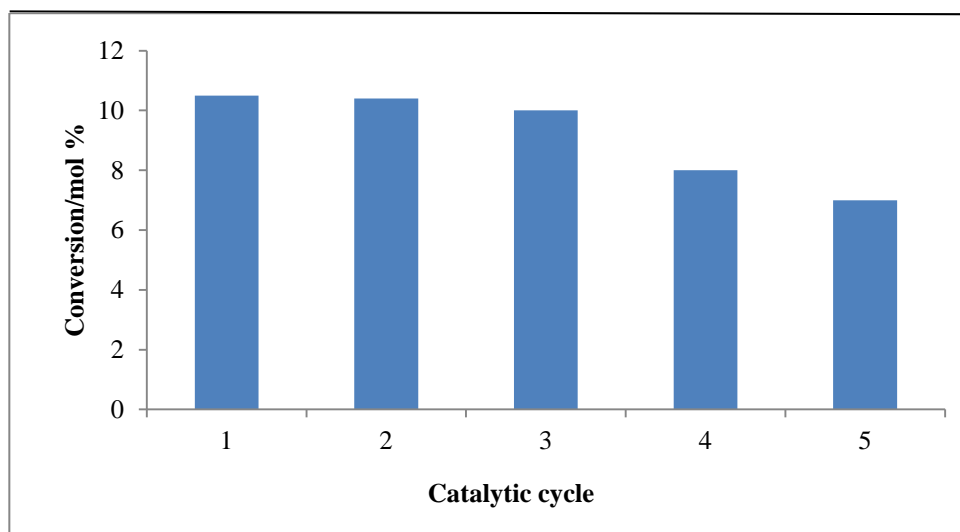


**Figure 3.16:** Catalytic conversion of octane and reuse of the catalytic system.

The loss of catalytic activity after the third cycle might be attributed to the leaching of the catalyst from the IL phase to the product layer at higher temperatures, which was eventually extracted/washed out with the products, hence reducing the amount of active species after the third cycle.<sup>42,43</sup>

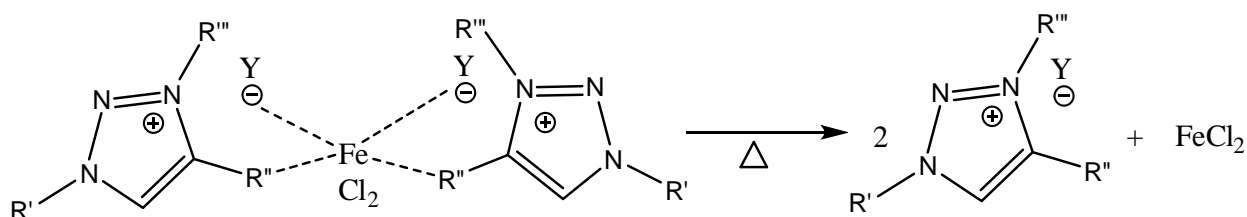


**Figure 3.17:** Possible decomposition of catalytic system.

Inductively coupled plasma (ICP) analyses of the system indicated a decrease of iron content after each catalytic cycle. Similar observation has been reported in the literature and used to explain drop in activity of recyclable catalyst systems.<sup>44-46</sup> The leaching was suspected to be as a result of weakening of the interaction between the IL and the metal salts which resulted in loss of the active species.

#### 2.8.4 Testing of systems 3.1-3.6 at the optimum conditions

Further catalytic experiments were carried out to study the influence of varying the substituent groups (R', R'' and R''') around the triazolium ring for compounds **3.1-3.6**. The catalytic results (Figure 3.18) indicated that **3.1** returned the highest catalytic conversion (12 %) whilst **3.2** was the least active (6 %). It is believed that the introduction of hydrophobicity (alkyl chain) around the triazolium salts enhanced catalytic activity. The hydrophobic regions promoted compatibility with the substrate allowing for better contact with the metal centre. Evidence from the literature shows that the hydrophobic regions of proteins (monooxygenase enzymes like cytochrome P-450) enabled the ready uptake, correct orientation and subsequent functionalization (hydroxylation) of C-H containing compounds.<sup>47</sup>

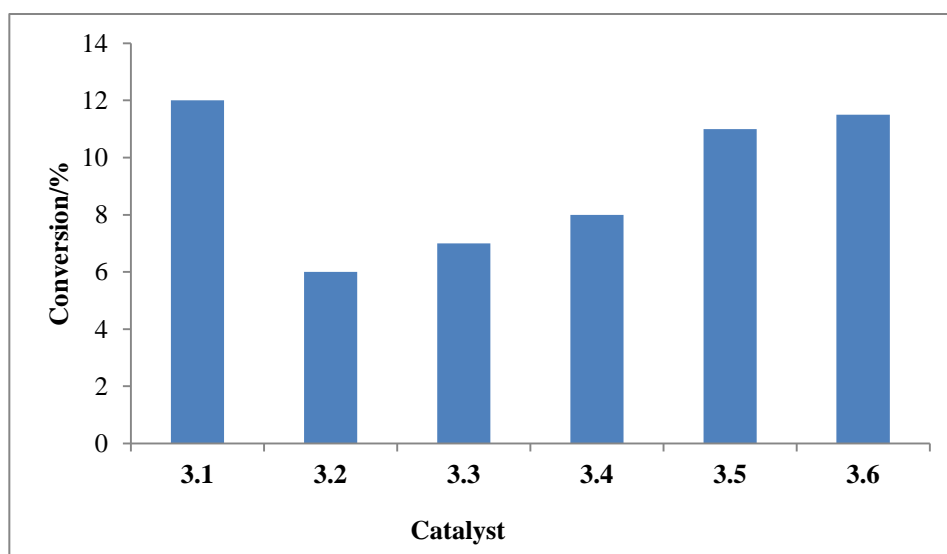


**Figure 3.18** : Catalytic conversion of octane to oxygenated products using system **3.1-3.6**

For all six systems (**3.1-3.6**) tested, overall activity was highest for the formation of ketone products. Of the alcoholic products, all six were significantly more selective for the formation of 2-octanol at low temperatures (60 °C) however increase in temperature resulted in drop in catalyst selectivity and higher product distribution that included 2-, 3-, and 4-octanols.

## 2.9 Summary and conclusions

The main focus of this work was to prepare a series of related 1,2,3-triazolium salts which were then converted into ILs by anion metathesis and used as solvents for the oxidation of octane in the presence of oxidants. The catalyst ( $\text{FeCl}_2$ ) was dissolved in the IL phase with the aim to providing a cheap, recyclable and environmentally friendly catalytic route to valuable oxygenated products. The result shows that the ILs were suitable for the development of biphasic systems for the oxidation of octane. Recycling and re-usage of the systems was demonstrated and were found to be reproducible up to three cycles after which catalytic activity dropped on successive runs. The leaching of the catalyst to the product phase was suspected to be associated with the decrease of catalytic activity.

## 2.10 Experimental

### 2.10.1 Synthesis of ionic salts

Unless stated otherwise, all reagents and solvents were purchased from commercial suppliers and were used without further purification. Glassware was oven dried at 110 °C. All NMR experiments were done using a 400 MHz Bruker ultrashield spectrometer and samples were dissolved in deuterated solvents. The solvents used in column chromatography were obtained from commercial suppliers and used without distillation. Chemical shifts ( $\delta$ ) are reported with respect to tetramethylsilane (TMS) as the internal standard in ppm. The following abbreviations are used to describe peak splitting patterns where appropriate: br = broad, s = singlet, d = doublet, t = triplet, q = quartet, m = multiplet. Infrared spectra (FTIR) were recorded on a Perkin Elmer FT-IR 1600 spectrophotometer.

### 2.10.2 General

The syntheses of 1,2,3-triazolium salts consist of two major steps, which are: construction of 1,2,3-triazole ring system and then its *N*-alkylation (Scheme 3.1).

### 2.10.3 Synthesis of 1,4-triazoles

1,4-triazoles were synthesised using the CuAAC “click” chemistry technique which involved cycloaddition of an organic azide with a terminal alkyne in the presence of Cu(I) as a catalyst. Refer to Chapter 2 for more details.

## 2.10.4 Synthesis of 1,2,3-triazolium salts

Triazolium ionic salts were synthesised by: (a) *N*-Alkylation of the triazole ligands with alkyl halide followed by (b) salt metathesis using silver nitrate.

### 2.10.4.1 General procedure

To a solution of the 1,4-disubstituted triazole (1 equiv. mmol) in acetonitrile (20 mL) was added alkyl halide (2 equiv. mmol). The mixture was heated to 70 °C in a two-neck round bottom flask. After 24hr, the solvent was evaporated under reduced pressure and the crude oil was then purified by column chromatography, first by ethyl acetate to wash out unreacted starting materials and hence methanol to elute the product. Removal of volatiles quantitatively yielded a solid product.

**3-benzyl-1,4-dibutyl-1H-1,2,3-triazol-3-ium bromide<sup>49</sup> (3.1a)** . The starting materials used: 1,4-dibutyl-1H-1,2,3-triazole (2.131 g, 11.2 mmol) and benzyl bromide (4.023 g, 23.3 mmol). Yellow solid product (2.801 g, 70 %). mp: 172-174 °C. <sup>1</sup>H-NMR (CD<sub>3</sub>OD 400 MHz): δ 9.24 (s, 1H, triazole C=CH), 7.35 (s, 5H, Ar), 5.89 (s, 2H, Ar-CH<sub>2</sub>), 4.60 (t, 2H, CH<sub>2</sub>), 2.79 (t, 2H, CH<sub>2</sub>), 1.83-1.87 (m, 2H, CH<sub>2</sub>), 1.43-1.47 (m, 2H, CH<sub>2</sub>), 1.19-1.24 (m, 4H, 2xCH<sub>2</sub>), 0.74-0.80 (m, 6H, 2xCH<sub>3</sub>); <sup>13</sup>C NMR (CD<sub>3</sub>OD 400 MHz): δ 143.9, 132.4, 128.9, 128.1, 53.6, 52.9, 30.4, 28.3, 22.3, 21.2, 18.6, 18.6, 13.3, 13.0

**1-benzyl-3-methyl-4-phenyl-1H-1,2,3-triazol-3-ium iodide<sup>49</sup> (3.2a)**. The starting materials used: 1-benzyl-4-(phenyl)-1H-1,2,3-triazole (1.601 g, 7.4 mmol) and methyl iodide (1.920 g, 13 mmol). Reddish-brown solid product (1.821 g, 79 %). mp: 181-183 °C. <sup>1</sup>H-NMR (CD<sub>3</sub>OD 400 MHz): δ 9.37 (s, 1H, triazole C=CH), 8.06 (s, 1H), 7.72-7.28 (m, 10H), 6.03 (s, 2H), 4.30 (s, 3H); <sup>13</sup>C NMR (CD<sub>3</sub>OD 400 MHz): δ 143.1, 131.7, 130.8, 129.7, 129.6, 129.4, 121.6, 57.6, 31.4.

**4-ethyl-3-methyl-1-phenyl-1H-1,2,3-triazol-3-ium iodide (3.3a)**. The starting materials used: 4-ethyl-1-phenyl-1H-1,2,3-triazole (3.124 g, 11.3 mmol) and methyl iodide (1.92 g, 13.4 mmol). Off-white solid product (1.8 g, 79 %). mp: 181-183 °C. <sup>1</sup>H NMR (CD<sub>3</sub>OD 400 MHz): (s, 1H), δ 9.02 (s, 1H, triazole C=CH), 7.82-7.80 (m, 2H, Ar), 7.68-7.66 (t, 3H, Ar), 4.34 (s, 3H, CH<sub>3</sub>), 2.19-2.13 (m, 2H, CH<sub>2</sub>), 1.05 (m, 3H, CH<sub>3</sub>); <sup>13</sup>C NMR (CD<sub>3</sub>OD 400 MHz): δ 11.2, 23.9, 39.7, 56.8, 124.0, 130.0, 130.7, 130.8, 132.9, 144.6: HRMS (ESI) m/z for C<sub>11</sub>H<sub>13</sub>N<sub>3</sub>[M-I]:calculated : 189.1, found : 190.0.

**1-butyl-3-methyl-4-phenyl-1H-1,2,3-triazol-3-ium iodide<sup>49</sup> (3.4a).** The starting materials used 1-butyl-4-phenyl-1H-1,2,3-triazole (4.013 g, 19.3 mmol) and methyl iodide (5.64 g, 39.2 mmol). Yellow-orange oily product (5.31 g, 81 %). <sup>1</sup>H NMR (CDCl<sub>3</sub> 400 MHz): δ 9.010 (s, 1H, triazole C=CH), 7.81-7.79 (d, 2H, Ar), 7.68 (t, 3H, Ar), 4.77 (m, 2H, CH<sub>2</sub>), 4.34 (s, 3H, CH<sub>3</sub>), 2.13-2.09 (m, 2H, CH<sub>2</sub>), 1.53-1.51 (m, 2H, CH<sub>2</sub>), 1.05 (m, 3H, CH<sub>3</sub>); <sup>13</sup>C NMR (CDCl<sub>3</sub> 400 MHz): δ 13.8, 20.5, 32.3, 39.7, 55.1, 124.0, 130.0, 130.7, 130.8, 132.9, 144.6.

**1-hexyl-3-methyl-4-phenyl-1H-1,2,3-triazol-3-ium iodide (3.5a).** The starting materials used: 1-hexyl-4-phenyl-1H-1,2,3-triazole (4.012 g, 19.2 mmol) and methyl iodide (5.641 g, 39.2 mmol). Yellow-orange solid product (4.259 g, 93 %). mp: 218-220 °C. <sup>1</sup>H NMR (CD<sub>3</sub>OD 400 MHz): δ 9.02 (s, 1H, triazole C=CH), 7.82 (d, 2H, Ar), 7.68 (t, 3H, Ar), 4.76 (t, 2H, CH<sub>2</sub>), 4.34 (s, 3H, CH<sub>3</sub>), 2.15-2.11 (m, 2H, CH<sub>2</sub>), 1.51-1.40 (m, 6H, 3xCH<sub>2</sub>), 0.95 (t, 3H, CH<sub>3</sub>); <sup>13</sup>C NMR (CD<sub>3</sub>OD 400 MHz): δ 14.4, 23.5, 27.0, 30.3, 32.3, 39.7, 55.3, 124.0, 130.0, 130.7, 132.9, 144.6.

**3-benzyl-1-hexyl-4-phenyl-1H-1,2,3-triazol-3-ium bromide (3.6a).** The starting materials used: 1-hexyl-4-phenyl-1H-1,2,3-triazole (6.015 g, 26.3 mmol) and benzyl bromide (8.924 g, 52.1 mmol). Brown-oily product (8.484 g, 81 %). <sup>1</sup>H NMR (CD<sub>3</sub>OD 400 MHz): δ 9.02 (s, 1H, triazole C=CH), 7.61-6.65 (m, 5H, Ar), 7.34-7.36 (m, 3H, Ar), 7.18-7.20 (m, 2H, Ar), 5.89 (s, 2H, Ar-CH<sub>2</sub>-), 4.76 (t, 2H, CH<sub>2</sub>), 2.11-2.14 (m, 2H, CH<sub>2</sub>), 1.37-1.41 (m, 6H, 3xCH<sub>2</sub>), 0.94 (t, 3H, CH<sub>3</sub>); <sup>13</sup>C NMR (CD<sub>3</sub>OD 400 MHz): δ 144.6, 132.9, 130.7, 130.0, 124.0, 55.3, 39.7, 32.3, 30.3, 27.0, 27.0, 27.0, 23.5, 14.4; HRMS (ESI) m/z for C<sub>21</sub>H<sub>25</sub>N<sub>3</sub> [M-Br]: calculated: 320.21, found: 320.21.

### 2.10.5 Synthesis of ionic liquids

To a solution of triazolium salt (1 equiv. mmol) in dry DCM (20 mL) was added a solution of AgNO<sub>3</sub> (1 equiv. mmol) in DCM (10 mL). The resulting mixture was then allowed to stir at room temperature overnight. The precipitate of AgX (X = I or Br) formed was filtered through celite and the solvent was evaporated and the residue was washed with diethyl ether and allowed to dry under vacuum.

**3-benzyl-1,4-dibutyl-1H-1,2,3-triazol-3-ium nitrate (3.1).** The starting materials used **3.1a** (4.731 g, 12.4 mmol) and AgNO<sub>3</sub> (4.012 g, 23.2 mmol). Brown oily liquid (3.832 g, 94%). <sup>1</sup>H-NMR (CD<sub>3</sub>OD 400 MHz): δ 9.01 (s, 1H, triazole C=CH), 7.12-7.30 (s, 5H, Ar), 5.62 (s, 2H, Ar-CH<sub>2</sub>), 4.62 (t, 2H, CH<sub>2</sub>), 2.12 (t, 2H, CH<sub>2</sub>), 1.81-1.83 (m, 2H, CH<sub>2</sub>), 1.32-1.24 (m, 2H, CH<sub>2</sub>) 1.19-1.24 (m, 4H, 2xCH<sub>2</sub>), 0.85-0.90 (m, 6H, 2xCH<sub>3</sub>); <sup>13</sup>C NMR (CD<sub>3</sub>OD 400 MHz): δ 143.7, 132.4, 128.8, 128.3, 53.4, 52.9, 30.5, 28.7, 22.4, 21.6, 18.7, 18.7, 13.5, 13.3. IR ν<sub>max</sub> (cm<sup>-1</sup>): 3442 (s), 3334 (b), 3214 (s), 1627 (m), 1614 (m), 1501(s), 1435 (s), 1358 (s), 805 (s), 758 (s), 724 (m), 523 (m), 484 (m). HRMS (ESI) m/z for C<sub>17</sub>H<sub>26</sub>N<sub>3</sub>[M-NO<sub>3</sub>]: calculated: 272.2, found: 272.9.

**1-benzyl-3-methyl-4-phenyl-1H-1,2,3-triazol-3-ium nitrate (3.2).** The starting materials used **3.2a** (2.187 g, 6.4 mmol) and AgNO<sub>3</sub> (1.984 g, 12.2 mmol). Light brown oily product (1.801 g, 98%). <sup>1</sup>H NMR (CDCl<sub>3</sub> 400 MHz): δ 8.996 (s, 1H, triazole C=CH), 8.061 (s, 1H), 7.358-7.582 (m, 10H, Ar), 5.801 (s, 2H, Ar-CH<sub>2</sub>-), 4.229 (s, 3H, N-CH<sub>3</sub>); <sup>13</sup>C NMR (CDCl<sub>3</sub> 400 MHz): δ 143.3, 131.7, 131.6, 129.7, 129.6, 129.3, 121.9, 57.4, 38.6. IR ν<sub>max</sub> (cm<sup>-1</sup>): 3442 (s), 3334 (b), 3214 (s), 1627 (m), 1614(m), 1501(s), 1435 (s), 1358 (s), 805(s), 758(s), 724 (m), 523(m), 484(m). C<sub>16</sub>H<sub>13</sub>N<sub>3</sub>[M-NO<sub>3</sub>]: calculated: 250.2, found: 250.1.

**4-ethyl-3-methyl-1-phenyl-1H-1,2,3-triazol-3-ium nitrate (3.3).** The starting materials used **3.3a** (2.012 g, 5.4 mmol) and AgNO<sub>3</sub> (0.907 g, 6.2 mmol). Colourless oily product (1.601 g, 98%). <sup>1</sup>H NMR (CDCl<sub>3</sub> 400 MHz): δ 9.18 (s, 1H, triazole C=CH), 7.53-7.62 (m, 5H, Ar), 4.37 (m, 3H, N-CH<sub>3</sub>), 1.30-1.33 (m, 3H, CH<sub>3</sub>); <sup>13</sup>C NMR (CDCl<sub>3</sub> 400 MHz): δ 165.0, 143.3, 131.9, 130.9, 129.7, 129.6, 124.4, 121.8, 63.2, 53.8, 38.7, 13.9; IR ν<sub>max</sub> (cm<sup>-1</sup>): 3411 (b), 3067 (m), 2936 (s), 1747 (s), 1616 (m), 1436 (s), 1324 (s), 1223 (s), 1078 (m), 1016 (s), 767 (s), 697 (m), 548(m). HRMS (ESI) m/z for C<sub>11</sub>H<sub>13</sub>N<sub>3</sub>[M-NO<sub>3</sub>]: calculated: 188.118, found: 190.098.

**1-butyl-3-methyl-4-phenyl-1H-1,2,3-triazol-3-ium nitrate (3.4).** The starting materials used **3.4a** (4.140 g, 12.0 mmol) and AgNO<sub>3</sub> (2.038 g, 12.3 mmol). Light brown oily liquid (3.214 g, 96 %). <sup>1</sup>H NMR (CDCl<sub>3</sub> 400 MHz): δ 9.47 (s, 1H, triazole C=CH), 7.55-7.79 (m, 5H, Ar), 4.78-4.82 (m, 2H, CH<sub>2</sub>), 4.36 (s, 3H, CH<sub>3</sub>), 2.07-2.11 (m, 2H, CH<sub>2</sub>), 1.44-1.49 (m, 2H, CH<sub>2</sub>), 0.96-0.99 (m, 3H, CH<sub>3</sub>); <sup>13</sup>C NMR (CDCl<sub>3</sub> 400 MHz): δ 142.9, 131.8, 129.6, 129.6, 129.4, 121.7, 54.2, 39.5, 31.2, 19.4, 13.3. IR ν<sub>max</sub> (cm<sup>-1</sup>): 3460 (b), 3067 (m), 2936 (s), 1737 (m), 1616 (m), 1436 (s), 1319 (s), 1358 (s), 829 (m), 765 (s), 694 (m), 548 (m). HRMS (ESI) m/z for C<sub>11</sub>H<sub>13</sub>N<sub>3</sub>[M-NO<sub>3</sub>]: calculated: 216.150, found: 216.715.



**1-hexyl-3-methyl-4-phenyl-1H-1,2,3-triazol-3-ium nitrate (3.5).** The starting materials used **3.5a** (4.710 g, 13.1 mmol) and AgNO<sub>3</sub> (2.217 g, 12.2 mmol). Oily product (4.259 g, 93%). <sup>1</sup>H NMR (CDCl<sub>3</sub> 400 MHz): δ 9.26 (s, 1H, triazole C=CH), 7.56-7.66 (dd, 5H, Ar), 4.69 (t, 2H, CH<sub>2</sub>), 4.29 (s, 3H, -N-CH<sub>3</sub>), 2.49 (m, 2H, CH<sub>2</sub>), 2.24-2.28 (m, 2H, CH<sub>2</sub>), 1.30 -1.39 (m, 6H, 3xCH<sub>2</sub>), 0.88 (t, 3H, CH<sub>3</sub>); <sup>13</sup>C NMR (CDCl<sub>3</sub> 400 MHz): 143.3, 131.8, 129.9, 129.5, 129.4, 122.0, 68.5, 67.3, 54.3, 38.5, 33.2, 30.9, 27.8, 25.8, 23.9, 22.3, 22.1, 13.9. IR ν<sub>max</sub> (cm<sup>-1</sup>): 3465 (b), 3077 (m), 2938 (s), 1739 (m), 1655 (m), 1446 (s), 1384 (s), 1321 (s), 767 (s), 692 (m), 448 (m).

**3-benzyl-1-hexyl-4-phenyl-1H-1,2,3-triazol-3-ium nitrate (3.6).** The starting materials used **3.6a** (5.381 g, 13.4 mmol) and AgNO<sub>3</sub> (2.271 g, 13.4 mmol). Brown-oily product (5.104 g, 82%). <sup>1</sup>H NMR (CDCl<sub>3</sub> 400 MHz): δ 9.02 (s, 1H, triazole C=CH), 7.61-6.65 (m, 5H, Ar), 7.34-7.36 (m, 3H, Ar), 7.18-7.25 (m, 2H, Ar), 5.89 (s, 2H, Ar-CH<sub>2</sub>-), 4.76 (t, 2H, CH<sub>2</sub>), 2.11-2.14 (m, 2H, CH<sub>2</sub>), 1.37-1.41 (m, 6H, 3xCH<sub>2</sub>), 0.94 (t, 3H, CH<sub>3</sub>); <sup>13</sup>C NMR (CDCl<sub>3</sub> 400 MHz): δ 144.6, 132.9, 130.7, 130.0, 124.0, 55.3, 39.7, 32.3, 30.3, 27.0, 27.0, 27.0, 23.5, 14.4. IR ν<sub>max</sub> (cm<sup>-1</sup>): 3465 (b), 3077 (m), 2938 (s), 1739 (m), 1655 (m), 1446 (s), 1384 (s), 1321 (s), 767 (s), 692 (m), 448 (m). HRMS (ESI) m/z for C<sub>21</sub>H<sub>25</sub>N<sub>3</sub>[M-NO<sub>3</sub>]: calculated: 320.216, found: 320.217.

## 2.11 Catalytic studies

### 2.11.1 Procedure for oxidation of octane to oxygenated products in water

The oxidants H<sub>2</sub>O<sub>2</sub> (30%) and *t*-BuOOH (70%) were respectively purchased from Sigma-Aldrich and DLD Scientific and used as supplied. The reagents utilised for the calibration of the GC: 1-octanol (99%), 2-octanol (97%), 3-octanol (98%), 4-octanone (99%), octanal (99%) and octanoic acid (99%) were obtained from Sigma-Aldrich, 2-octanone (98%), 3-octanone (97%), 4-octanol (98%) and *n*-octane (99%) were sourced from Fluka, and pentanoic acid (98%) from Merck. Double distilled water was used as solvent.

The paraffin oxidation study was carried out with *n*-octane as the substrate in an aqueous-IL biphasic system. Each catalytic run was performed in air, in a 50 mL round bottom flask equipped with a magnetic stirrer and a condenser. At the end of the reaction, the mixture was allowed to cool to room temperature before it was transferred to a centrifuge vial and centrifuged

for 10 min at a speed of 2500 rpm to allow for phase separation and product extraction. Contents of the aqueous phase were analysed by injecting 0.5  $\mu\text{L}$  into the GC. In all samples, excess solid triphenylphosphine ( $\text{PPh}_3$ ) was added to neutralise any alkyl hydroperoxides (if present) which is known to gradually decompose to produce corresponding ketones (aldehydes) and alcohols in the hot injector chamber and columns. All measurements were conducted in an Agilent Technology 6820 GC System fitted with a flame ionization detector (FID) and an Agilent DB-Wax column with a length of 30m, inner diameter of 0.25 mm and a thickness of 0.25 mm. The GC was calibrated with octane solutions and was found to have a linear correlation from 0.025-0.10 g/mL octane.

Samples were run using HP Chemstation software with the following parameters:

Injector temperature: 240  $^{\circ}\text{C}$

Oven temperature: 90  $^{\circ}\text{C}$

Detector temperature: 220  $^{\circ}\text{C}$

Pressure: 0.052 MPa

Air pressure: 420 kPa

Hydrogen pressure: 410 kPa

## 2.12 Reference list

1. G. Guisado-Barrios, J. Bouffard, B. Donnadiou and G. Bertrand, *Angew. Chem. Int. Ed.*, 2010 28, 4759–4762.
2. P. Wasserscheid and W. Keim, *Angew. Chem., Int. Ed.*, , 2000, 39.
3. S. G. Cull, J. D. Holbrey, V. Vargas-Mora, K. R. Seddon and G. J. Lye, *Biotechnology and bioengineering* 2000, 69, 227-233.
4. S. H. Schöfer, N. Kafzik, P. Wasserscheid and U. Kragl, *Chem Comm.* , 2001, 425-426.
5. N. V. Plechkova and K. R. Seddon, *Chem. Soc. Rev.* , 2008, 37, 123-150.
6. M. Koel, *Crit. Rev. Anal. Chem.* , 2005, 35, 177-192.
7. P. J. Kubisa, *Polym. Chem.* , 2005, 43, 4675-4683.
8. A. J. Carmichael, M. J. Earle, J. D. Holbrey, P. B. McCormac and K. R. Seddon, *Org. Lett.*, 1999, 7, 997-1000.
9. K. R. Seddon and A. Stark, *Green Chem.*, 2002, 4, 119-123.
10. C. Hardacre, J. D. Holbrey, S. P. Katdare and K. R. Seddon, *Green Chem.*, 2002, 4, 143-146.
11. A. Sivaramakrishna , P. Suman, E. V. Goud, S. Janardan, C. Sravani, C. S. Yadav and H. S. Clayton, *Research and Reviews in Materials Science and Chemistry*, 2012, 1, 75-103.
12. J. Z. Miao Sun , Piotr Putaj, Valerie Caps, Frédéric Lefebvre,Jeremie Pelletier, and a. J.-M. Basset, *Chem. Rev.*, 2014, 114, 981–1019.
13. M. Smiglak, A. Metlen and R. D. Rogers, *Acc. Chem. Res.* , 2007, 40.
14. J. H. D. Jr, *Chem. Lett.*, 2004, 33
15. T. Welton, *Coord. Chem. Rev.*, 2004, 248
16. V. I. Parvulescu and C. Hardacre, *Chem. Rev.* , 2007, 107.
17. R. Sebesta, I. Kmentova and S. Toma, *Green Chem.* , 2008, 10
18. Z. Yacob and J. Liescher, in *Ionic Liquids 4 – Classes and Properties*, Humboldt-University Berlin, Germany, 2001.
19. V. V. Rostovtsev, L. G. Green, V. V. Fokin, K. B. Sharpless and K. Barry, *Angew. Chem. Int. Ed.*, 2002, 41, 2596-2599.
20. P. Li and L. Wang, *Letters in Organic Chemistry*, 2007, 4, 23-26.
21. L. Pinhua and L. Wang, *Letters in Organic Chemistry*, 2007, 4, 23-26.
22. D. Wang, *Green Chem.*, 2010, 12, 2120-2123.
23. F. Wang, H. Fu, Y. Jianga and Y. Zhaoa, *Green Chem.*, 2008, 10, 452–456.
24. L. Xiao and K. E. J. Johnson, *Electrochem. Soc.* , 2003, 150 307-311.
25. L. Liang and D. Astruc, *Coord. Chem. Rev.*, 2011, 255, 2933-2940.
26. H. Struthers, T. L. Mindt and R. Schibli, *Dalton Trans.* , 2010, 39, 675-679.
27. R. M. Meudtner, M. Ostermeier, R. Goddard, C. Limberg and S. J. Hecht, *Chem. Eur.* , 2007, 13, 9834-9839.
28. G. F. Manbeck, W. W. Brennessel and R. Eisenberg, *Inorg. Chem.*, 2011, 50, 3431-3440.
29. A. Bondi, *J. Phys. Chem.* , 1964, 68, 441-445.
30. A. R. Katritzky, J. Cobo-Domingo, B. Yang and P. G. Steel, *J. Chem. Res.* , 1999, 162, 452-456.
31. J. Catalan, J. L. G. d. Paz, M. R. Torres and J. D. J. Tomero, *Chem. Soc. Perkin Trans. Faraday Soc.*, 1997, 93, 1691-1697.
32. C. A. Hunter and J. K. M. Sanders, *J. Am. Chem. Soc.* , 1990, 112, 5525–5534.
33. A. Dhotel, Z. Chen, L. Delbreilh, B. Youssef, J. Saiter and L. Tan, *Int. J. Mol. Sci.* , 2013, 14 2303-2333.
34. R. Fasan, R. L. A. Dias, K. Moehle, O. Zerbe, D. Obrecht, P. R. E. Mittl, M. G. Grütter and J. A. Robinson, *Org. Biomol. Chem.*, 2006, 7, 515–526.

35. C. F. Matta, N. Castillo and R. J. Boyd, *J. Phys. Chem.* , 2005, 110, 563–578.
36. J. Pavlinac, M. Zupan, K. K. Laali and S. Stavber, *Tetrahedron Lett.*, 2009 65, 5625–5662.
37. T. Welton, *Coordination Chemistry Reviews*, 2004, 248, 2459–2477.
38. X. K. Hu, L. F. Zhu, X. Q. Wang, B. Guo, J. Q. XuLi and C. W. Hu., *J. Mol. Catal.*, 2011, 342, 41-49.
39. R. H. Crabtree, *Journal of the Chemical Society, Dalton Transactions*, 2001, 2437-2450.
40. J. Peng, F. Shi, Y. Gu and Y. Deng, *Green Chem.*, 2003, 5, 224–226.
41. H. L. Ngo, A. Hu and W. Lin, *Chem. Commun.*, 2003, 1912-1917.
42. V. Cimpeanu, V. I. Pa<sup>^</sup>rvulescu, P. A. s, D. B. a. n, J. M. Thompson and C. Hardacre, *Chem. Eur. J.* , 2004, 10, 4640 – 4646.
43. V. Cimpeanu, A. N. Pa<sup>^</sup>rvulescu, V. I. Pa<sup>^</sup>rvulescu, D. T. On, S. Kaliaguine, J. M. Thompson and C. Hardacre, *J. Catal.*, 2005, 232, 60 – 67.
44. L.C . Branco and C. A. M. Afonso, *Chem. Commun.*, 2002, 3036 – 3037.
45. A. Wada, S. Ogo, S. Nagatomo, T. Kitagawa, Y. Watanabe, K. Jitsukawa and H. Masuda, *Inorg. Chem.*, 2002, 41, 616-618.
46. Z. Yacob and J. Liebscher, in *Ionic Liquids as Advantageous Solvents for Preparation of Nanostructures*, ed. S. T. Handy, 2011 DOI: 10.5772/24349, pp. 3 – 22.
47. A. Wada, S. Ogo, S. Nagatomo, T. Kitagawa, Y. Watanabe, K. Jitsukawa and H. Masuda, *Inorg. Chem.*, 2002, **41**, 616-618.
48. H. Xiao-ke, Z. Liang-fang, G. Bin, L. Qiu-yuan, L. Gui-ying and H. Chang-wei, *Chem. Res. Chin. Univ.* 2011, **27**, 503–507.
49. Z. Yacob and J. Liebscher, *Ionic Liquids as Advantageous Solvents for Preparation of Nanostructures*, ed. S. T. Handy, 2011 pp. 3–22.

## Chapter 4

### Synthesis and application of 1,2,3-triazolium-based nickel complexes as catalysts for the oxidation of alkanes

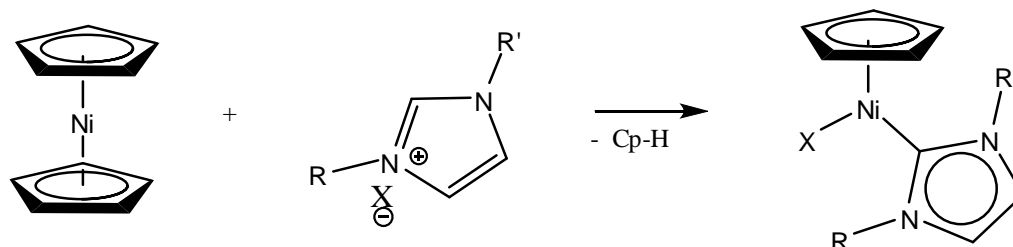
#### 2.13 General introduction

In this chapter the synthesis and characterisation of 1,2,3-triazolium-based nickel complexes are described. The complexes were also tested for the catalytic oxidation of alkanes in the presence of an oxidant under mild reaction conditions.

##### 2.13.1 Synthesis of triazolium nickel complexes

The use of 1,2,3-triazolium salts in organometallic chemistry as sources of ancillary NHC ligands has been recognized due largely to four key properties: i) relatively large covalent contribution to the M–NHC bond therefore lessening dissociation; ii) strong donor ability enabling favourable rates of metal catalysed oxidative addition; iii) the presence of sterically encumbering groups bound to the N-atoms facilitate reductive elimination of products from the metal; iv) the activity of NHC ligands can be remotely modified by introduction of electronic directing substituents.<sup>1</sup>

Since the first synthesis of the complex  $[(\eta^5\text{-C}_5\text{H}_5)\text{Ni}(\text{Cl})(\text{IMes})]$  (**1**; IMes = 1,3-dimesitylimidazol-2-ylidene; Scheme 4.1) by Abernethy, *et al.*<sup>2</sup> from nickelocene and an imidazolium salt, a series of  $[(\eta^5\text{-C}_5\text{H}_5)\text{Ni}(\text{X})(\text{NHC})]$  (X = Cl, Br, I; NHC = *N*-heterocyclic carbene) have been synthesised in a similar fashion (Scheme 4.1).<sup>3-5</sup>



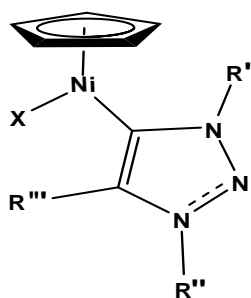
**Scheme 4.1** : Synthesis of  $[(\eta^5\text{-C}_5\text{H}_5)\text{Ni}(\text{X})(\text{NHC})]$ .

## 2.14 Results and discussion

### 2.14.1 Synthesis and characterisation of nickel complexes

It is evident from current literature that only imidazolium salts from the azole family have been widely used for the synthetic method of Abernethy, *et al.*<sup>2</sup> Hence, a modified methodology was developed for the synthesis of the triazolium nickel complexes which involved modification of Abernethy's original synthetic method by applying longer reaction times and an extra product extraction step. The acidity of the 1,2,3-triazolium salts (C-H bond) is weaker than that of the imidazolium salts, which makes imidazolium salts more reactive in this aspect. The two *N*-atoms around *C*-2 of imidazolium ion make it more acidic, thus accessible through basic environments for deprotonation.<sup>6</sup> Therefore, when the unmodified version of the Abernethy's method was employed for this project, comparatively lower yields were obtained.

The method used involve the treatment of a series of triazolium salts with nickelocene in THF under reflux where a rapid colour change from deep green to reddish-violet was observed as the first signs of formation of the triazolium-nickel complexes. Complexes **4.1-4.4** were isolated as violet crystalline solids while **4.5** and **4.6** were reddish pastes. The synthesized nickel complexes were fully characterised by spectroscopic analysis and X-ray crystallography. All complexes were stable towards air and soluble in acetonitrile, dichloromethane and DMSO while sparingly soluble in THF and insoluble in hexane.



**4.1** R' = phenyl , R'' = methyl , R''' = phenyl (X = I)

**4.2** R' = ethyl propionate, R'' = methyl , R''' = phenyl (X= I)

**4.3** R' = propyl , R'' = methyl, R''' = phenyl (X = I)

**4.4** R' = benzyl , R'' = methyl, R''' = phenyl (X = I)

**4.5** R' = butyl , R'' = methyl, R''' = phenyl (X = I)

**4.6** R' = octyl, R'' = methyl, R''' = phenyl (X= I)

**Figure 0.1** : Triazolium-based nickel complexes prepared in this study.

Representative <sup>1</sup>H NMR spectra of the triazolium halide salt and its corresponding nickel complex **4.6** are depicted in Figure 4.2. The <sup>1</sup>H-NMR spectra of all the complexes showed the disappearance of the characteristic triazolium proton (**a**, in Figure 4.2) which resonated around

9-10 ppm in their corresponding triazolium salts, thus indicating successful deprotonation and complexation. However, the effect of the paramagnetic Ni centre resulted in complications in assigning some peaks due to line broadening, signal integration error and abnormal chemical shifts. Hence, some peaks from the  $^1\text{H-NMR}$  assigned to the triazolium ring substituents ( $\text{R}'$ ,  $\text{R}''$  and  $\text{R}'''$ ) were not fully resolved. A similar phenomenon has been reported by Buchowicz, *et al.*<sup>7</sup> Presence of an intense singlet peak around  $\sim 5$  ppm indicated the presence of one  $\eta^5$ -bonded cyclopentadienyl ligand. Other peaks noted in the NMR spectrum indicated the presence of the bonded triazolium ligand with peak positions shifted slightly from their original resonating positions.

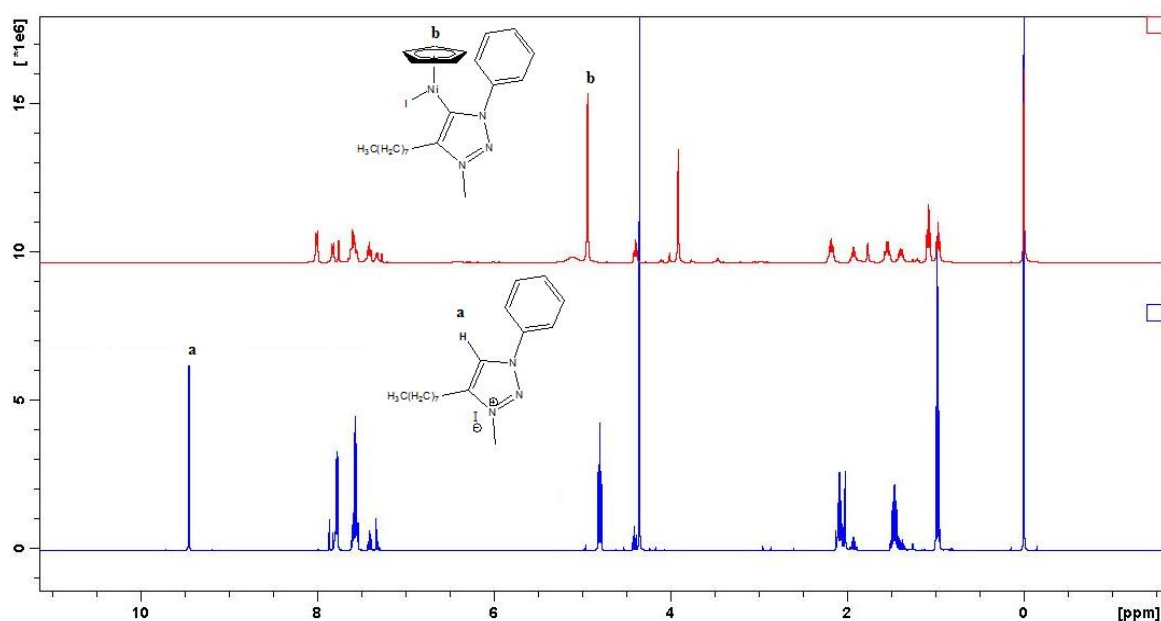


**Figure 0.2 :**  $^1\text{H}$  NMR spectra of a 1,2,3-triazolium salt (bottom) and the corresponding nickel complex **4.6** (top).

The carbene carbon atom which usually resonates around 166-200 ppm was not observed in the  $^{13}\text{C}$  NMR spectra of all prepared complexes. However, a sharp peak which resonated around  $\sim 90$  ppm believed to be the Cp signal was observed in all complexes which indicated formation of the proposed complexes. Similarly, other peaks noted in the  $^{13}\text{C}$  NMR spectra corresponded with the presence of a bonded triazolium ligand in the complex.

### 2.14.1.1 Structural characterisation by single crystal X-ray diffraction

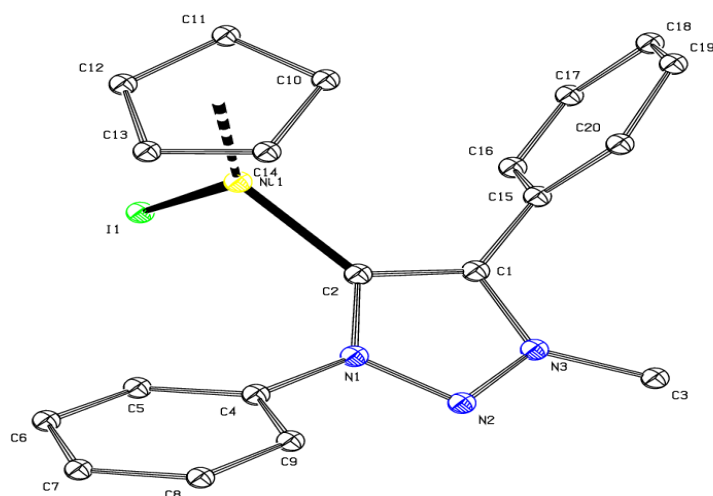


**Figure 0.3** : Molecular structure of **4.1**. For clarity, all hydrogen atoms have been omitted. Displacement ellipsoids are drawn at the 50% probability.

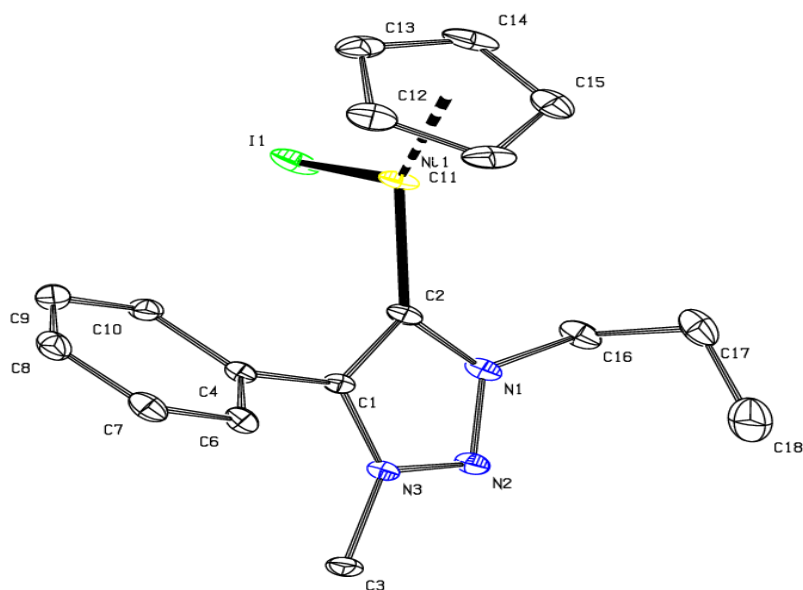


**Figure 0.4** : Molecular structure of **4.3**. For clarity, all hydrogen atoms have been omitted. Displacement ellipsoids are drawn at the 50% probability.



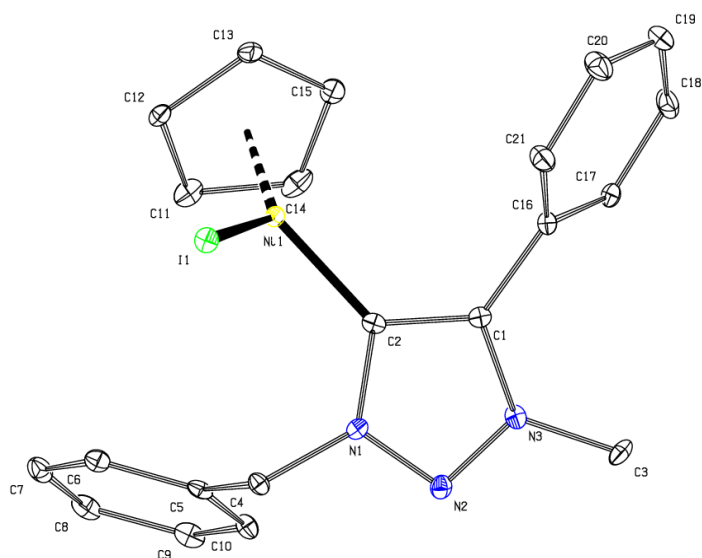


**Figure 0.5** : Molecular structure of **4.4**. For clarity, all hydrogen atoms have been omitted. Displacement ellipsoids are drawn at the 50% probability.

Violet single crystals of **4.1**, **4.3** and **4.4** were obtained from slow diffusion of hexane into dichloromethane solution of **4.1**, **4.3** and **4.4** and their molecular structures were determined by X-ray diffraction. Molecular plots of **4.1**, **4.3** and **4.4** are shown in Figures 4.3, 4.4 and 4.5 respectively, while selected bond lengths and angles are shown in Table 4.1.

Compound **4.1** crystallised in the orthorhombic *Pna21* space group while **4.3** and **4.4** both crystallised in the monoclinic crystal system with space groups *Cc* and *P21/c* respectively. In all three complexes, nickel coordination is trigonal-planar. The Ni-Cp bonds (Table 4.1) are considerably different from each other within every complex. Similar results were reported by Buchowicz, *et al.*<sup>3</sup> No major deviations were observed in the bond lengths and angles of all the complexes when compared with related compounds reported in the literature.<sup>2, 3, 7</sup>

**Table 4.1:** Selected bond lengths (Å) and angles (°) for complexes **4.1**, **4.3** and **4.4**.

d/Å	4.1	4.3	4.4
Ni(1)-I(1)	2.505(4)	2.4951(5)	2.5130(7)
Ni(1)-C(2)	1.89(2)	1.881(3)	1.872(5)
N(1)-C(2)	1.353(4)	1.363(4)	1.376(7)
N(1)-N(2)	1.352(3)	1.337(3)	1.330(8)
N(2)-N(3)	1.303(3)	1.318(3)	1.319(7)
N(3)-C(3)	1.462(5)	1.468(4)	1.451(8)
N(3)-C(1)	1.385(4)	1.369(3)	1.360(8)
I(1)-Ni(1)-C(2)	98.6(7)	97.49(9)	100.1(2)
N(1)-C(2)-C(1)	103.0(2)	102.0(2)	102.0(4)
N(1)-N(2)-N(3)	104.0(2)	103.0(2)	103.4(5)
N(2)-N(3)-C(1)	113.0(3)	112.8(2)	112.4(5)

#### 2.14.1.2 FT-IR analysis of the complexes

There were no significant shifts in the vibration bands of functional groups for FT-IR spectroscopic analysis to be used to distinguish between the synthesised complexes and their corresponding triazolium precursors. However, it was possible to identify some distinctive functional groups which were present due to bonded triazolium ligands which also confirm the formation of complexes. All IR spectra for the prepared complexes are presented in Appendix 4. From an analysis of the FTIR spectra, the  $C_{sp^3}$ -H stretching vibration bands which appeared around 3000–2850  $cm^{-1}$  is due to alkyl chains and the methylene groups.

The presence of -HC=N- from the triazolium rings was confirmed by the appearance of strong vibrational bands around 1335–1250  $cm^{-1}$ . The strong band around 3100–3000  $cm^{-1}$  is associated with C–H stretch from the aromatics due to the phenyl and benzyl rings.

### 2.14.1.3 Thermogravimetric analysis (TGA)

The thermal stabilities of three complexes (**4.1**, **4.2** and **4.3**) were investigated by thermogravimetric analysis (TGA). Heating was conducted at a rate of 10 °C/min in both air and nitrogen over the temperature range of 0-400 °C. A representative example of TGA and DTA data of **4.1** is shown in Figure 4.6. The total weight loss from room temperature to 400 °C is 58%. The TGA curve shows initial weight loss of 1-4% from room temperature to 100 °C which was believed to be due to solvents used for synthesis and extraction of metal complexes.

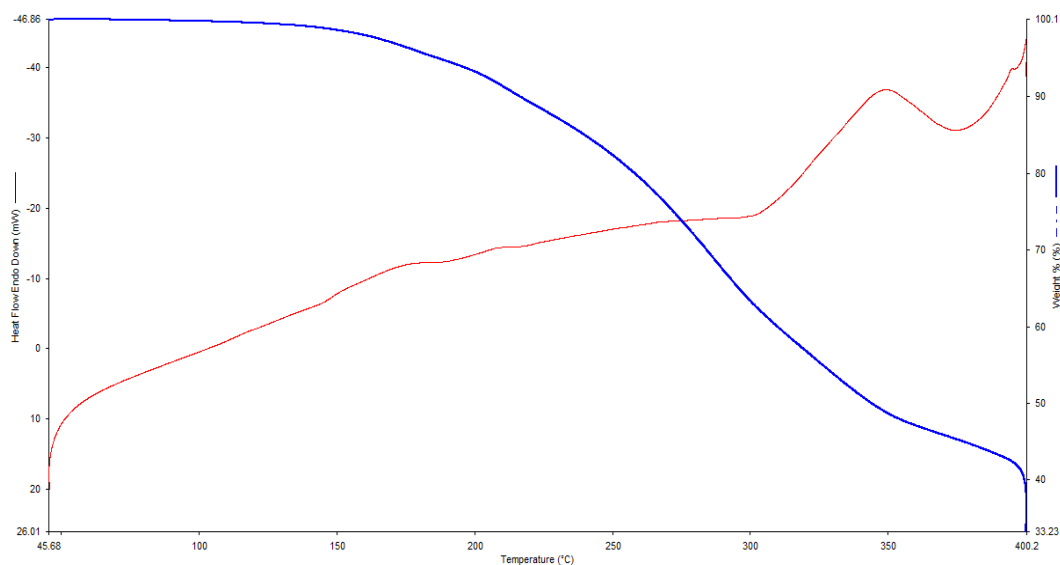
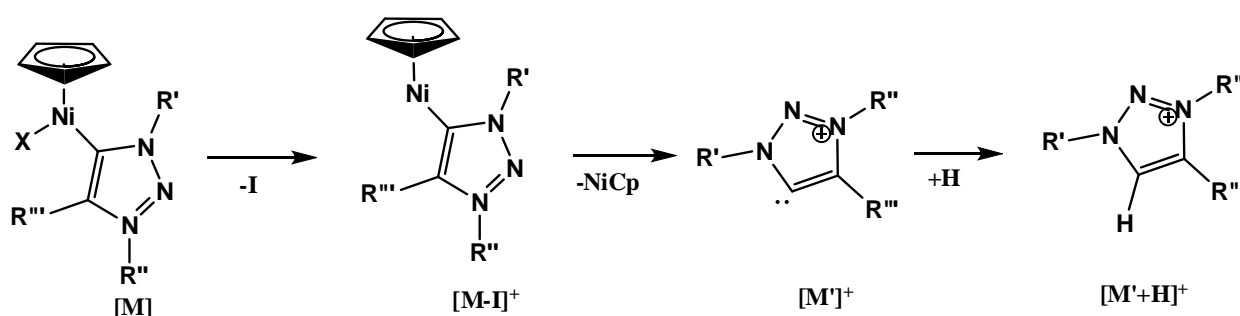


**Figure 0.6:** Thermo gravimetric analysis for **4.1**.

Significant weight loss in all complexes was due to loss of the NHC–triazolium ligand observed at 180 °C in the TGA with a weight loss of 40%. In the DTA, a broad exothermic peak was observed at 350 °C which was due to a loss of the triazolium ligand. The next decomposition was observed at 380 °C which might be due to loss of the Cp from nickel. An endothermic peak was observed in the DTA at 390 °C. There was no significant difference in weight loss from analysis in air or nitrogen. All TGA curves for the prepared complexes are presented in Appendix A4.

#### 2.14.1.4 Mass spectrometry

Mass spectrometry of complexes (**4.1-4.6**) revealed the same fragmentation pattern (Scheme 4.2). Except for **4.2**, the parent molecular peak  $[M]$  was not observed in all metal complexes synthesised. The loss of a halide ( $X=I$ ) anion was the first noted followed by the loss of NiCp to give the uncomplexed carbene ligand  $[M']$  which was protonated to give  $[M'+H]^+$ . The results are summarised in Table 4.2.



**Scheme 4.2:** Possible fragmentation pathways of the generated ions.

**Table 4.2:** Summary of HRMS fragmentation results.

$[M]$	$[M-I+H]^+$	$[M-I]^+$	$[M']^+$	$[M' + H]^+$
<b>4.1</b>	360.0833	358.0866	236.1190	237.1228
<b>4.2</b>	372.0336	-	254.0943	255.0976
<b>4.3</b>	325.1240	324.1071	202.1374	207.0124
<b>4.4</b>	340.1184	338.1218	216.1512	217.1566
<b>4.5</b>	373.0125	372.0851	250.1217	251.1266
<b>4.6</b>	426.0241	425.0716	254.0943	255.0976

### 2.15 Catalytic studies

#### 2.15.1 Oxidation of cyclohexane

A set of reactions were conducted as previously reported<sup>8</sup> with **4.1** as the catalyst and cyclohexane as a substrate. Cyclohexane was first tested since it is a recognized model substrate and in view of the importance of the products.<sup>8-10</sup>

Hydrogen peroxide (H<sub>2</sub>O<sub>2</sub>) was first used as an oxidant since it is a common oxygen source used in research for hydrocarbon oxidations.<sup>11, 12</sup> Results are summarised in Table 4.3.

**Table 4.3:** Catalytic oxidation of cyclohexane using complex **4.1**.

Entry	System	Conversion/ (mol %)	Selectivity		
			Alcohol(s) (mol %)	Ketones(s) (mol %)	A/K*
1†	H <sub>2</sub> O <sub>2</sub>	≤0.1	-	-	-
2	<b>4.1</b> -H <sub>2</sub> O <sub>2</sub>	67	56	43	1.3
3‡	<b>4.1</b> -H <sub>2</sub> O <sub>2</sub>	52	32	63	0.5
4	<b>4.1</b> -H <sub>2</sub> O <sub>2</sub> -HCl	70	41	54	0.8
5	<b>4.1</b> -H <sub>2</sub> O <sub>2</sub> -AcOH	78	58	44	1.3
6	<b>4.1</b> -TBHP-AcOH	62	59	38	1.5

\* A/K = alcohol/ketone ratio; 1† = blank run; all entries (MeCN, 50 °C) except 3‡ (H<sub>2</sub>O, 50 °C).

A blank reaction (entry 1) was performed without a catalyst, no oxygenated products were observed. When the catalyst **4.1** was added, conversion of substrates to oxygenated products was observed (entry 2). Water has been referred to as an environmentally friendly and useful solvent for many reactions including oxidation reactions. When water was tested as the solvent for the catalytic oxidation reaction (entry 3), the conversion dropped with a higher selectivity for ketones. The effect of some acidic additives on the reaction was investigated (entries 4 and 5). It was observed that the addition of a strong acid (i.e. hydrochloric acid) accelerated the oxidation reaction; however, change of the solution colour indicated some decomposition of the catalyst. While addition of the weaker acetic acid yielded no colour change due to catalyst decomposition and a higher conversion was obtained with higher selectivity for the desired alcohol. The effect of changing acid concentration did not have much change on the final product obtained, however higher concentration was associated with catalyst decomposition.

## 2.15.2 Oxidation of *n*-octane

### 2.15.2.1 Influence of temperature

To optimise the system, the influence of temperature was first investigated using **4.1** as model catalyst. The conversion of octane with variation of reaction temperatures is presented in Figure 4.7. In order to obtain the correct concentration of oxygenated products, the reaction was monitored by GC before and after reduction with solid triphenylphosphine. The results show increase in conversion of octane with increase in temperature from 40 to 80 °C. The same phenomenon was reported by others researches.<sup>13, 14</sup> From these results, 80 °C was used as optimum temperature for the remainder of the catalytic testing.

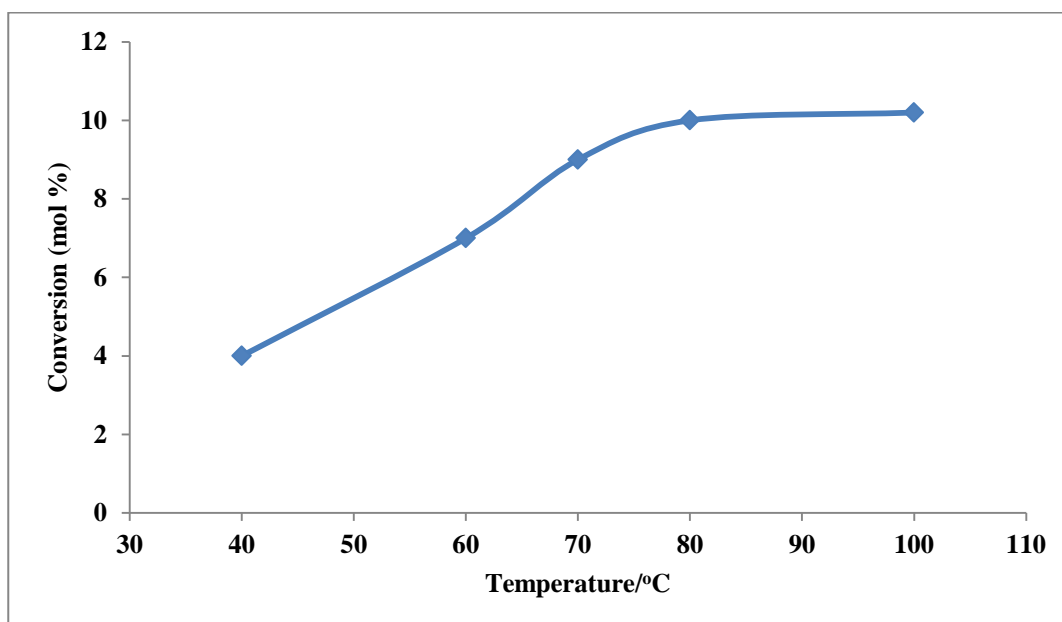


**Figure 0.7:** Effect of temperature in catalytic oxidation of *n*-octane.

The selectivity of the catalyst to the products is presented in Table 4.4. The products obtained were identified by a comparison of their retention times with standard samples. Products (formaldehyde and formic acid) associated with oxidation of MeCN reported by Bonon, *et al.*<sup>15</sup> were not observed. Depending on temperature used, different concentrations of isomeric alcohols and ketones at positions 1, 2, 3 and 4 of the octane chain were observed.

Alcohols were the main products at low temperatures, however, their concentration dropped as the temperature increased. Along the octane backbone carbon C(2) was the more reactive since it gave the highest concentration of oxygenated products while carbon C(1) was least reactive.

This is reflected by the regioselectivity parameter C(1), C(2), C(3), C(4) which correlates the reactivity of hydrogen atoms at position 1, 2, 3 and 4 of the octane chain. The values were calculated according to the method reported by Shul'pin, *et al.*<sup>16</sup>

**Table 4.4:** Catalyst selectivity in the oxidation of *n*-octane.

Temperature	Selectivity		Regioselectivity parameter	
	Alcohol (s)	Ketone (s)	C(1) : C(2) : C(3) : C(4)	A/K
40	59	31	1 : 9 : 4 : 6	1.4
60	57	35	1 : 18 : 13 : 12	1.6
70	51	38	1 : 32 : 26 : 22	1.3
80	47	43	1 : 36 : 27 : 24	1.1
100	43	57	1 : 31 : 28 : 24	0.7

A/K = alcohol/ketone ratio

### 2.15.2.2 Effect of time

To determine the optimum reaction time, a set of reactions were performed under reflux (at 80 °C) and the reaction was monitored after 6, 12, 24 and 36 hr. The results were summarised in Figure 4.8. From these results, it was observed that during the first 6 hr, isomeric alcohols were the major products, however, after 24 hr the concentration of alcohols began to drop. Slow accumulation of ketones was also observed within the first 12 hr, but after 24 hours the rate of their formation was faster. This phenomenon was due to over-oxidation of the alcohols by H<sub>2</sub>O<sub>2</sub> to afford the corresponding ketones. Similar observation has been reported by Leod, *et al.*<sup>17</sup>

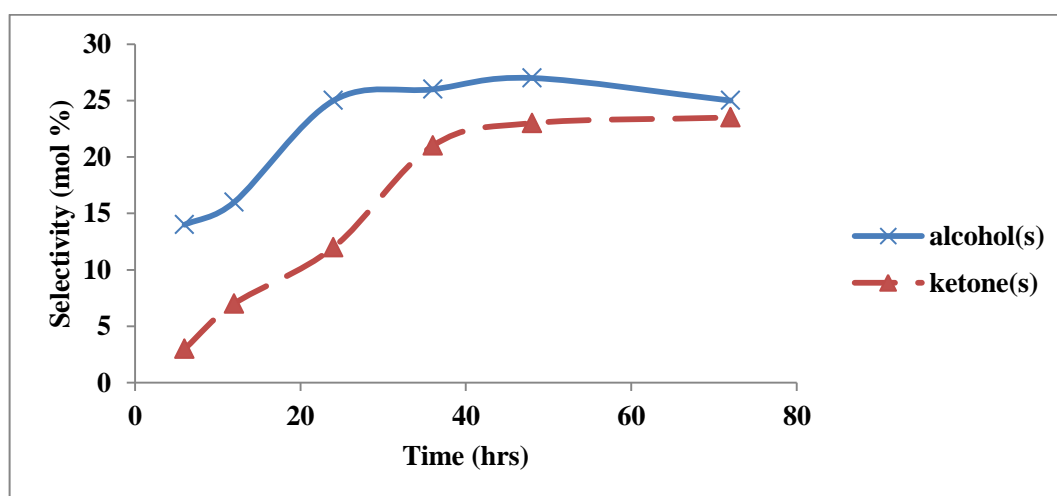
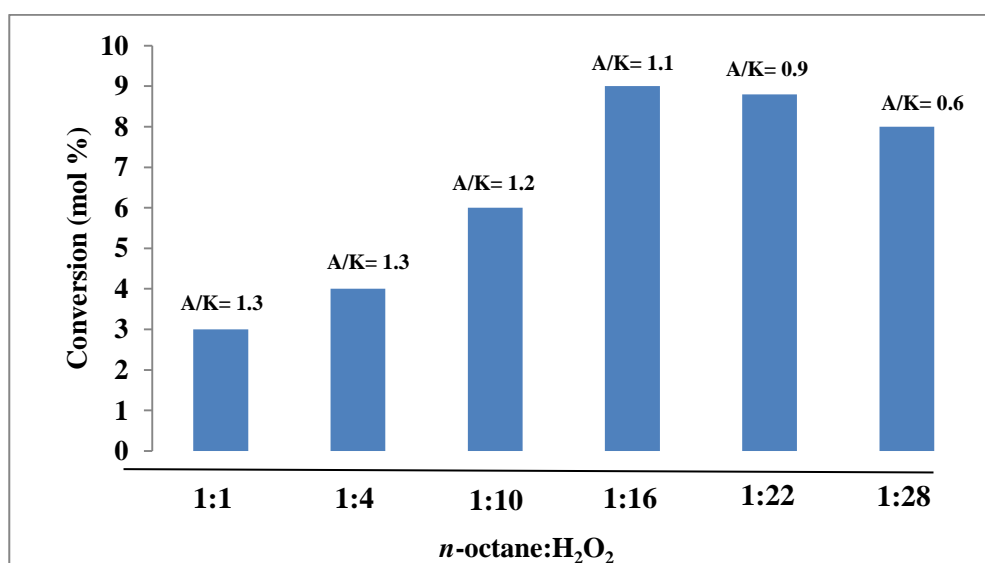


**Figure 0.8:** Effect of time on product distribution.

### 2.15.2.3 The effects of catalyst to oxidant ratio

As indicated in Figure 4.9, the molar ratio of octane to H<sub>2</sub>O<sub>2</sub> was evaluated from 1:1 to 1:28. The results indicated an increase in total products yield as the ratio increase from 1:1 to 1:16, which is also accompanied by a gradual drop in the proportion of the alcohol products (lower A/K ratio). This could be interpreted as increasing the H<sub>2</sub>O<sub>2</sub> concentration efficiently led to oxidation of both the substrate and the alcohols. The active intermediate from the H<sub>2</sub>O<sub>2</sub> was therefore involved in over-oxidation of the alcohols to ketones. The substrate to oxidant ratio 1:16 was therefore chosen as the optimum ratio, as it yielded the highest conversion at low over-oxidation rate. All the remaining catalytic testing was carried out at this mole ratio.



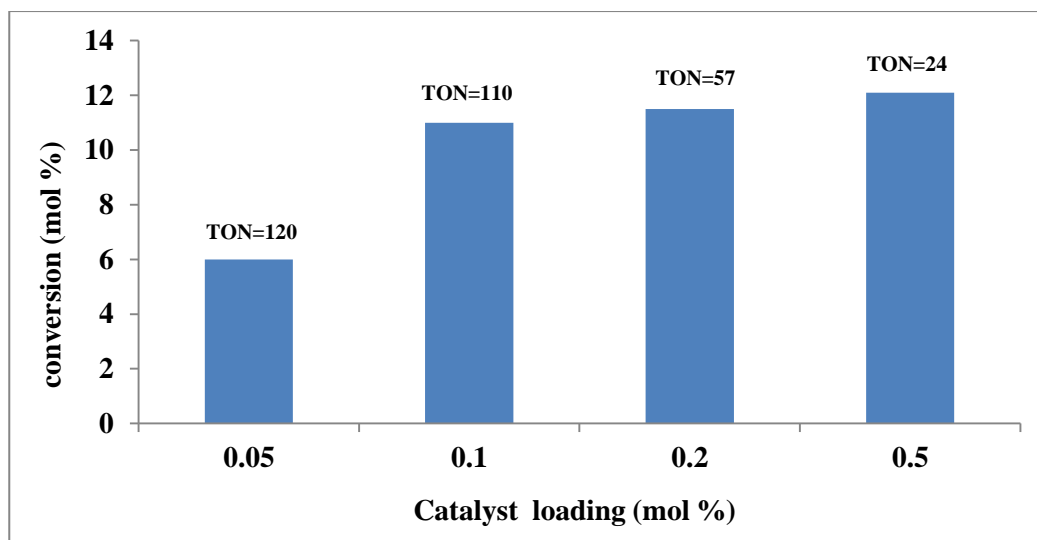
\* A/K = alcohol/ketone

**Figure 0.9:** Effect of substrate to oxidant ratio.

### 2.15.2.4 Effect of catalyst loading

The effect of catalyst loading was investigated using complex **4.1** at 80 °C. Catalyst loading tested were 0.05, 0.1, 0.2 and 0.5 mol%. The results are summarised in Figure 4.10 from which an increase in conversion was observed when the catalyst loading was increased from 0.05 to 0.5 mol%. The best loading was 0.1 mol% which gave the highest TON (110) with conversion of 11 mol%. Higher catalyst loading did not give any significant increase in conversion.





\*TON (turnover number) = (total moles of alkane converted)/moles of catalyst.

**Figure 0.10:** Effect of catalyst loading.

### 2.15.3 Testing of complexes 4.1-4.6 under the optimised conditions

The effects of ring substituents (-R', -R'' and -R''') around the triazolium ligand were evaluated under established optimum reaction conditions using catalysts **4.1-4.6**. The results presented in Figure 4.11 showed that because all the catalysts tested dissolved completely in MeCN all were active for the oxidation of *n*-octane. Compound **4.3** is the most active as it showed the highest conversion of 15 mol% to oxygenated products. The less sterically hindered substituent (propyl, -R' group) bonded to nitrogen allowed for easy access of the substrate to the metal centre and consequently enhanced catalytic activity. It was also observed, as the -R' groups alkyl chain increased, the conversion decreased indicating the effects of steric hindrance. **4.2** with an ester group in the -R''' position gave good conversion (8 mol%) compared to **4.1** and **4.2** with bulky benzyl and phenyl groups respectively.

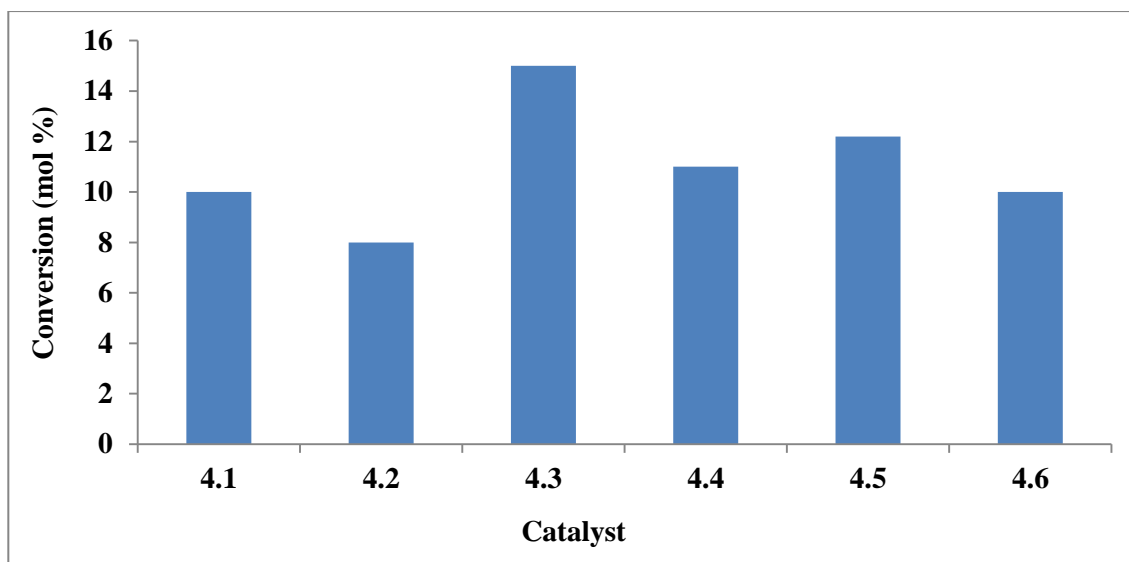


**Figure 0.11:** Total conversion of *n*-octane at the optimum conditions for catalysts **4.1-4.6**.

Electronic effects of the ligands were observed to also play a fundamental role in the catalytic activity of the complexes tested. A comparison of the activities of **4.1** and **4.3**, shows that **4.1** with more electron withdrawing phenyl group had a lower conversion while **4.3** with electron donating alkyl (propyl) group -R' had a higher conversion. Further comparing **4.1** with **4.4**, 1 mol% conversion difference was observed. Complexes **4.3**, **4.5** and **4.6** with alkyl chain substituents propyl, butyl and octyl respectively were used to analyse the balance between electronic and steric influences in the catalytic study. **4.3** showed the highest catalytic activity of 15 mol% conversion while **4.5** and **4.6** had 12 and 11.5 mol% respectively. The difference in conversions did not follow the expected trend where an increase in chain length increases conversion. However, an inverse relationship was observed relating catalyst activity to chain length, indicating that steric bulk of the R' side chain dominated over electron donation. Leod, *et al.*<sup>17</sup> have also reported a similar trend of observation.

Based on selectivity, for all six catalysts tested, averaging ketones were the foremost products formed. The carbon at position **C(2)** on the alkane backbone was more reactive since more oxygenated products were observed for this position, with ketones been the major products. Position **C(1)** was least reactive in all catalysts tested since low terminal products were observed with octanoic acid as the major product of terminal oxidation.

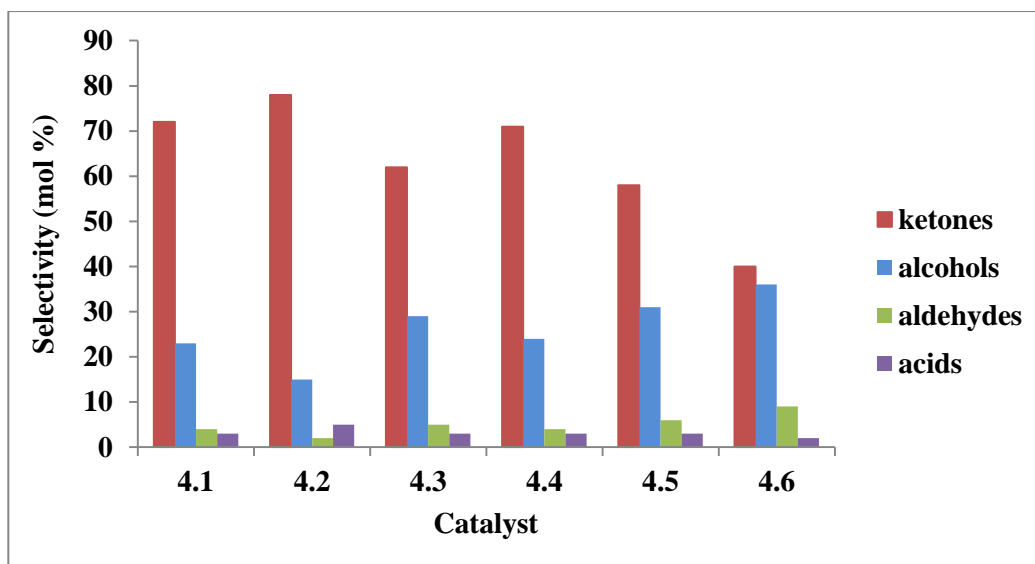


**Figure 0.12:** Oxygenated product distribution for catalysts **4.1-4.6**.

Summarised selectivity results are shown in Figure 4.12. From these results it was observed that catalyst **4.2** has higher selectivity for ketones, while **4.6** has the highest selectivity for alcohols compared to all other catalysts. A comparison of the molecular composition of the two catalysts shows that at the -R' position **4.2** is functionalised by an ester group while **4.6** contained a long alkyl chain. Hence, it is obvious that the presence of a long hydrophobic chain minimised the interaction of oxygenated alcohol products with the catalyst active site hence minimising over-oxidation in **4.6**.

Furthermore, the steric effect offered by the octyl substituent in catalyst **4.6** may have influenced the reductive elimination of the products compared to other catalysts with shorter alkyl chain substituents (**4.3** and **4.5**) at the same position. Similar observation was reported by Leod, *et al.*<sup>17</sup> where they suggested that over-oxidation of alcohol products can be minimised by introducing bulky substituents in the catalyst structure. Same phenomenon was observed when comparing catalyst **4.1** with phenyl substituent in -R' position, with catalyst **4.4** with benzyl substituent in same position. The results for terminal carbon activation are presented in Figure 4.13 where catalyst **4.6** was more selective for terminal products as more oxygenated products were observed compared to other catalysts tested. The presence of the hydrophobic alkyl chain substituent in **4.6** is helpful in the orientation of the long alkyl chain substrate C(1) activation.

The results are summarised in Figure 4.13. Similar phenomenon have been reported in biological systems where the hydrophobic region of the enzyme is involved in the ready uptake, correct orientation and subsequent hydroxylation of the C-H compounds.<sup>18</sup>

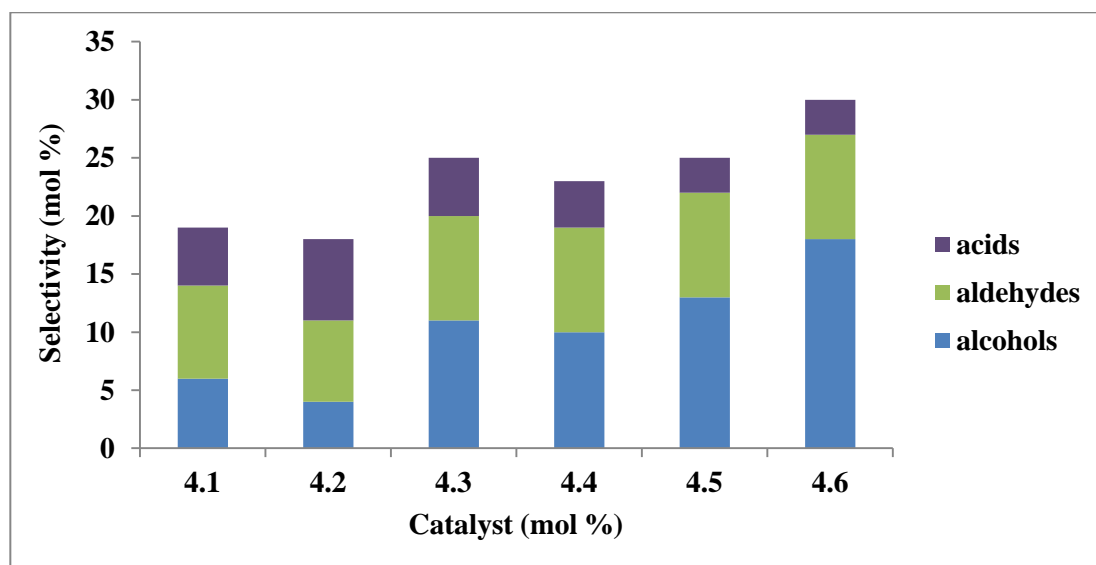


**Figure 0.13:** Selectivity and product distribution at C(1) for compounds 4.1-4.6.

## 2.16 Summary and conclusions

This chapter reported on the synthesis of a series of related triazolium-based nickel complexes by modification of reported methods. The metal complexes were fully characterised by spectroscopic analysis and thermal stability techniques. The effect of the paramagnetic centre resulted in complications in assigning some peaks due to line broadening, signal integration error and unusual chemical shifts. Single crystal X-ray diffraction studies were performed to determine the solid state structures of some of the compounds. The metal complexes were further tested as catalysts for the oxidation of alkanes in the presence of an oxidant. All complexes were found to be active as catalysts under optimum reaction conditions with ketones observed as the major products of all the catalyst systems tested. The system based on catalyst **4.3**, with less sterically bulky substituents bonded to nitrogen maximised the contact of substrates to the active metal centre and consequently enhanced the catalytic activity to yield the highest catalytic conversion of 15 mol% at a turnover rate (TON) of 117.

## 2.17 Experimental

Toluene and tetrahydrofuran (THF) were dried over sodium wire and benzophenone, dichloromethane (DCM) was dried over phosphorous pentoxide. All solvents were freshly distilled before used. High purity nitrogen gas was purchased from Afrox. Glassware was oven dried at 110 °C. All NMR experiments were done using a 400 MHz Bruker ultrashield spectrometer and samples were dissolved in deuterated solvents. Chemical shifts ( $\delta$ ) in ppm were reported with respect to tetramethylsilane (TMS) as internal standard. The following abbreviations were used to describe peak splitting patterns when appropriate: br = broad, s = singlet, d = doublet, t = triplet, q = quartet, m = multiplet. Infrared spectra (FTIR) were recorded on a Perkin Elmer FT-IR 1600 spectrophotometer.

### 2.17.1 General procedure for synthesis of 1,3,4-trisubstituted-1,2,3-triazolium salts

To a solution of 1,4-disubstituted triazole (1 equiv.) in acetonitrile (20 mL) under N<sub>2</sub> atmosphere was added the required alkyl halide (2 equiv.). The mixture was heated to 70 °C in a two-neck round bottom flask. After 24 hr, the solvent was evaporated under reduced pressure and the crude product was purified by column chromatography (ethyl acetate eluted unreacted starting materials and a switch to methanol eluted the solid product).

**3-methyl-1,4-diphenyl-1H-1,2,3-triazol-3-ium iodide (4.1a).** The starting materials used: 1,4-diphenyl-1H-1,2,3-triazole (3.011 g, 15.4 mmol) and methyl iodide (4.231 g, 30.2 mmol). Yield: (4.821 g 89%). <sup>1</sup>H NMR (CDCl<sub>3</sub> 400 MHz):  $\delta$  9.66 (s, 1H, triazole C=CH), 7.49-8.16 (s, 10H, Ar), 4.43 (s, N-CH<sub>3</sub>). <sup>13</sup>C NMR (CDCl<sub>3</sub> 400 MHz):  $\delta$  144.1, 134.6, 132.0, 131.9, 130.5, 130.1, 129.8, 129.6, 128.9, 127.2, 125.8, 122.0, 121.3, 120.5, 40. IR  $\nu_{\max}$  (cm<sup>-1</sup>): 3412 (m) 3001 (m), 2928 (m), 1753 (s), 1604(m), 1555 (m), 1465 (m), 1172 (m), 777 (s), 722 (m), 694 (s), 501 (m). HRMS (ESI) m/z for C<sub>15</sub>H<sub>14</sub>N<sub>3</sub> [M-I]<sup>+</sup>: calculated: 236.1, found: 236.1.

**1-(2-ethoxy-2-oxoethyl)-3-methyl-4-phenyl-1H-1,2,3-triazol-3-ium iodide (4.2a).** The starting materials used: ethyl-2-(4-phenyl-1H-1,2,3-triazol-1-yl) acetate (3.124 g, 13.5 mmol) and methyl iodide (3.120 g, 27.0 mmol). White solid product (4.201 g, 83%). mp: 141-143 °C. <sup>1</sup>H NMR (CDCl<sub>3</sub> 400 MHz):  $\delta$  9.51 (s, 1H, triazole C=CH), 7.56-7.73 (m, 5H, Ar), 5.90 (s, 2H, Ar-CH<sub>2</sub>), 4.37 (s, 3H, CH<sub>3</sub>), 4.32 (t, 2H, CH<sub>2</sub>), 1.32-1.35 (m, 3H, CH<sub>3</sub>); <sup>13</sup>C NMR (CDCl<sub>3</sub> 400 MHz):  $\delta$  164.4, 142.9, 132.1, 131.0, 129.8, 129.7, 129.6, 129.4, 125.7, 121.4, 63.4, 54.6, 39.8, 14.1. IR  $\nu_{\max}$  (cm<sup>-1</sup>): 3134 (m) 2993 (m), 2948 (m), 1752 (s), 1711 (m), 1466 (m), 1346 (m),

1197 (m), 763 (s), 692 (s), 511 (m). HRMS (ESI)  $m/z$  calculated for  $C_{12}H_{13}N_3O_2[M-I]$ : 246.1, found: 246.1.

**3-methyl-4-phenyl-1-propyl-1H-1,2,3-triazol-3-ium iodide<sup>6</sup> (4.3a).** The starting materials used: 1-propyl-4-phenyl-1H-1,2,3-triazole (5.210 g, 27.2 mmol) and methyl iodide (7.881 g, 55.4 mmol). Yellow-orange solid product (7.801 g, 87%).  $^1H$  NMR ( $CD_3OD$  400 MHz):  $\delta$  9.020 (s, 1H, triazole C=CH), 7.82-7.80 (m, 2H), 7.68-7.66 (t, 3H), 4.76 (m, 2H), 4.34 (s, 3H), 2.19-2.13 (m, 2H), 1.05 (t, 3H);  $^{13}C$  NMR ( $CD_3OD$  400 MHz):  $\delta$  11.2, 23.9, 39.7, 56.8, 124.0, 130.0, 130.7, 130.8, 132.9, 144.6.

**1-benzyl-3-methyl-4-phenyl-1H-1,2,3-triazol-3-ium iodide<sup>6</sup> (4.4a).** The starting materials used: 1-benzyl-4-(phenyl)-1H-1,2,3-triazole (1.602 g, 6.8 mmol) and methyl iodide (1.920 g, 13.6 mmol). Reddish-brown solid product (1.801 g, 79%). mp: 181-183 °C.  $^1H$  NMR ( $CD_3OD$  400 MHz):  $\delta$  9.37 (s, 1H, triazole C=CH), 8.06 (s, 1H), 7.72-7.28 (m, 10H), 6.03 (s, 2H), 4.30 (s, 3H);  $^{13}C$  NMR ( $CD_3OD$  400 MHz):  $\delta$  143.1, 131.7, 130.8, 129.7, 129.6, 129.4, 121.6, 57.6, 31.4.

**1-butyl-3-methyl-4-phenyl-1H-1,2,3-triazol-3-ium iodide<sup>6</sup> (4.5a).** The starting materials used: 1-butyl-4-phenyl-1H-1,2,3-triazole (4.010 g, 19.3 mmol) and methyl iodide (5.641 g, 39.4 mmol). Brown needle product (5.31 g, 81%).  $^1H$  NMR ( $CD_3OD$  400 MHz):  $\delta$  9.01 (s, 1H, s, 1H, triazole C=CH), 7.81-7.79 (d, 2H), 7.68 (t, 3H), 4.77 (m, 2H), 4.34 (s, 3H), 2.13-2.09 (m, 2H), 1.53-1.51 (m, 2H), 1.05 (m, 3H);  $^{13}C$  NMR ( $CD_3OD$  400 MHz):  $\delta$  13.8, 20.5, 32.3, 39.7, 55.1, 124.0, 130.0, 130.7, 130.8, 132.9, 144.6.

**1-octyl-3-methyl-4-phenyl-1H-1,2,3-triazol-3-ium iodide<sup>6</sup> (4.6a).** The starting materials used: 1-octyl-4-phenyl-1H-1,2,3-triazole (3.513 g, 15.33 mmol) and methyl iodide (4.323 g, 30.70 mmol). Off-white solid product (5.124 g, 90%).  $^1H$  NMR ( $CD_3OD$  400 MHz):  $\delta$  9.02 (s, 1H, triazole C=CH), 7.66-7.82 (m, 5H, Ar), 4.76 (m, 2H,  $CH_2$ ), 4.34 (s, 3H, N- $CH_3$ ), 2.11-2.11 (m, 2H,  $CH_2$ ), 1.40-1.51 (m, 6H, 3x $CH_2$ ), 0.95 (m, 3H,  $CH_3$ );  $^{13}C$  NMR ( $CD_3OD$  400 MHz):  $\delta$  144.6, 132.9, 130.8, 130.7, 130.0, 124.0, 55.3, 36.7, 32.3, 30.3, 27.0, 23.5, 14.4.

### 2.17.2 General procedure for synthesis of [(Cp)Ni(X)(NHC)] complexes.

The reported method<sup>2</sup> was modified: Under  $N_2$  atmosphere, 1,3,4-trisubstituted-1,2,3-triazolium salts (1 equiv.) and  $NiCp_2$  (1 equiv.) were charged into a flame-dried Schlenk tube and THF (20 mL) was added. The resultant mixture was heated to reflux at 70 °C for 24 hr to give a red solution in which a large brown insoluble solid was suspended. The solvent was evaporated

under reduced pressure and the crude product was extracted with hot toluene and filtered through celite to give a crude mixture of unreacted nickelocene and Ni-NHC complex. The crude product was then purified by column chromatography (hexane eluted the nickelocene and a switch to dichloromethane eluted the reddish solid product). The same procedure was used to prepare all Ni-NHC complexes (**4.1-4.6**) in good yields.

**[CpNi(I){3-methyl-1,4-diphenyl-1H-1,2,3-triazol-3-ylidene}] (4.1).** The starting materials used: 3-methyl-1,4-diphenyl-1H-1,2,3-triazol-3-ium iodide (0.801 g, 2.2 mmol) and NiCp<sub>2</sub> (0.417 g, 2.5 mmol). Reddish powder (0.781 g, 73%). Crystals suitable for X-ray crystallography were grown by layering hexane to a dichloromethane solution of **4.1**. <sup>1</sup>H-NMR (CDCl<sub>3</sub> 400 MHz) δ 7.17-7.54 (bm, Ar), 4.81 (s, Cp), 4.00 (s, N-CH<sub>3</sub>), <sup>13</sup>C-NMR (CDCl<sub>3</sub> 400 MHz): 148.5, 130.7, 129.9, 129.8, 129.7, 129.1, 128.7, 128.4, 128.3, 128.0, 125.8, 120.5, 117.7, 91.8, 37.9. IR ν<sub>max</sub> (cm<sup>-1</sup>): 3054 (m), 2922 (m), 2853 (m), 1695 (m), 1593 (m), 1400 (m), 1042 (m), 917(m), 756 (s), 607 (s), 513 (m). HRMS (ESI) m/z for C<sub>20</sub>H<sub>20</sub>N<sub>3</sub>NiI [M]: calculated: 358.1, found: 358.1.

**[CpNi(I){1-(2-ethoxy-2-oxoethyl)-3-methyl-4-phenyl-1H-1,2,3-triazol-3-ium}] (4.2).** The starting materials used: 1-(2-ethoxy-2-oxoethyl)-3-methyl-4-phenyl-1H-1,2,3-triazol-3-ium iodide (0.813 g, 3.4 mmol) and NiCp<sub>2</sub> (0.411 g, 2.2 mmol). Reddish solid product (0.713 g, 66%). <sup>1</sup>H-NMR (CDCl<sub>3</sub> 400 MHz): δ 7.26-7.92 (bm, Ar), 5.21 (s, N-CH<sub>3</sub>), 4.29 (s, Cp), 4.14 (s, CH<sub>2</sub>), 1.13-1.33 (m, 5H, CH<sub>2</sub>+CH<sub>3</sub>); <sup>13</sup>C NMR (CDCl<sub>3</sub> 400 MHz): δ 166.2, 148.2, 130.3, 129.1, 128.8, 125.8, 120.9, 96.0, 62.4, 50.39, 22.6, 11.4. IR ν<sub>max</sub> (cm<sup>-1</sup>): 3429 (b), 2929 (m), 2360 (m), 1730 (b), 1616 (m), 1464 (m), 1370 (m), 1213 (b), 1025 (s), 765 (s), 695 (s), 502 (m). HRMS (ESI) m/z for C<sub>18</sub>H<sub>20</sub>N<sub>3</sub>NiIO<sub>2</sub> [M]: calculated: 495.0, found: 497.1.

**[CpNi(I){3-methyl-4-phenyl-1-propyl-1H-1,2,3-triazol-3-ylidene}] (4.3).** The starting materials used: 3-methyl-4-phenyl-1-propyl-1H-1,2,3-triazol-3-ium iodide (0.801 g, 3.5 mmol) and NiCp<sub>2</sub> (0.459 g, 3.3 mmol). Reddish crystalline product (0.501 g, 63%). Crystals suitable for X-ray crystallography were grown by layering hexane to a dichloromethane solution of **4.3**. <sup>1</sup>H-NMR (CDCl<sub>3</sub> 400 MHz): δ 7.26-8.19 (bm, Ar), 4.82 (s, N-CH<sub>3</sub>), 4.35 (s, Cp), 4.02 (s, CH<sub>2</sub>); <sup>13</sup>C-NMR (CDCl<sub>3</sub>, 400 MHz): δ 148.0, 130.4, 129.7, 129.6, 128.0, 127.6, 125.6, 91.4, 55.9, 37.1, 31.9, 19.9, 13.7. IR ν<sub>max</sub> (cm<sup>-1</sup>): 3439 (m), 3350 (m), 2987 (m), 1608 (s), 1579 (m), 1483 (s), 1464 (s), 1433 (s), 1345 (s), 1227 (m), 1073 (s), 1045 (m), 765 (s), 691 (s), 508 (s). HRMS (ESI) m/z for C<sub>17</sub>H<sub>20</sub>N<sub>3</sub>NiI [M]: calculated: 324.1, found: 324.1.

**[CpNi(I){1-benzyl-3-methyl-4-phenyl-1H-1,2,3-triazol-3-ylidene}] (4.4).** The starting materials used: 1-benzyl-3-methyl-4-phenyl-1H-1,2,3-triazol-3-ium iodide (0.711 g, 2.4 mmol) and NiCp<sub>2</sub> (0.356 g, 2.4 mmol). Reddish solid product (0.501 g, 63%). Crystals suitable for X-ray crystallography were grown by layering hexane to a dichloromethane solution of **4.4**. <sup>1</sup>H-NMR (CDCl<sub>3</sub> 400 MHz): δ 7.26-8.19 (bm, Ar), 4.82 (s, N-CH<sub>3</sub>), 4.35 (s, Cp), 4.02 (s, CH<sub>2</sub>); <sup>13</sup>C-NMR (CDCl<sub>3</sub> 400 MHz): δ 130.7, 129.9, 129.8, 128.9, 128.8, 125.8, 125.4, 120.5, 91.8, 61.4, 37.5. IR ν<sub>max</sub> (cm<sup>-1</sup>): 3433(b), 2927 (m), 1695 (s), 1622 (m), 1450 (s), 1338 (s), 1073(s), 780 (m), 727 (s), 694 (m), 698 (s). HRMS (ESI) m/z for C<sub>21</sub>H<sub>18</sub>N<sub>3</sub>INi [M]: calculated: 372.1, found: 372.1.

**[CpNi(I){1-butyl-3-methyl-4-phenyl-1H-1,2,3-triazol-3-ylidene}] (4.5).** The starting materials used: 1-butyl-3-methyl-4-phenyl-1H-1,2,3-triazol-3-ium iodide (0.813 g, 2.4 mmol) and NiCp<sub>2</sub> (0.447 g, 2.4 mmol). Reddish crystalline product (0.565 g, 51%). <sup>1</sup>H-NMR (CDCl<sub>3</sub> 400 MHz): δ 7.26-8.19 (bm, Ar), 4.82 (s, N-CH<sub>3</sub>), 4.35 (s, Cp), 4.02 (s, CH<sub>2</sub>); <sup>13</sup>C-NMR (CDCl<sub>3</sub> 400 MHz): δ 148.0, 130.4, 129.7, 129.6, 128.0, 127.6, 125.6, 91.4, 55.9, 37.1, 31.9, 19.9, 13.7. IR ν<sub>max</sub> (cm<sup>-1</sup>): 3119 (s) 3064 (m), 2955 (m), 2934 (m), 1674 (m), 1608 (s), 1464 (s), 1078 (s), 839 (s), 761 (m), 693 (m), 501 (m). HRMS (ESI) m/z for C<sub>18</sub>H<sub>22</sub>N<sub>3</sub>INi [M]: calculated: 338.1, found: 338.1.

**[CpNi(I){3-methyl-4-phenyl-1-octyl-1H-1,2,3-triazol-3-ylidene}] (4.6).** The starting materials used: 3-methyl-4-phenyl-1-propyl-1H-1,2,3-triazol-3-ium iodide (0.801 g, 2.4 mmol) and NiCp<sub>2</sub> (0.459 g, 2.4 mmol). Reddish crystalline product (0.501 g, 63%). Crystals suitable for X-ray crystallography were grown by layering hexane to a dichloromethane solution of **4.6**. <sup>1</sup>H-NMR (CDCl<sub>3</sub> 400 MHz): δ 7.26-8.19 (bm, Ar), 4.82 (s, N-CH<sub>3</sub>), 4.35 (s, Cp), 4.02 (s, CH<sub>2</sub>); <sup>13</sup>C-NMR (CDCl<sub>3</sub> 400 MHz): δ 148.0, 130.4, 129.7, 129.6, 128.0, 127.6, 125.6, 91.4, 55.9, 37.1, 31.9, 19.9, 13.7. IR ν<sub>max</sub> (KBr, cm<sup>-1</sup>): 3403(b), 2924 (m), 1895 (s), 1633 (m), 1450 (s), 1338 (s), 1073(s), 780 (m), 727 (s), 696 (s). HRMS (ESI) m/z for C<sub>22</sub>H<sub>30</sub>N<sub>3</sub>INi [M]: calculated: 324.1, found: 324.10.

## 2.18 Catalytic studies

The oxidants H<sub>2</sub>O<sub>2</sub> (30%) and *t*-BuOOH (70%) were respectively purchased from Sigma-Aldrich and DLD Scientific and used as supplied. The reagents utilised for the calibration of the GC: 1-octanol (99%), 2-octanol (97%), 3-octanol (98%), 4-octanone (99%), octanal (99%) and octanoic acid (99%) were obtained from Sigma-Aldrich, 2-octanone (98%), 3-octanone (97%), 4-octanol (98%) and *n*-octane (99%) were sourced from Fluka, and pentanoic acid (98%) from Merck. Where required, double distilled water was used.



The oxidation reaction of *n*-octane was studied under a nitrogen atmosphere in dry acetonitrile with the respective oxidant (H<sub>2</sub>O<sub>2</sub> or *t*-BuOOH), *n*-octane and the required catalyst.

The reaction mixture was stirred in an oil bath at the optimum temperature and after the required time period, an aliquot of sample was removed using a Pasteur pipette and filtered through a cotton wool plug, after which 0.5 µL of the aliquot was injected into the GC for analysis and quantification.

In all samples, excess solid triphenylphosphine (PPh<sub>3</sub>) was added in order to capture alkyl hydroperoxides (if present) which is known to gradually decompose with the production of corresponding ketones (aldehydes) and alcohols in the hot injector and columns. Total conversion was calculated as total moles of product/initial moles of substrate while selectivity was calculated as moles of product/total moles of product and both were expressed as a percentage. 2,4,6-trichlorobenzene was used as the internal standard and all experiments were conducted in an Agilent Technology 6820 GC System equipped with a flame ionization detector (FID) and an Agilent DB-Wax column with a length of 30 meters, inner diameter of 0.25 mm and a thickness of 0.25 mm. The GC was calibrated with octane solutions and was found to have a linear correlation from 0.025-0.07 g/ml octane.

Samples were run using HP Chemstation software with the following parameters:

Injector temperature: 240 °C

Oven temperature: 90 °C

Detector temperature: 220 °C

Pressure: 0.052 MPa

Air pressure: 420 kPa

Hydrogen pressure: 410 kPa

## 2.19 Reference list

1. W. A. Herman, *Angew. Chem. Int. Ed.*, 2002, **41**, 1290-1309.
2. C. D. Abernethy, A. H. Cowley and R. A. Jones, *J. Organomet. Chem.*, 2000, **596**, 3–5.
3. W. Buchowicz, A. Koziół, L. B. Jerzykiewicz, T. Lis, S. Pasynekiewicz, A. Pecherzewska and A. Pietrzykowski, *J. Mol. Catal. A: Chem.*, 2006, **257**, 118–123.
4. F. E. Hahn, C. Radloff, T. Pape and A. Hepp, *Organometallics*, 2008, **27**, 6408–6410.
5. F. E. Hahn, B. Heidrich, A. Hepp and T. Pape, *J. Organomet. Chem.*, 2007, **692**, 4630–4638.
6. Z. Yacob and J. Liebscher, in *Ionic Liquids as Advantageous Solvents for Preparation of Nanostructures*, ed. S. T. Handy, 2011 pp. 3 – 22.
7. W. Buchowicz, W. Wojtczak, A. Pietrzykowski, A. Lupa, L. B. Jerzykiewicz, A. Makal and K. Wozniak, *Eur. J. Inorg. Chem.*, 2010, 648–656.
8. G. B. Shul'pin, M. V. Kirillova, T. Sooknoi and A. J. L. Pombeiro, *Catal. Lett.*, 2008, **123**, 135–141.
9. U. Schuchardt, D. Cardoso, R. Sercheli, R. Pereira, R. S. d. Cruz, M. C. Guerreiro, D. Mandelli, E. V. Spinace and E. L. Pires, *Appl. Catal. A*, 2001, **211**, 1-13.
10. M. V. Kirillova, Y. N. Kozlov, L. S. Shul'pina, O. Y. Lyakin, A. M. Kirillov, E. P. Talsi, A. J. L. Pombeiro and G. B. Shul'pin, *J. Catal.*, 2009, **268**, 26–38.
11. A. E. Shilov and G. B. Shul'pin, *Chem. Rev.*, 1997, **97**, 2879-2884.
12. G. B. Shul'pin and G. J. Süß-Fink, *Chem. Soc. Perkin Trans.*, 1995, **2**, 1459-1463.
13. M. J. L. Kishore, G. S. Mishra and A. Kumar, *Indian J. Chem.*, 2005, **44**, 349-355.
14. R. H. P. R. Poladi and C. C. Landry, *Microporous and Mesoporous Materials*, 2002, **52**, 11–18.
15. A. J. Bonon, D. Mandelli, O. A. Kholdeeva, M. V. Barmatova, Y. N. Kozlov and G. B. Shul'pin, *Appl. Catal. A*, 2009, **365**, 96–104.
16. G. B. Shul'pin, T. Sooknoi, V. B. Romakh, G. Süß-Fink and L. S. Shul'pina, *Tetrahedron Lett.*, 2006, **47**, 3071–3075.
17. T. C. Leod, M. V. Kirillova, A. J. L. Pombeiro, M. A. Schiavon and M. D. Assis, *Appl. Catal. A*, 2010, **372**, 191–198.
18. A. Wada, S. Ogo, S. Nagatomo, T. Kitagawa, Y. Watanabe, K. Jitsukawa and H. Masuda, *Inorg. Chem.*, 2002, **41**, 616-618.
19. F. Haber and H. Weiss, *Proc. R. Soc.*, 1934, **147**, 332-339.

## Chapter 5

### Conclusions

A series of related 1,2,3-triazole compounds were synthesised and characterised by spectroscopic methods including NMR, IR, MS and X-ray diffraction. *N*-alkylation of the triazole compounds yielded 1,4-disubstituted triazolium ionic liquids (**3.1-3.6**). The ionic liquids were found to act as “green” solvent systems for the dissolution of an iron-based compound for the catalytic oxidation of *n*-octane. Recycling and re-usage of the system was found to be reproducible for three cycles and leaching of the catalyst to the product phase was associated with decrease of catalytic activity in subsequent cycles.

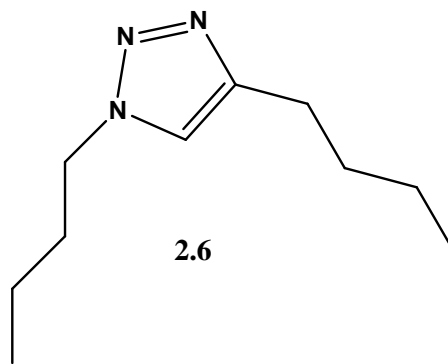
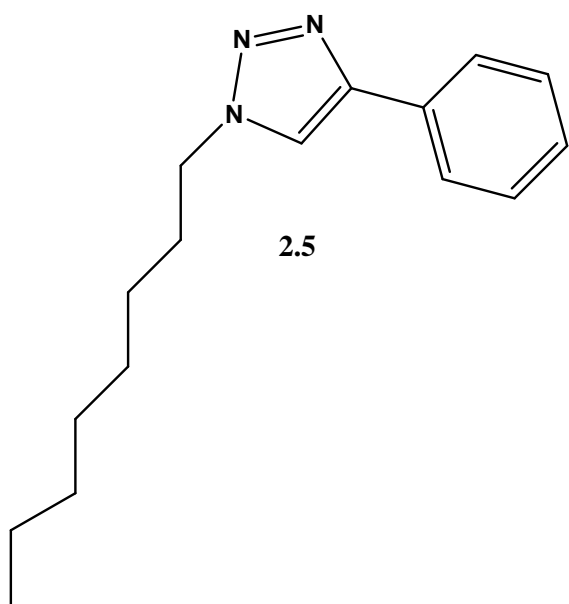
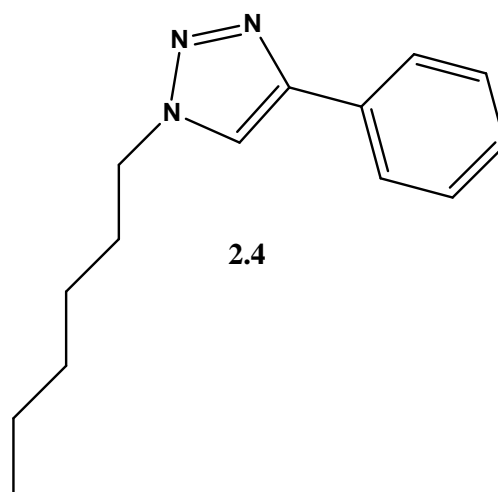
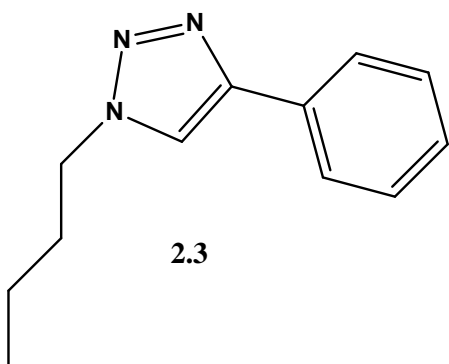
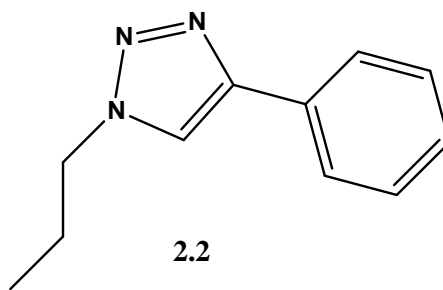
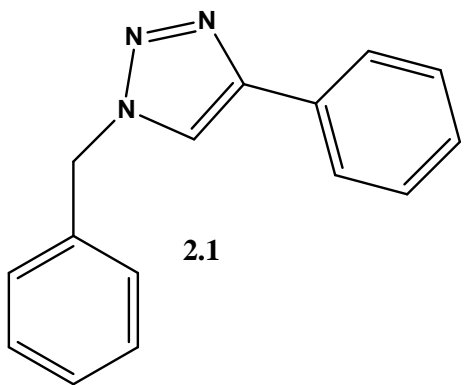
Synthesis and characterisation of 1,2,3-triazolium-based nickel carbene complexes by modification of reported synthetic methods was described (**4.1-4.6**). The crystal structures of three metal complexes (**4.1**, **4.3** and **4.4**) were reported and discussed. The complexes were then tested for catalytic oxidation of alkanes in the presence of various oxidants under mild reaction conditions. Catalyst (**4.3**) with less bulky substituents exhibited the highest catalytic activity (15%) with H<sub>2</sub>O<sub>2</sub> as the most productive oxidant.

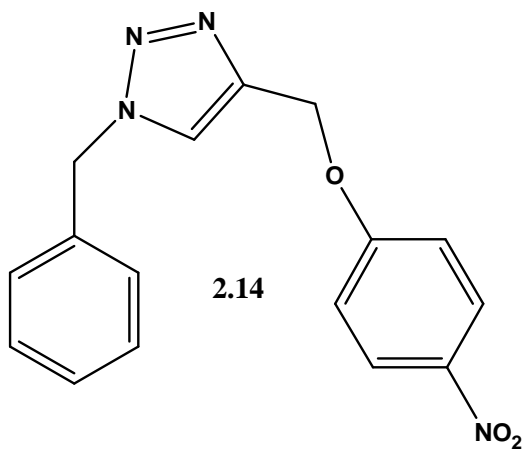
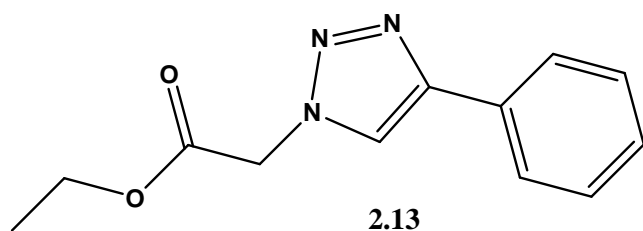
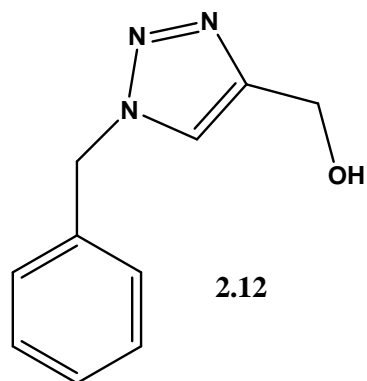
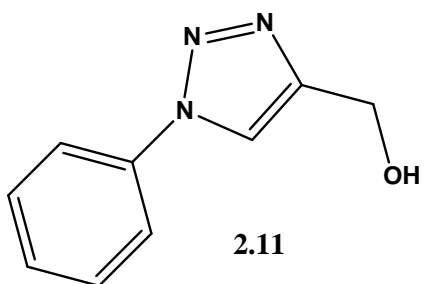
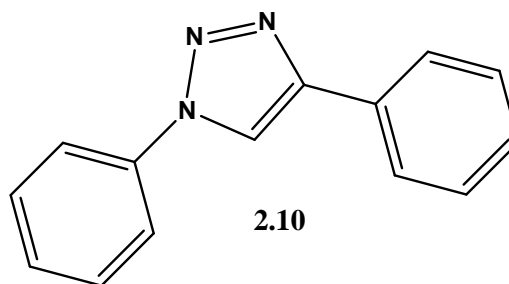
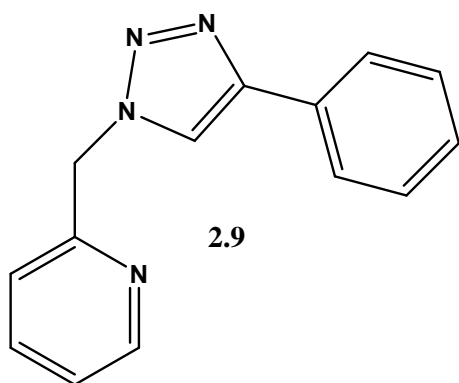
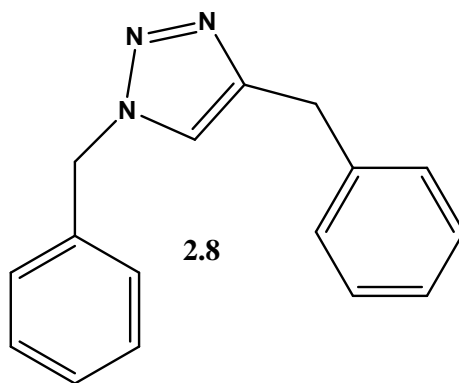
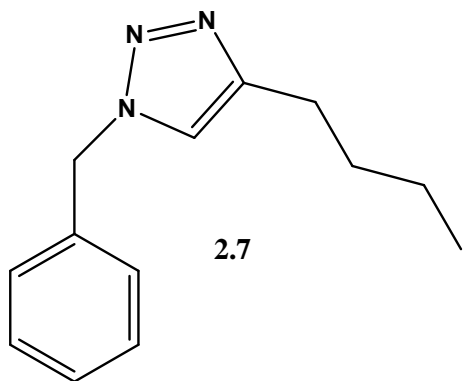
Finally, it can be concluded that the main goals of this study were achieved because the catalyst systems were successfully synthesised, characterised and tested for their activity in alkane oxidation. Indeed there was significant activity observed with all prepared catalysts, however from the results obtained, the nickel carbene catalysts in the presence of H<sub>2</sub>O<sub>2</sub> demonstrated the highest efficiency in this work.

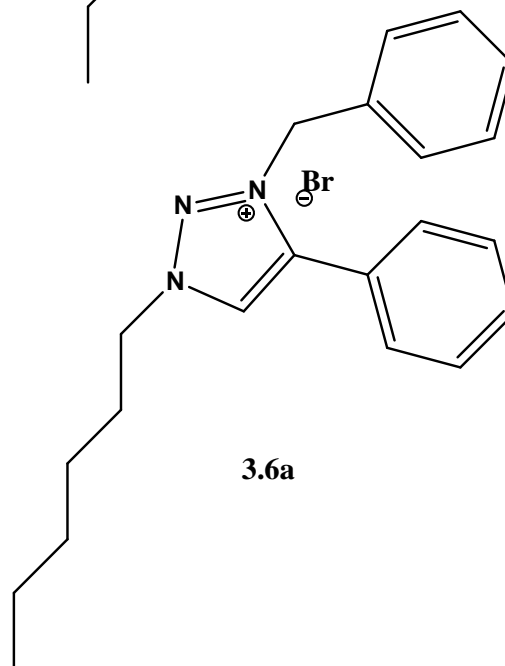
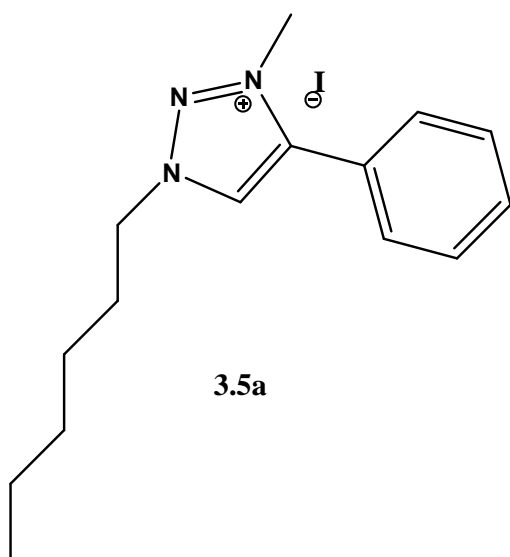
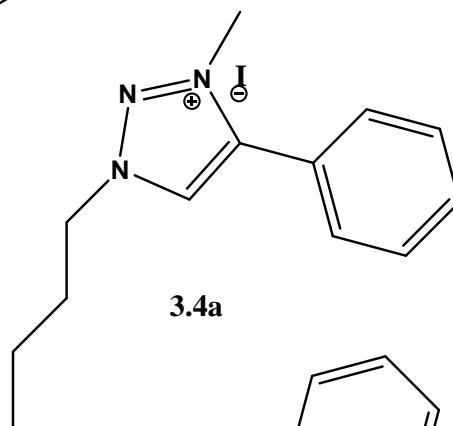
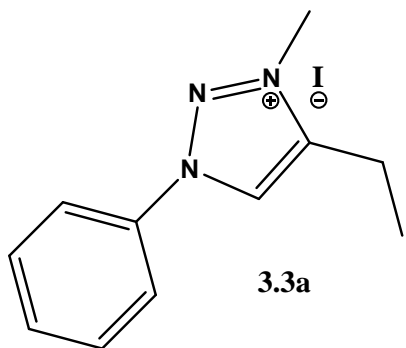
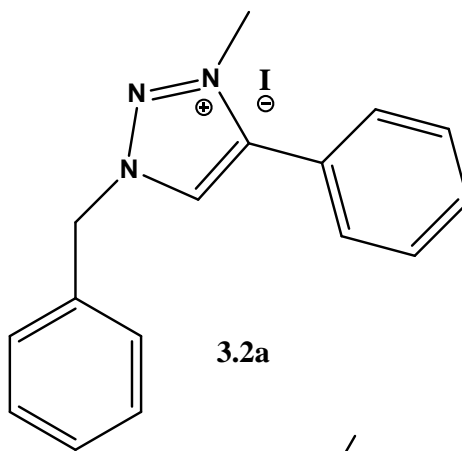
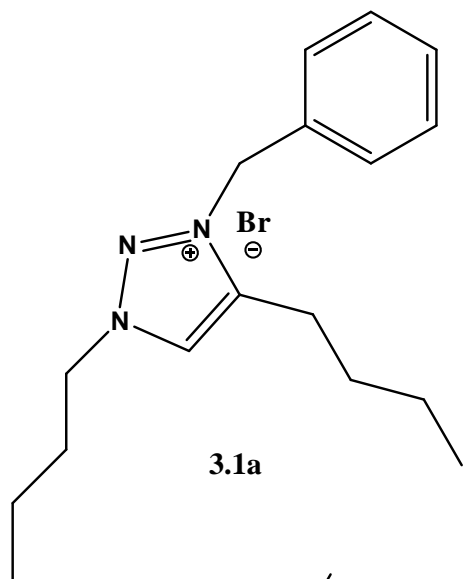
## List of compounds synthesised

- 1-Benzyl-4-phenyl-1*H*-1,2,3-triazole<sup>1-3</sup> (2.1).
- 1-Propyl-4-(Phenyl)-1*H*-1,2,3-triazole (2.2).
- 1-Butyl-4-phenyl-1*H*-1,2,3-triazole<sup>4</sup> (2.3).
- 1-Hexyl-4-(Phenyl)-1*H*-1,2,3-triazole (2.4).
- 1-Octyl-4-phenyl-1*H*-1,2,3-triazole<sup>5</sup> (2.5).
- 1,4-Dibutyl-1*H*-1,2,3-triazole (2.6).
- 1-Benzyl-4-butyl-1*H*-1,2,3-triazole<sup>6</sup> (2.7).
- 1,4-Dibenzyl-1*H*-1,2,3-triazole (2.8).
- 2-((4-Phenyl-1*H*-1,2,3-triazol-1-yl)methyl)pyridine<sup>7</sup> (2.9).
- 1,4-Diphenyl-1*H*-1,2,3-triazole<sup>8-10</sup> (2.10).
- (1-Phenyl-1*H*-1,2,3-triazol-4-yl)methanol (2.11).
- (1-Benzyl-1*H*-1,2,3-triazol-4-yl)methanol<sup>11</sup> (2.12).
- Ethyl- 2-(4-phenyl-1*H*-1,2,3-triazol-1-yl)acetate<sup>12-14</sup> (2.13).
- 1-Benzyl-4-((4-nitrophenoxy)methyl)-1*H*-1,2,3-triazole (2.14).
- 3-Benzyl-1,4-dibutyl-1*H*-1,2,3-triazol-3-ium bromide<sup>15</sup> (3.1a ).
- 1-Benzyl-3-methyl-4-phenyl-1*H*-1,2,3-triazol-3-ium iodide<sup>15</sup> (3.2a).
- 4-Ethyl-3-methyl-1-phenyl-1*H*-1,2,3-triazol-3-ium iodide (3.3a).
- 1-Butyl-3-methyl-4-phenyl-1*H*-1,2,3-triazol-3-ium iodide (3.4a).
- 1-Hexyl-3-methyl-4-phenyl-1*H*-1,2,3-triazol-3-ium iodide (3.5a).
- 3-Benzyl-1-hexyl-4-phenyl-1*H*-1,2,3-triazol-3-ium bromide (3.6a).
- 3-Benzyl-1,4-dibutyl-1*H*-1,2,3-triazol-3-ium nitrate (3.1).
- 1-Benzyl-3-methyl-4-phenyl-1*H*-1,2,3-triazol-3-ium nitrate (3.2).
- 4-Ethyl-3-methyl-1-phenyl-1*H*-1,2,3-triazol-3-ium nitrate (3.3).
- 1-Butyl-3-methyl-4-phenyl-1*H*-1,2,3-triazol-3-ium nitrate (3.4).

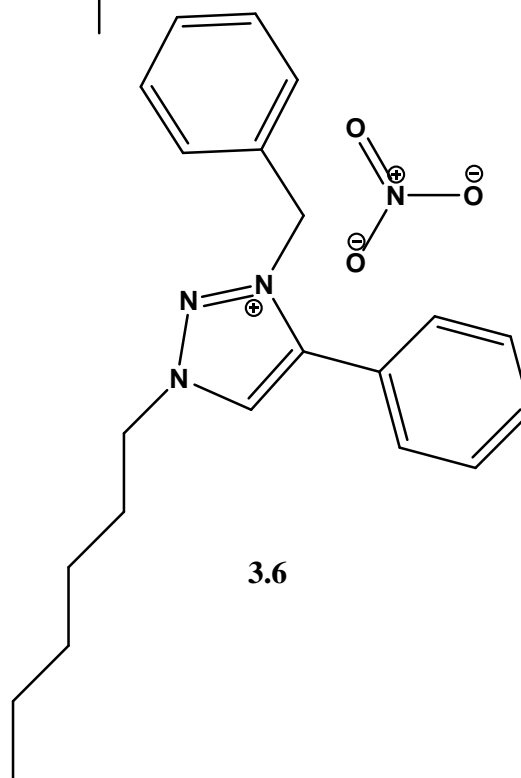
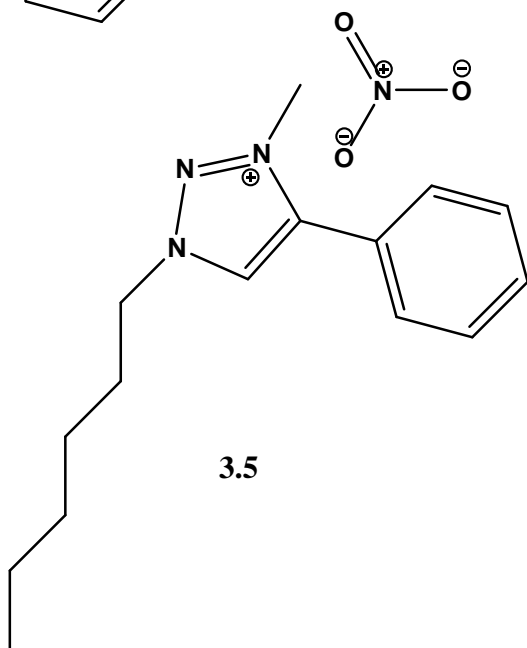
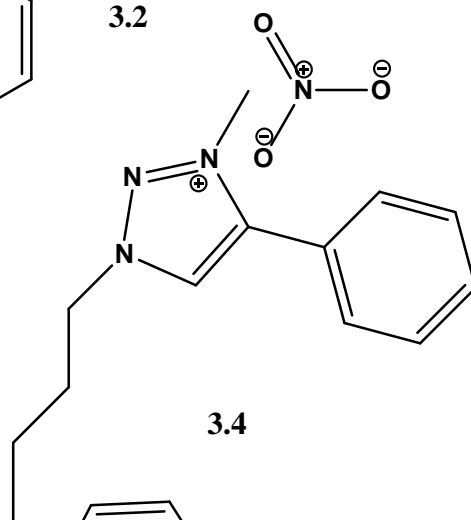
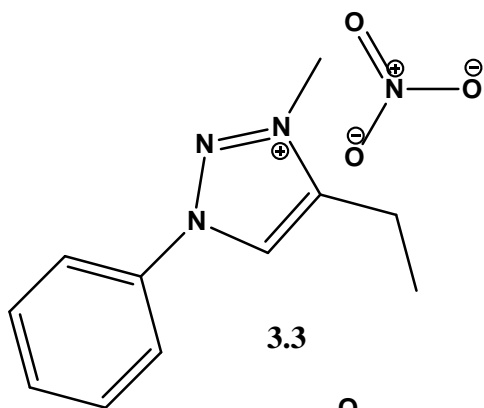
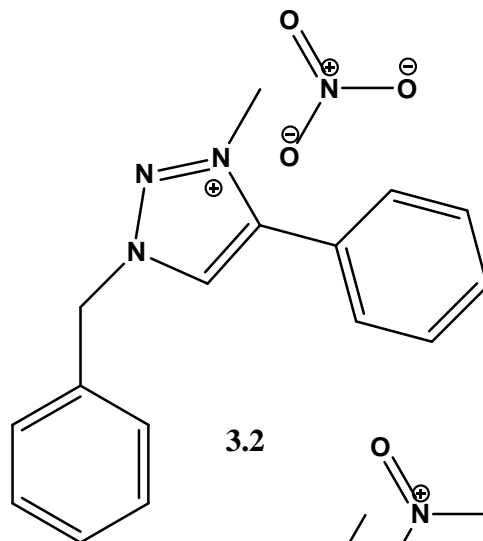
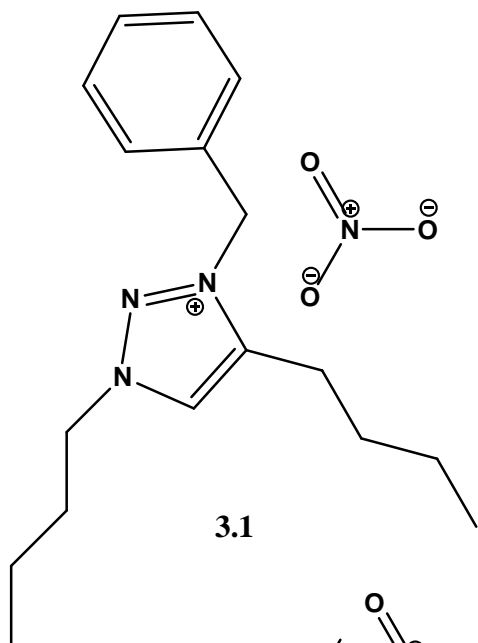
- 1-Hexyl-3-methyl-4-phenyl-1H-1,2,3-triazol-3-ium nitrate (3.5).**
- 3-Benzyl-1-hexyl-4-phenyl-1H-1,2,3-triazol-3-ium nitrate (3.6).**
- 3-Methyl-1,4-diphenyl-1H-1,2,3-triazol-3-ium iodide (4.1a).**
- 1-(2-Ethoxy-2-oxoethyl)-3-methyl-4-phenyl-1H-1,2,3-triazol-3-ium iodide (4.2a).**
- 1-Benzyl-3-methyl-4-phenyl-1H-1,2,3-triazol-3-ium iodide<sup>15</sup> (4.4a).**
- 1-Butyl-3-methyl-4-phenyl-1H-1,2,3-triazol-3-ium iodide<sup>15</sup> (4.5a).**
- 1-Octyl-3-methyl-4-phenyl-1H-1,2,3-triazol-3-ium iodide<sup>15</sup> (4.6a).**
- [CpNi(I){3-methyl-1,4-diphenyl-1H-1,2,3-triazol-3-ylidene}] (4.1).**
- [CpNi(I){1-(2-ethoxy-2-oxoethyl)-3-methyl-4-phenyl-1H-1,2,3-triazol-3-ium}] (4.2).**
- [CpNi(I){3-methyl-4-phenyl-1-propyl-1H-1,2,3-triazol-3-ylidene}] (4.3).**
- [CpNi(I){1-benzyl-3-methyl-4-phenyl-1H-1,2,3-triazol-3-ylidene}] (4.4).**
- [CpNi(I){1-butyl-3-methyl-4-phenyl-1H-1,2,3-triazol-3-ylidene}] (4.5).**
- [CpNi(I){3-methyl-4-phenyl-1-octyl-1H-1,2,3-triazol-3-ylidene}] (4.6).**

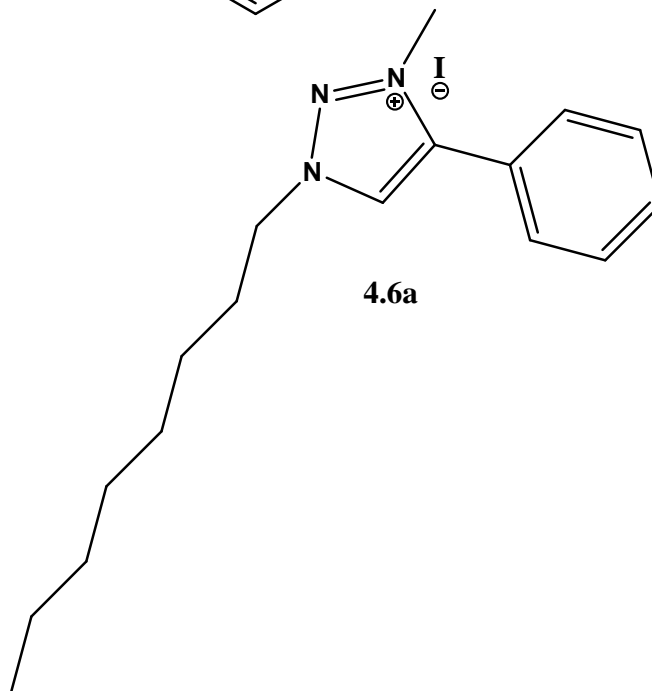
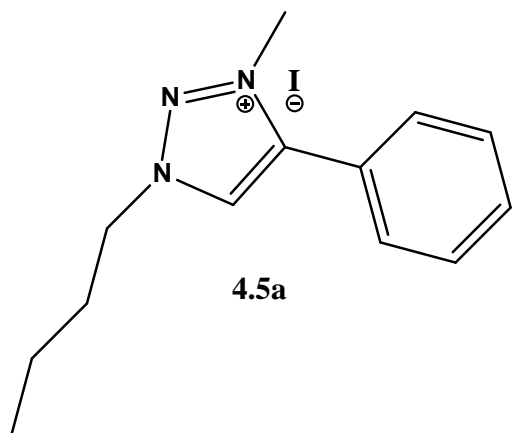
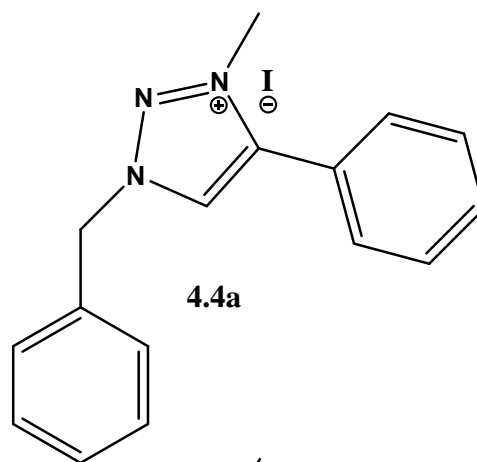
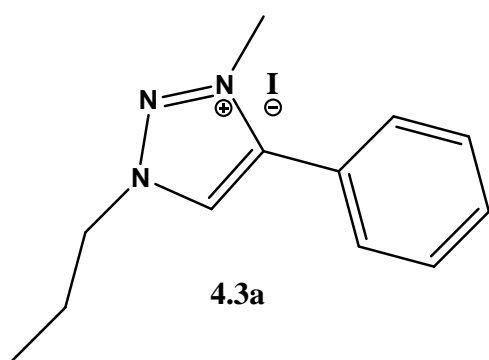
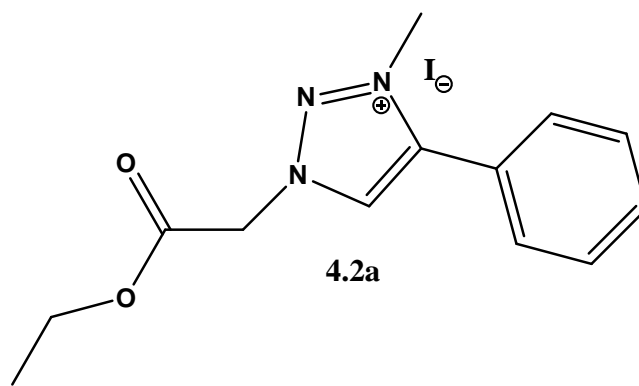
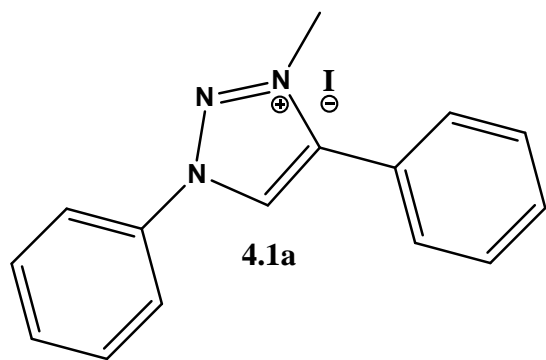


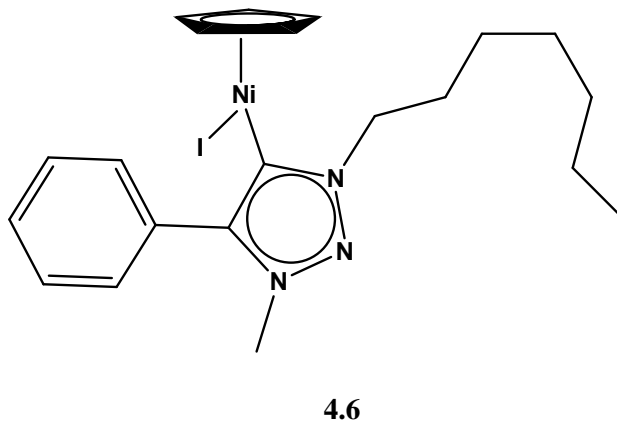
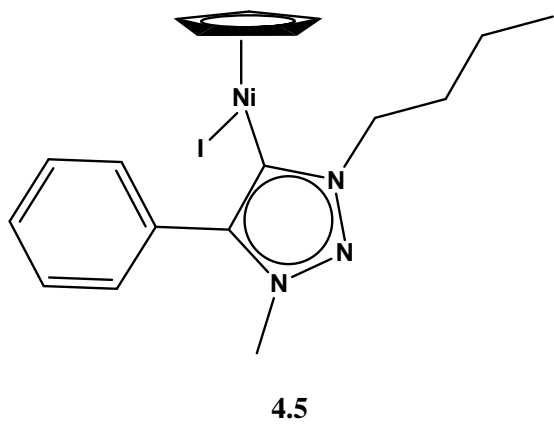
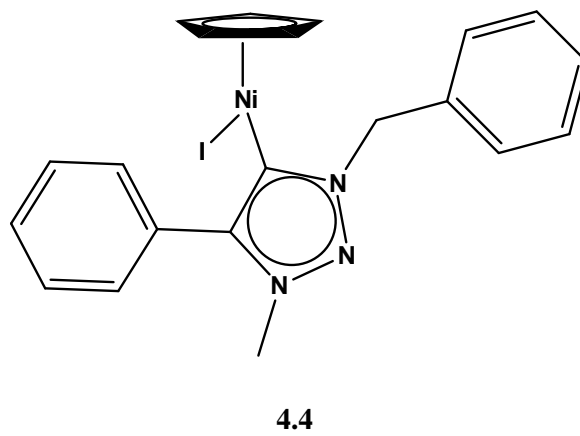
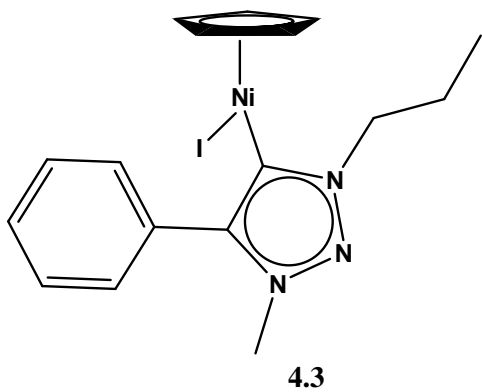
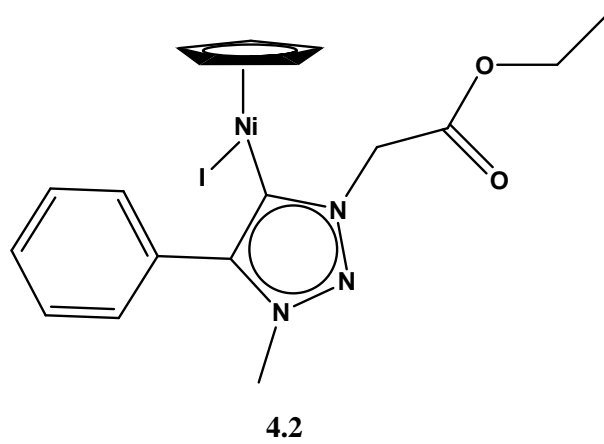
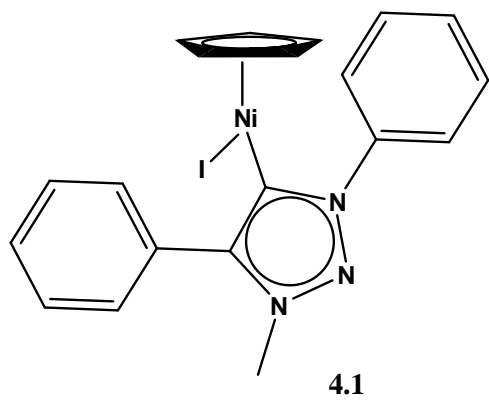












## Key references

1. J. C. Sheehan, *J. Am. Chem. Soc.*, 1951, **73**, 1207-1210.
2. P. Li and L. Wang, *Lett. Org. Chem.*, 2007, **4**, 23-26.
3. F. Wang, H. Fu, Y. Jiang and Y. Zhao, *Green Chem.*, 2008, **10**, 452-456.
4. L. Pinhua and L. Wang, *Lett. Org. Chem.*, 2007, **4**, 23-26.
5. S. Lal and S. Díez-González, *J. Org. Chem.*, 2011, **76**, 2367-2373.
6. N. Candelon, D. Lastécouères, A. K. Diallo, J. R. Aranzaes, D. Astruc and J. M. Vincent, *Chem. Commun.*, 2008, **6**, 741-747.
7. J. D. Crowley, P. H. Bandeen and L. R. Hanton, *Polyhedron*, 2010, **29**, 70-83.
8. M. Sun, J. Zhang, P. Putaj, V. Caps, F. Lefebvre, J. Pelletier, J.-M. Basset *Chem. Rev.*, 2014, **114**, 981-1019
9. C. Jia, T. Kitamura and Y. Fujiwara, *Acc. Chem. Res.*, 2001, **34**, 633-639.
10. A. Sivaramakrishna, P. Suman, E. V. Goud, S. Janardan, C. Sravani, C. S. Yadav and H. S. Clayton, *Res. Rev. Mat. Sci. Chem.*, 2012, **1**, 75-103.
11. R. A. Periana, D. J. Taube, E. R. Evitt, D. G. Loffler, P. R. Wentreck, G. Voss and T. Masuda, *Science*, 1993, **259**, 340-345.
12. C. W. Tornøe, C. Christensen and M. Meldal, *J. Org. Chem.*, 2002, **67**, 3057-3064.
13. K. Odlo, E. A. Høydahl and T. V. Hansen, *Tetrahedron Lett.*, 2007, **48** 2097-2099.
14. K. Barral, *Org. Lett.*, 2007, **9**, 1809-1811.
15. Z. Yacob and J. Liebscher, in *Ionic Liquids as Advantageous Solvents for Preparation of Nanostructures*, ed. S. T. Handy, 2011 pp. 3-22.